Resource and Interference Management in UAV-Cellular Network

by

Amr Salaheldin Hashem Matar

A thesis
presented to the University of Waterloo
in fulfillment of the
thesis requirement for the degree of
Doctor of Philosophy
in
Electrical and Computer Engineering

Waterloo, Ontario, Canada, 2022

Examining Committee Membership

The following served on the Examining Committee for this thesis. The decision of the Examining Committee is by majority vote.

External Examiner:	Abdallah Shami Professor, Dept. of Electrical and Computer Engineering, Western University
Supervisor(s):	Xuemin (Sherman) Shen Professor, Dept. of Electrical and Computer Engineering, University of Waterloo
Internal Member:	Catherine Gebotys Professor, Dept. of Electrical and Computer Engineering, University of Waterloo
Internal Member:	Xiaodong Lin Professor, School of Computer Science, University of Guelph
Internal-External Member:	Samer Al-Kiswany Associate Professor, David R. Cheriton School of Computer Science, University of Waterloo

Author's Declaration

I hereby declare that I am the sole author of this thesis. This is a true copy of the thesis, including any required final revisions, as accepted by my examiners.

I understand that my thesis may be made electronically available to the public.

Abstract

The future Sixth-Generation (6G) network is anticipated to extend connectivity for millions of Unmanned Aerial Vehicles (UAVs) worldwide and support various innovative use cases, such as cargo transport, inspection, and intelligent agriculture. The terrestrial cellular networks provide real-time information exchange between UAVs and Ground Control Stations (GCS), which facilitates the evolution of UAV communication systems while bringing promising economic benefits to cellular network operators. However, the tremendous growth in the UAV data traffic, with diverse and stringent service requirements, would add another pressure on the already congested terrestrial cellular network that is facing a rigorous challenge to increase network capacity with the limited spectrum resources. Moreover, since Macro Base Station (MBS) antennas are typically downtilt, UAVs, which are served by the MBS antenna's side lobes, suffer from sharp signal fluctuations causing throughput reduction and coverage drop. Besides, due to the Line-of-Sight (LoS) between UAVs and MBSs, UAVs experience higher uplink/downlink interference compared to ground Cellular Users (CUs). In this thesis, we propose two novel aerial network architectures in which we design efficient interference and resource management strategies to support the UAV Quality-of-Service (QoS) guarantee while considering different types of interference.

Firstly, we propose a novel standalone aerial multi-cell network where multiple UAV Base Stations (UAV-BSs) provide cellular services to UAV Users by reusing the licensed and unlicensed spectrum. Our objective is to jointly optimize the subchannels and power allocations of UAV-Users in the licensed and unlicensed spectrum to maximize the network uplink sum rate, considering inter-cell interference, co-existence with terrestrial cellular and WiFi systems, and the QoS of UAV-Users. We prove mathematically that the formulated optimization problem is an NP-hard problem. Therefore, the original problem is decomposed into three subproblems to solve it efficiently. We first use convex optimization and the Hungarian algorithm to obtain the global optimal of power and subchannel allocations in the licensed spectrum, respectively. Then, we design a matching game with externalities and coalition game algorithms to obtain the Nash stable of the subchannel allocation in the unlicensed band. Local optimal power assignment in the unlicensed spectrum is obtained using the successive convex approximation method. Lastly,

we develop an iterative algorithm to solve the three subproblems sequentially until convergence is reached. Simulation results demonstrate that the proposed algorithm achieves a significantly higher uplink sum rate compared with other resource allocation schemes. Moreover, the proposed algorithm improves the network throughput and capacity by nearly two times comparing to the Long Term Evolution-Advanced (LTE-A).

Secondly, we propose a novel integrated aerial-terrestrial multi-operator network. In the network, each operator deploys a number of UAV-BSs besides the terrestrial MBS, where each BS reuses the operator's licensed spectrum to provide downlink connectivity for UAV-Users. Moreover, the operators allow the UAV-Users, whose demand cannot be satisfied by the licensed band, to compete with others to obtain bandwidth from the unlicensed spectrum. Given the QoS requirements of UAV-Users, we aim to maximize the total sum rate by jointly optimizing user association, BSs transmit power, and dynamic spectrum allocation considering inter-cell interference in the licensed band and inter-operator interference in the unlicensed spectrum. In particular, we divide the resulting non-convex Mixed-Integer Non-Linear Programming (MINLP) optimization problem into two sequential subproblems: user association and power control in the licensed spectrum; and dynamic spectrum allocation and user association in the unlicensed spectrum. Furthermore, the former subproblem is decomposed into multiple subproblems for distributed and parallel problem-solving. Since the resulting former subproblem is still a non-convex MINLP problem, we propose a distributed iterative algorithm consisting of a matching game, coalition game, and successive convex approximation technique to solve it. Afterwards, in the latter subproblem, we first use a matching game to associate UAV-Users with the UAV-BSs for each operator in the unlicensed spectrum. Then, we propose a three-layers auction algorithm to allocate the unlicensed spectrum among operators dynamically. Extensive simulation results demonstrate that the proposed algorithm in the licensed spectrum significantly improves network throughput per operator than the conventional terrestrial network alone. Moreover, the achieved system throughput of the proposed algorithms in both licensed and unlicensed spectrum is 86.8% higher compared with that of using the licensed spectrum only.

In summary, we have proposed integrated aerial-terrestrial network architectures that leverage the aerial network to complete the terrestrial network to serve cellular-connected UAVs by reusing licensed and unlicensed spectrum considering multi-cell and multi-operator scenarios. Under

the proposed network architectures, we have investigated the subchannel allocation, UAV-Users' transmit power, user association, BSs' transmit power, and dynamic spectrum management to maximize the network throughput considering the QoS of UAV-User. The proposed architectures and algorithms should provide valuable guidelines for future research in designing resource and interference management schemes, improving network capacity, and enhancing spectrum utilization for complex interference environments in integrated UAV-cellular networks.

Acknowledgements

My unreserved gratitude and praises are for Allah, the Most Compassionate and the Most Merciful. He has blessed me with his bounties, and He has given me the strength and courage to reach my goals during the course of this research.

I would like to express my deepest and sincerest gratitude to my supervisor, Professor Xuemin (Sherman) Shen, for his continuous guidance, inspiration, deep insight, invaluable advice, and support during my graduate studies at the University of Waterloo. His guidance and encouragement have inspired and motivated me throughout the completion of this thesis, and he has made my experience at the Broadband Communications Research (BBCR) Group worthwhile and enjoyable. I would also like to thank the examining committee members of this thesis, Professor Catherine Gebotys, Professor Xiaodong Lin, and Associate Professor Samer Al-Kiswany. Their insightful comments have significantly improved the quality and presentation of my work. In addition, I would like to thank Professor Abdallah Shami for serving as my thesis external examiner and for his insights on my thesis with me.

Special thanks are due to my friends and colleagues at the BBCR group for their support and kindness, and for making my stay memorable. I would like to express special gratitude to Dr. Ahmed Abdalrahman, Dr. Manaf Ben-Yahya, Dr. Omar Alhussein, Dr. Hesham Moussa, Dr. Haixia Peng, Dr. Dongxiao Liu, Dr. Weisen Shi, Dr. Junling Li, Dr. Wen Wu, Dr. Huaqing Wu, and many other current and former BBCR members.

With great appreciation, I acknowledge the scholarship and financial support from my employer, Helwan University in Egypt, for granting me the scholarship and allowing me to enhance my experience and education. Acknowledgment is also extended to the Egyptian Cultural Bureau in Canada for their assistance. They have been very helpful in the administration of my scholarship during my academic journey in Canada.

Finally, my greatest thanks to my devoted parents, Salaheldin Matar and Fawzia Al-Sheikh, and my sister Heba Matar, all of whom have constantly given me love, support, motivation, and sincere prayers. Last, but certainly not least, I would like to thank my beloved wife, Noura Nasar, for the love, patience, and continued encouragement she has provided me during my graduate

study. Special thanks also go to my children, Ali, Sara, and Jumana, who fill my life with joy and happiness. Nothing would have been possible without Allah, the Creator and Lord of the universe, and my family support.

Dedication

This work is dedicated to my beloved parents, sister, wife, children, and siblings for giving me love, support, and encouragement.

Table of Contents

List of Figures

List of Tables

Chapter 1

Introduction

Unmanned Aerial Vehicles (UAVs) are expected to be an essential component of the future Sixth-Generation (6G) networks. Based on the Federal Aviation Administration (FAA) report, the number of UAVs (commonly known as drones) is predicted to be around 1.8 million vehicles by 2027 [2]. The applications of UAVs are expected to overgrow during the next decade, such as aerial imaging, package/cargo transport, inspection, and intelligent agriculture [3, 4]. However, current UAVs depend on simple direct communication with their Ground Control Station (GCS) over the WiFi band within the visible line-of-sight space, limiting future UAVs' applications [5]. Providing reliable and high-performance connectivity between UAV and GCS is necessary to achieve real-time command and control for UAV safe operation besides the data payload transmission and pave the road to large-scale UAV deployment [6]. Therefore, integrating UAVs into the cellular network as new aerial users (UAV-UEs), also known as cellular-connected UAVs, is a promising solution which anticipates achieving significant performance enhancement in terms of reliability, coverage, and throughput [7]. In this chapter, we provide an overview of UAV, discuss the main components of Unmanned Aircraft System (UAS), and elaborate on the challenges that face cellular-connected UAVs. We then present three key research problems investigated in this thesis.

1.1 Overview of Unmanned Aerial Vehicle

In this section, the main characteristics and factors of Unmanned Aerial Vehicle (UAV) are explained and summarized [8, 9].

1.1.1 Payload

The maximum weight that a UAV can carry is called a payload. As more sensors and equipment are needed, a larger payload is required at the expense of increasing the size of the UAV and shorter flight times [10].

1.1.2 Mechanism of Flying

The UAV flying mechanisms can be divided into three categories [11]:

- *Fixed-wing UAVs* can carry a heavy load over a wide area at high speed while maintaining energy efficiency simultaneously. However, the drawbacks of this type are that it cannot hover over a fixed area and does not take off and land vertically.
- *Rotary-wings UAVs* (a.k.a Multi-rotor UAVs) allow vertical lift and landing, and can hover over a certain area to complete the cellular coverage above it. However, this high maneuverability comes at the cost of limited mobility and significant power consumption compared to fixed-wing UAVs.
- *Hybrid fixed/rotary wing UAVs* provide a compromise between the two previously mentioned types; where the UAV can take off vertically, glide over the air, and then use its rotors to switch to hovering over a fixed location.

1.1.3 Operating Platform

Overall, UAVs as aerial platforms can be categorized into two types based on their altitude [12]:

- *Low Altitude Platform (LAP)* is usually employed to complement the mobile network since it operates at an altitude of 10 km or less. In addition, the LAP UAV is characterized by its cost-effective, fast deployment and its Line of Sight (LoS) links that significantly enhance cellular communications' performance.

- *High Altitude Platform (HAP)* operates at an altitude between 17 km and 22 Km. Compared to LAP, vehicles that fall under this platform can stay much longer time in the stratosphere layer, but their deployment is more complex. HAP is used to provide Internet connectivity to rural areas that are currently not served by cellular networks. Examples of these UAV platforms are balloons, airships, and aircraft.

1.1.4 Industry Projects on UAVs

In this subsection, we give small details about the recent projects targeting UAV applications.

- ***Nokia F-Cell*** is a novel infrastructure composed of a massive MIMO wireless backhaul that serves autonomous self-configured and solar-powered UAVs which form small cells [13]. The F-Cell architecture can spatially multiplex up to 8 autonomous F-Cells (which mount a solar panel no more than the cell itself to consume less processing power) by connecting them to a closed loop 64 massive MIMO antenna array located at the center.

- ***Huawei Digital Sky*** was activated by Huawei's Lab in 2017 in Shanghai city in order to promote the experiments of specific use cases involving connected UAVs [14]. It creates an end-to-end ecosystem consists of two 6km diameter flying zones and a maximum height of 200 m covered by cellular networks to ensure Command & Control (C&C) traffic between UAVs and either control stations or wireless charging locations deployed in the ground.

1.2 Unmanned Aircraft System (UAS)

An Unmanned Aircraft System (UAS) is composed of two main components: a UAV and Ground Control Station (GCS). For UAV safe operation, it is necessary to provide reliable and high-

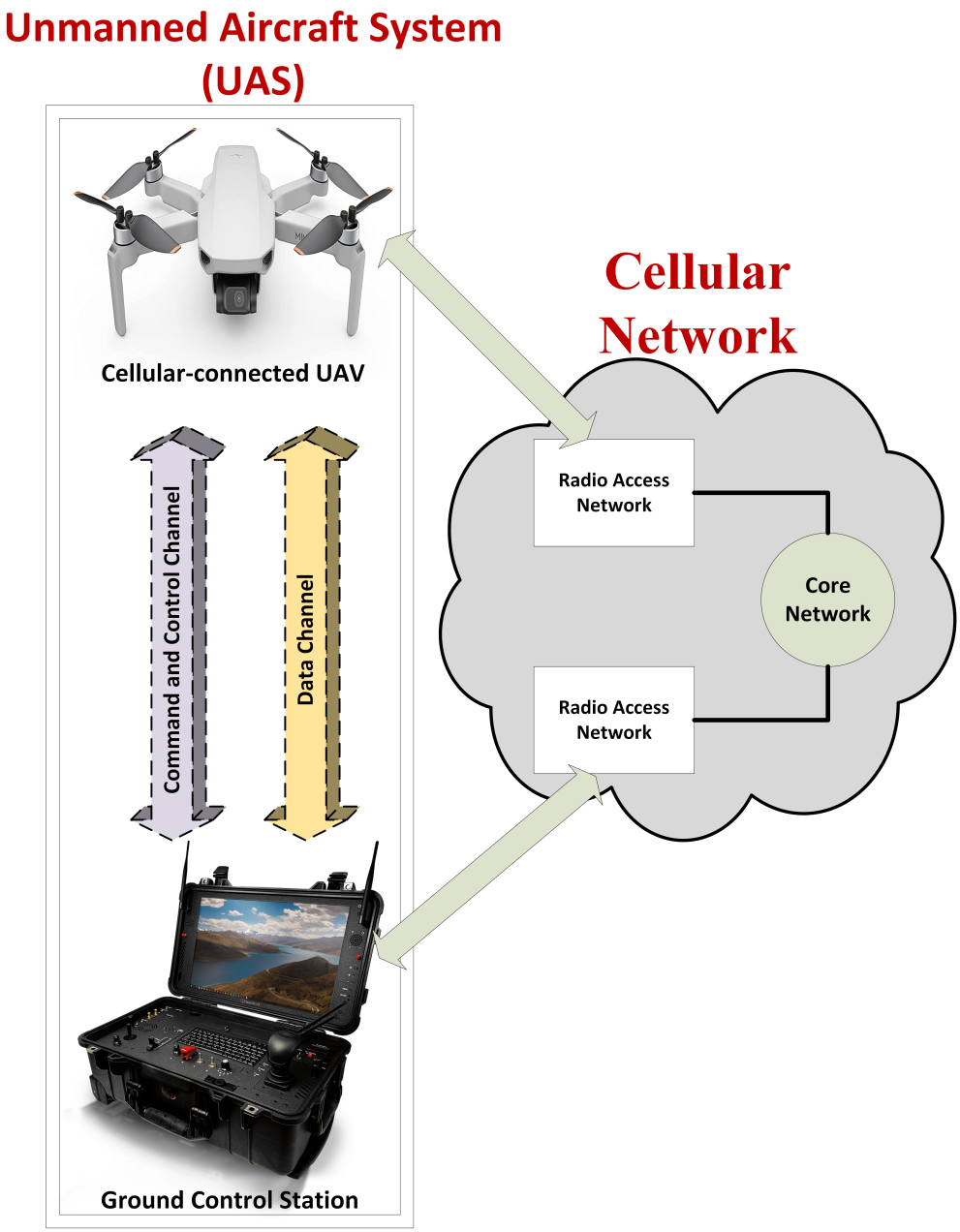

Figure 1.1: Unmanned Aircraft System (UAS).

performance connectivity between UAV and GCS to support two types of traffic channels [15], which are defined as follows:

- **Command & Control (C&C) Traffic** includes telemetry, real-time piloting, identity, authentication, and trajectory location update. It needs critical Quality-of-Service (QoS) requirements regarding reliability and latency.
- **Data Traffic** includes data from sensors carried by UAVs, images, real-time videos, etc.

In order to move toward long-range control and autonomous operation of UAVs, reliable and widely available wireless connectivity between UAV and GCS is needed because it is the only way to remotely control a UAV or take control of an autonomous UAV flight [16, 17]. Therefore, the cellular network, which has broad coverage, has been introduced as a critical solution for the UAS [18]. Thus, as seen in Figure 1.1, integrating UAVs with the cellular network, known as cellular-connected UAVs, expect to anticipate achieving significant performance enhancement in terms of reliability, coverage, and throughput.

1.3 Challenges of Cellular-connected UAVs

As discussed in Section 1.2, the cellular network has emerged as a key enabler of cellular-connected UAVs that can significantly enhance UAV traffic safety and efficiency and enable ubiquitous access to support new UAV data services and applications [19]. However, how to guarantee the performance of the cellular-connected UAVs to achieve their essential role as expected by industry and academia still faces challenges. In this section, we will investigate the major challenges faced by cellular-connected UAVs, which have been explained and summarized in the study item [1] of the 3rd Generation Partnership Project (3GPP) .

1. **Traffic performance requirements:** The 3GPP defined the performance requirements of the Command & Control (C&C) and data traffic channels that should be provided for UAV-UE, as summarized in Table 1.1.

Table 1.1: UAV-UE traffic performance requirements [1]

Traffic	Data Rate	latency
Command & Control Traffic	60 - 100 Kbps for UL/DL	50ms (one way)
Data Traffic	up to 50 Mbps for UL	similar to LTE UE

2. **Uplink transmission interference:** The cellular infrastructure performance assessment has demonstrated that UAV-UEs experience interference issues in the uplink transmissions as UAV-UE receives Line-of-Sight (LoS) transmissions from many BSs when it increases its altitude [20]. Therefore, when UAV-UEs transmit data toward their serving cellular BS, they generate substantial interference on the other ground BSs that cause critical issues in the cellular network. The resulting interference can damage the uplink connection of existing terrestrial cellular users, who are likely to have non-LoS uplink transmissions.

3. **Downlink transmission interference:** According to some field measurements, a UAV-UE flying at an altitude of 100 meters can receive signals from BSs located 10 kilometres apart [21]. In other words, UAV-UEs can experience significant interference from multiple cellular BSs that transmit toward other terrestrial cellular users or UAV-UEs. Therefore, downlink transmissions towards UAV-UEs commonly suffer from degradation in Signal to Interference plus Noise Ratio (SINR) compared to ground cellular users.

4. **Association and handover:** Due to the down-tilt of cellular BSs antennas, UAV-UEs are connected to the BS through the sidelobes of its directive antennas, as seen in Fig. 1.2. Consequently, UAV-UEs are usually associated with BSs other than this physically adjacent BS due to insufficient signal strength received from the latter. Therefore, UAV-UEs face an increase in handover failure and outage probabilities compared to ground users due to the antenna's radiation pattern nulls and the high power of the interference signals [22].

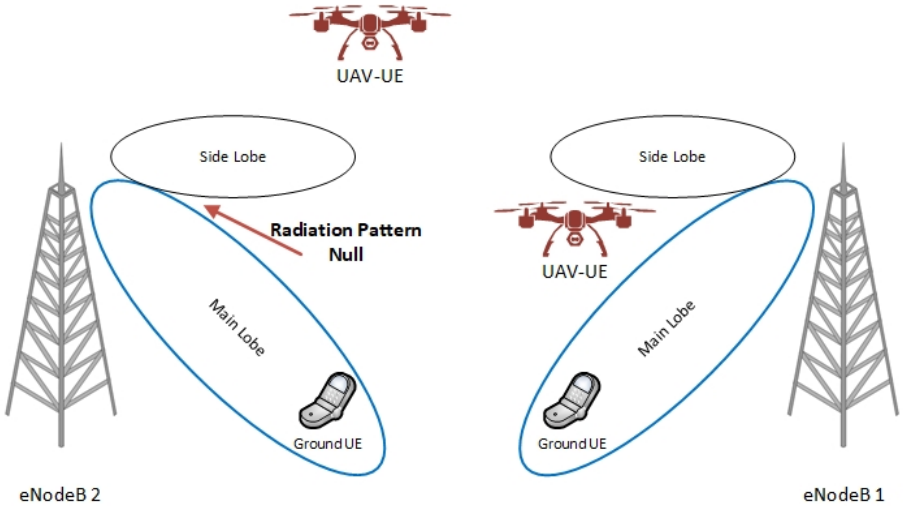

Figure 1.2: Challenges of cellular-connected UAV.

1.4 Research Motivations and Contributions

As we mentioned above, benefiting from advances in the UAV industry and wireless communication technologies, the cellular network has emerged as a critical enabler of cellular-connected UAVs [23]. Therefore, integrating UAVs into the cellular network as new aerial users (UAV-UEs), also known as cellular-connected UAVs, is a promising new solution which anticipates achieving significant performance enhancement in terms of reliability, coverage, and throughput. Moreover, allowing real-time information exchange between UAV-UEs and GCS would enhance UAV safety and efficiency and support new UAV services and applications.

However, several challenges need to be solved to realize this integration efficiently [24]. Specifically, since Macro Base Station (MBS) antennas are typically downtilt, UAVs suffer from sharp signal fluctuations since they are received only by the MBS antenna's side lobes. According to [25], UAVs flying at an altitude of 100 m suffer from a throughput reduction of factor 10 and a coverage drop from 76% to 30% compared to ground cellular users. Moreover, UAVs at that height could receive signals from MBSs located 10 kilometres apart [21], which produce high uplink/downlink interference. Furthermore, with more and more UAV services and applications, data and C&C traffic generated by UAV-UEs would increase, and the issue of the

overloaded terrestrial cellular network would get worse [26]. Because of the limited spectrum resources, promoting terrestrial cellular networking to support the emerged cellular-connected UAVs' services and applications, especially those requiring sensitive delay and diverse resources, is challenging [27].

Several recent research works have tackled these issues through UAV trajectory optimization. However, most existing schemes that aim to minimize the coverage outage probability only consider one cellular-connected UAV with a predefined start and end point. The trajectories computation of large numbers of UAV-UEs, defining the conflict between these trajectories, and the impact on the terrestrial network have not been considered. Moreover, these studies have shown the significant effect of UAV movement change on coverage probability [28, 29]. Furthermore, the vast predicted data rate demand of UAV-UEs would produce more pressure on the overloaded terrestrial cellular network since UAV-UEs need to share the limited spectrum available with ground cellular users. Therefore, an aerial network architecture which provides seamless connectivity for cellular-connected UAVs is a promising solution that allows mobility freedom for UAV-UEs without a trajectory restriction by providing broad coverage above the actual coverage height of Macro BS.

In this thesis, we propose two novel aerial networks in which channel resource allocation, power control, user association, and spectrum management are designed to increase the network throughput considering the QoS of UAV-UE and different types of interference. Specifically, the main contributions of this thesis are summarized as follows,

1. We propose a novel standalone aerial multi-cell network in which UAV-BSs are deployed to provide uplink cellular services to UAV-UEs through reusing both licensed and unlicensed spectrum. Considering the coexistence of the proposed network, terrestrial cellular network, and WiFi system, we jointly optimize the subchannel allocation and the transmit power of UAV-UEs to maximize the network uplink sum rate in the licensed and unlicensed spectrum considering the QoS of UAV-UE and the inter-cell interference. The formulated optimization problem, which we prove to be an NP-hard problem, is decomposed into three subproblems. Afterwards, we propose an iterative algorithm which consists of convex optimization, the Hungarian algorithm, a matching game with externalities and a coalition

game, and a successive convex approximation technique to solve the formulated problem. Simulations show that the proposed algorithms improve the cellular operator's network capacity by at least two-fold while ensuring coexistence with the existing terrestrial and WiFi systems.

2. We propose a novel integrated aerial-terrestrial multi-operator network architecture in which each operator deploys a number of UAV-BSs besides the terrestrial Macro BS (MBS), where each BS reuses the operator's licensed spectrum to provide downlink connectivity for UAV-UEs. Moreover, the operators allow the UAV-UE, whose demand cannot be satisfied by the licensed band, to compete with others to obtain bandwidth from the unlicensed spectrum. Given the QoS requirements of UAV-UEs, we aim to maximize the proposed network's total sum rate by jointly optimizing user association, BSs transmit power, and dynamic spectrum allocation considering inter-cell interference in the licensed spectrum and inter-operator interference in the unlicensed spectrum. The formulated non-convex mixed integer non-linear programming (MINLP) optimization problem is divided into two sequential subproblems, which are explained as follows:

    - First, we jointly optimize the user association and the transmit power of BSs to maximize the network throughput in the licensed spectrum, considering the coupling issue caused by the multi-cell scenario. To cope with the complexity of the non-convex MINLP subproblem, we further decompose the optimization problem into multiple subproblems to be solved in a distributed and parallel manner. Afterwards, we propose a distributed iterative algorithm for efficient solving. Simulation results demonstrate that the proposed architecture and algorithm allow operators to achieve significantly higher network throughput in the licensed spectrum with low complexity compared to other schemes and only use terrestrial networks.
    - Second, we jointly optimize the user association and dynamic spectrum management to maximize the network throughput in the unlicensed spectrum, considering the QoS of UAV-UE and the inter-operator interference issue due to the multi-operator scenario. We first use a matching game to associate UAV-UEs with UAV-BSs; then, we design a three-layers auction framework to dynamically allocate the unlicensed

spectrum band among the UAV-UEs of different operators. The simulation results demonstrate the effectiveness of the proposed spectrum management approach in increasing the network throughput and user satisfaction compared to other spectrum management schemes. Moreover, the proposed architecture enables the cellular operators to significantly enhance the total network throughput by close to double through reusing both licensed and unlicensed spectrum compared with using licensed band only.

1.5 Thesis Outline

The remainder of the thesis is organized as follows: In Chapter 2, we provide a comprehensive review of cellular-connected UAV's state-of-the-art resource and interference management strategies. In Chapter 3, we propose a joint subchannel allocation and power control to maximize the network uplink throughput in the licensed and unlicensed spectrum for a novel standalone aerial multi-cell network. In Chapter 4, we propose a novel integrated aerial-terrestrial multi-operator network architecture, in which we design a user association, power control, and dynamic spectrum management to maximize the network downlink throughput. The proposed optimization approach considers the QoS of UAV, inter-cell interference in the licensed spectrum, and inter-operator interference in the unlicensed spectrum. Finally, we conclude the thesis and discuss future research works in Chapter 5.

Chapter 2

Background and Literature Survey

This chapter presents the background of the UAV-cellular network and the LTE-Unlicensed (LTE-U) and surveys state-of-the-art resource and interference management strategies for cellular-connected UAVs.

2.1 UAV-Cellular Network and LTE-Unlicensed

In this section, we intend to explain the background of the UAV-Cellular Network and the LTE-U.

2.1.1 UAV-Cellular Network

Supporting different multimedia service requirements while providing ubiquitous connectivity for mobile users are key challenges in Beyond 5G networks [30]. Therefore, future Radio Access Networks (RAN) need to support reliable and low-latency access to massive mobile devices with a significant level of flexible deployment required [31]. However, deployment of current cellular BS is according to long-term traffic behaviours with low flexibility to be re-distributed. Though the dense distribution of BSs is one intuitive strategy to improve RAN coverage, this method is unacceptable for cellular operators due to high expenditure and low efficiency [32]. Therefore,

to enhance the capacity, coverage, and reliability of the existing cellular networks, the emerging UAV as an aerial base station (UAV-BS) is a promising solution.

Latterly, there has been a significant effort to explore the potential of UAV-BS to enhance the performance of the terrestrial cellular network. In [33], the authors demonstrate the capability of UAV-BS as an aerial extension of cellular BS to improve the signal strength in coverage holes through field experiments. In [34], authors study the spectrum sharing of UAV Small Cells network modelled by the 3D Poisson point process. The optimal density of UAV-BSs to maximize the network throughput while maintaining the cellular network efficiency under a specific threshold. In [35], authors jointly optimize the UAV-BS trajectory and power control along with the multi-user communication scheduling and association in order to maximize the minimum downlink throughput over ground cellular users. Successive convex optimization and block coordinate descent algorithms are introduced for solving the mixed-integer non-convex optimization problem. In [36], in order to maximize the information collection gained from ground Internet of Things (IoT) devices, Mozaffari et al. design a clustering approach to finding the optimal locations and trajectories of UAV-BS.

Moreover, UAV can also operates as flying user (UAV-UE) [37]. Critical command and control information must be exchanged in real-time when using UAVs in applications such as surveillance, real-time monitoring, and precision agriculture [38]. Thus, a wireless technology that can provide ubiquitous coverage, sufficient connectivity, high throughput, and low latency between ground control stations and UAV-UEs is required [39]. Therefore, the current cellular infrastructure considers a promising solution to provide scheduling, licensed spectrum, and mobility management to UAV-UEs. However, based on [1], [25], UAVs as a new cellular user type could produce severe degradation in the overall performance of the cellular system. Studies that examined emerging issues from connecting UAV-UE to the cellular network are explained in detail in the next section.

2.1.2 LTE-Unlicensed

The phenomenal growth of data rate demand from mobile devices has brought about increasing scarcity in the available radio spectrum. Despite the many advanced technologies, the shortage

of spectrum resources is still the main bottleneck for capacity enhancement. To address these issues, LTE-Unlicensed, or LTE-U, is considered one of the latest groundbreaking innovations to provide high performance and seamless user experience under a unified radio technology by extending LTE to the readily available unlicensed spectrum [40]. This motivates cellular network operators to exploit the available unlicensed spectrum by allowing subscribers to adaptively use either licensed LTE spectrum or unlicensed WiFi spectrum to provide multimedia services.

LTE-U extends 3GPP LTE to the unlicensed spectrum and aggregates the unlicensed spectrum with the licensed spectrum leveraging the existing Carrier Aggregation (CA) technology. It can provide better coverage and larger capacity than cellular/WiFi inter-working while allowing seamless data flow between licensed and unlicensed spectrum through a single Evolved Packet Core (EPC) network [40]. For operators, LTE-U means synchronized integrated network management, the same authentication procedures, more efficient resource utilization, and thus lower operational costs. For wireless users, LTE-U means enhanced user experience, higher data rates, seamless service continuity between licensed and unlicensed bands, ubiquitous mobility, and improved reliability). LTE-U has been standardized in the 3GPP Releases 13, 14, and beyond [41].

Despite the many advantages of LTE-U, it also faces two critical technical challenges for practical deployment [42]. The first one is the coexistence with the WiFi networks. LTE is designed as an exclusive system to avoid uncontrolled interference on the same frequency band. In contrast, WiFi systems competitively manage unlicensed spectrum resources via distributed coordination function (DCF). Therefore, LTE-U will cause significant performance degradation on WiFi users without efficient coexistence mechanisms. The second challenge is resource management for LTE-U systems, which plays an essential role in determining system performance. The addition of unlicensed spectrum makes the current results of traditional LTE systems inappropriate for LTE-U systems. Specifically, several new research issues, such as the balance between the LTE-U and WiFi networks, and the spectrum sharing among operators on unlicensed spectrum, should be carefully considered.

2.2 Channel Resource and Interference Management

Channel resource and interference management are the keys to exploiting the full potential of UAV applications in the UAV-cellular networks. In this section, we survey existing Interference and resource management schemes for licensed and unlicensed spectrum.

2.2.1 Licensed Spectrum Resources

In what follows, we summarize the existing resource and interference management schemes from cellular-connected UAV and UAV-BS perspectives.

From UAV-UE perspective: Several studies investigate the interference and channel allocation issues related to integrating the cellular-connected UAVs into the cellular system while using the operator's licensed spectrum. In [43], a joint channel allocation and trajectory design scheme is proposed to achieve a balance between the uplink sum rate and the latency of sensing tasks for a multi-UAV-aided single cell network. The authors in [44] present a new 3D system model for the uplink/downlink transmission between the UAV-UE and the ground BS, where the UAV 3D coverage analysis for both uplink and downlink is proposed. In [45], an interference-aware path planning scheme is proposed for cellular-connected UAVs, which aims to strike a balance between minimizing UAV interference with terrestrial systems and maximizing the UAV energy efficiency. In [46], an interference-aware path planning scheme is proposed to minimize the mission completion time of a UAV-UE while maintaining the minimum QoS requirement with the ground BSs. The work in [47] jointly optimizes the trajectory, operation time, transmit power, and communication scheduling of the UAV-UE to maximize the throughput subject to the energy and QoS constraints. In [48], UAV-UEs collaboratively build a global outage probability model in the environment using Federated Learning (FL) to optimize the UAVs' paths for minimizing the UAV travel time. The UAV coverage probability analysis in the uplink transmission has been introduced in [28, 49]. In [49], the minimum UAV-UE flying height along a predefined trajectory is determined during a concurrent transmission with a ground cellular user using Non-Orthogonal Multiple Access (NOMA) and with a given QoS constraint. In [28], the authors propose a framework to derive the lower and upper bound coverage probability of UAV-UE served by ground BSs

using the Coordinated Multi-Point (CoMP) transmission to measure the UAV's speed, altitude, and collaboration distance on the achieved performance. In [50], a cooperative interference cancellation approach is introduced for a multi-beam UAV to maximize the uplink sum rate of the connected BS and, in the meanwhile, mitigate the UAV's uplink interference at each of the other ground BSs. In [51], a novel mechanism is proposed to dynamically tune the down-tilt angles of all the ground BSs for providing efficient mobility support to the UAVs moving in the sky through maximizing the received signal power while also maintaining good throughput performance of the ground users.

From UAV-BS perspective: As an extension of the cellular network to serve terrestrial users, the deployment and trajectory design of UAV-BSs have attracted high attention recently. The authors in [52] propose a multi-agent reinforcement learning framework to optimize the resource allocation, such that each UAV-BS can adjust its resource, power, and associated users separately without exchanging information among them. The joint design of UAV-BS trajectory and resource allocation is proposed in [53, 54] to maximize the network throughput while considering the ground cellular users' fairness through using deep reinforcement learning algorithms. In [55], the UAV-BS placement, user association, and resource allocation are jointly considered by designing an iterative algorithm to maximize the ground cellular users' throughput and achieve fairness among them. In [56], a UAV-BS equipped with a millimetre-Wave (mmWave) Multiple-Input Multiple-Output (MIMO) antenna is deployed to provide wireless access to IoT devices from different clusters in the downlink transmission. The authors jointly optimize the transmit power, beam pattern, and 3D placement of the UAV-BS to maximize the system's downlink sum rate.

Recently, a few articles investigated the performance of using the UAV-BS to provide cellular service to the UAV-UEs. The authors in [57] proposed a 3D placement algorithm for a UAV-BS equipped with a directional antenna to maximize the number of covered UAV-UEs subject to spectrum sharing policy with the terrestrial network. In [29], UAV-to-UAV (U2U) pairs sharing uplink band of ground cellular users are assumed, where the coverage probability and rate are evaluated under two spectrum sharing mechanisms through an analytical framework that considers channel models, antenna patterns, and practical power control schemes. The underlay mechanism showed that U2U communications might have a limited harmful effect on the ground user uplink performance since BSs receive the UAV power signals through their antenna sidelobes.

2.2.2 Unlicensed Spectrum Resources

The use of LTE in the unlicensed spectrum, *a.k.a* LTE-U, with UAV-BS was introduced in [58], [59]. In [58], the authors formulated a problem that jointly optimizes user association, content caching, and spectrum allocation of a UAV-BS that serves ground cellular users over the LTE licensed and unlicensed spectrum. A game for load balancing between UAV-BSs and WiFi access points in the unlicensed band was proposed in [59] to verify a sufficient throughput for all users. However, providing LTE service for cellular-connected UAVs in the unlicensed spectrum to fulfil their high demand data rate has not been considered yet.

2.3 Spectrum Management for Multiple Cellular Operators

The unlicensed spectrum is a promising candidate for cellular networks to seek more fruitful radio spectra to address the rigorous challenge of increasing network capacity due to the shortage of spectrum resources. However, since using unlicensed spectrum in UAV-cellular networks is a new scenario, no previous work considers the existence of multiple aerial network operators over the same unlicensed band. However, some research works have examined the inter-operator interference issue for heterogeneous cellular networks, but these works have some drawbacks, as explained below. In [60], the joint unlicensed subchannel allocation and WiFi coexistence problem is studied, aiming to maximize network sum-rate while ensuring user QoS constraint. The authors introduce an iterative algorithm in which a one-sided matching game solve the resource allocation subproblem, while the coexistence issue with WiFi access point is solved through a cooperative Nash bargaining game. In [61], authors formulate a coordinated hierarchical game to model the spectrum sharing between different operators in LTE-U small cells system. A Stackelberg multi-leader multi-follower game framework is introduced to examine the interaction between multiple small cell operators and users in the unlicensed spectrum. In this case, the operators profit from operating on unlicensed resources while the users choose which unlicensed bands to transmit based on the interference penalty price. Besides, the adopted game strategies ensure the interference to the WiFi system is kept under an acceptable level. In [62], authors formulate a sum-rate optimization problem under the constraints of achieving user QoS and coexistence

between LTE-U and WiFi Access Point (WAP) with considering multiple Small BSs from different operators. They use a Nash Bargaining Game (NBG) to find the optimum time sharing problem between the LTE-U system and WAP; and a heuristic algorithm for the LTE-U resource allocation problem. In [63], NBG is also used for the time-sharing problem and a Bankruptcy game for the resource allocation problem. A machine learning based optimization method is proposed in [64]. The authors introduced a Long Short-Term Memory (LSTM) cells based deep learning algorithm to develop a proactive spectrum reuse scheme for allocating the resources in an LTE-U network over a fixed time window. Based on the above, the main drawback in previous works is considered fixed spectrum sharing; that is, the unlicensed spectrum is partitioned into the fixed-length partition for each small cell network operator. Therefore, the dynamic traffic requirement of each operator has not been considered, which reduces the spectrum efficiency. In addition, in the previous works, only 2D small cells were considered, which is different from the 3D nature of the UAV-cellular network.

Spectrum sharing in licensed spectrum also received much attention recently as a promising technique to improve spectrum efficiency and increase operator profit [65]. The spectrum sharing method is based on the that each operator could lease a part of their licensed spectrum band to another operator. In [66],a spectrum sharing framework between two mobile network operators (MNOs) using MIMO techniques to enable licensed spectrum sharing is proposed. The authors develop an algorithm to determine resource allocation and user scheduling through fractional programming and block coordinate descent. In [67], the authors propose a blockchain trust framework for the licensed spectrum sharing in multiple operator networks, in which a smart contract is designed to implement the spectrum trading among multiple operators without the need for a trustless spectrum broker. However, there are critical differences in spectrum sharing strategies among multiple operators between the licensed and unlicensed spectrum. First, operators own their band in the licensed spectrum and lease a fraction of this band to other operators when the traffic demand is low to maximize the profit. In contrast, operators have no control over the unlicensed spectrum and who accesses it. Moreover, the licensed spectrum is not shared with other systems, unlike the unlicensed spectrum, which is shared with other networks such as WiFi systems.

2.4 User Association and Interference Management in Integrated Networks

Integrating the aerial network with the terrestrial network to serve the cellular-connected UAV has not been considered before; however, some research works investigated this integration for ground cellular users. The authors in [68] propose a service-oriented network slicing approach for an air-ground integrated Vehicular network. According to the paper, the ground roadside units (RSUs) provide on-demand unicast services to vehicles, while the High-Altitude Platforms (HAPs) broadcast contents proactively in a large area. In [69], the authors jointly optimize the coupled effects of UAV-BS's longitudinal mobility, air-to-ground communication, and computation dynamics to maximize the overall energy efficiency of UAV for an air-ground cooperative networking scenario. In [70], the authors propose a UAV-assisted cooperative transmission network, in which UAV location, UAV-user association, BS resource allocation, and the load allocation between the two systems were jointly optimized to maximize the energy efficiency of the network. In [71], the power allocation and cell association of the UAV are jointly optimized to maximize a weighted sum-rate of the UAV-UEs and the ground cellular users in the uplink transmission. A novel 3D fully-fledged UAV-cellular network is introduced in [72], where a framework was proposed to solve the two essential problems of 3D cell association and network planning. An integrated satellite-aerial-terrestrial network that supports smart vehicles on the ground is introduced in [73], where the user association, BS/UAV transmission power, and UAV trajectory are jointly optimized to maximize the average users' throughput, which is solved using an alternating iterative algorithm based on the block descent method. In [74], the authors analytically obtain the coverage probability (CP) and average rate expressions for an integrated aerial-terrestrial network by employing an optimal combination of mmWave and microwave radio access technology based on the proposed association strategy. In [75], the authors discuss the essential features of Non-terrestrial networks' integration into terrestrial networks and the synergies by delving into the new range of services and use cases. Moreover, they review the challenges and the new approaches being adopted to develop efficient integrated ground-air-space networks.

2.5 Summary and Discussions

In this chapter, we have surveyed the existing literature for resource and interference management for cellular-connected UAVs. Also, approaches applied for user association and spectrum management schemes for LET-U systems and integrated networks are summarized. Through this literature review, we identify the limitations of current studies, which we summarize as follows.

First, none of the previous works investigated leveraging aerial networks to provide cellular services for cellular-connected UAVs and reusing licensed and unlicensed spectrum to overcome the cellular operator challenge of increasing network capacity with spectrum resources deficiency. Moreover, the previous works that consider extending cellular service to unlicensed spectrum for heterogeneous small-cell networks focused only on time-sharing techniques with WiFi systems; none of them explored the interference threshold protection method as a promising solution for the co-existence with WiFi system. Furthermore, none of the previous works considered the coupling issue in resource allocation strategy due to the multi-cell scenario.

Second, even though some schemes for the small-cell networks explored the inter-operator interference issue in the unlicensed spectrum for multiple operators; however, they only considered the fixed assignment spectrum management, and none of them studied the dynamic spectrum management based on the cellular operators' traffic load demands, which reduces the spectrum efficiency. Moreover, these studies considered only small-cell networks to serve ground cellular users, not aerial networks.

Third, no previous works on user association and interference management schemes in the integrated aerial-terrestrial network investigated the multi-cell and multi-operator scenarios. In addition, they only considered ground cellular users, not cellular-connected UAVs.

Chapter 3

Subchannel Allocation and Power Control in Licensed and Unlicensed Spectrum for a Standalone Aerial Multi-Cell Network

In this chapter, we propose a novel standalone aerial multi-cell network in which resource and interference management strategies are developed. In the considered network, multiple UAV-BSs provide cellular services to UAV-UEs by reusing both licensed and unlicensed spectrum. Considering the co-existence of terrestrial cellular, WiFi and UAV-BSs, a joint optimization problem is formulated for subchannel allocation and power control of UAV-UEs over the licensed and unlicensed spectrum to maximize the network uplink sum rate while considering the QoS of UAV-UE and the inter-cell interference. Since the formulated problem is an NP-hard problem, which we prove in this chapter, we decompose it into three sub-problems. Specifically, we first use the convex optimization and the Hungarian algorithm to obtain the global optimal of power and subchannel allocations in the licensed spectrum, respectively. Afterwards, we propose a matching game with externalities and coalition game algorithms to obtain the Nash stable of the subchannel allocation in the unlicensed band. Local optimal power assignment in the unlicensed spectrum is obtained using the successive convex approximation (SCA) method. Finally, we develop an iterative algorithm to solve the three subproblems sequentially until convergence is

reached. Simulation results show that the proposed network and algorithm can improve the network capacity nearly two times more than the Long Term Evolution-Advanced (LTE-A).

3.1 Background and Motivation

There is a significant increase in using unmanned aerial vehicles (UAVs) for real-time monitoring, surveillance, precision agriculture, logistics, enhancing wireless coverage, etc. [76–78]. In those applications, a UAV is considered aerial user equipment, requiring appropriate techniques to ensure highly reliable communication between UAVs and ground control stations. As a new type of cellular user, UAV-UEs could produce severe degradation in the overall performance of the terrestrial cellular system [79], [80]. In particular, UAVs suffer from higher downlink/uplink interference due to the line-of-sight (LoS) connection with ground base stations (BSs). Besides, due to the radiation nulls and the down-tilt of the BS antennas [81], UAV-UEs are forced to associate with far BSs if they face one of these nulls, which raises the handover request rate and increases the possibility of handover failure. Therefore, the existing cellular network designed for terrestrial users cannot readily serve UAV-UEs. Meanwhile, a UAV can also work as a base station (UAV-BS) for providing broadband wireless connectivity during disasters due to its flexible deployment [82, 83]. According to [57, 72], UAV-BSs can be a promising solution to provide reliable wireless connectivity for UAV-UEs. Therefore, the need for a three-dimension (3D) cellular network consisting of both UAV-BSs and UAV-UEs has become essential.

The main contribution of this chapter is that we propose a novel standalone aerial multi-cell network allowing UAV-BSs to effectively serve UAV-UEs in uplink transmission through both licensed and unlicensed spectrum. A joint resource and interference management scheme is developed over the licensed and unlicensed bands to maximize the network uplink sum rate while considering the QoS of UAV-UE and the multi-cell scenario. Furthermore, interference threshold protection guarantees coexistence with the terrestrial cellular and WiFi systems is considered. To our best knowledge, this is the first work on a standalone aerial multi-cell network that reuses both licensed and unlicensed spectrum to maximize network uplink sum rate, considering the QoS of UAV-UE, multi-cell scenario, and the coexistence guarantee with both cellular and WiFi

networks. The main contributions of this work are as follows:

- We propose a novel aerial multi-cell network that reuses both licensed and unlicensed spectrum, in which we investigate subchannel allocation and power control to maximize the uplink sum rate of the system subject to the QoS constraint of UAV-UEs and the inter-cell interference.
- We consider mutual interference threshold protection constraints in the licensed/unlicensed band to ensure the harmonious coexistence of our proposed system concurrently with the cellular/WiFi networks, respectively.
- The formulated NP-hard optimization problem is decomposed into three subproblems. First, we use the convex optimization and Hungarian algorithm to get the global optimum power and subchannel allocations in the licensed spectrum. Second, the Nash-stable subchannel allocations in the unlicensed spectrum are reached using a matching game with externalities and coalition game algorithms. Third, we use the successive convex approximation technique to obtain the local optimum power values in the unlicensed band. Finally, an iterative algorithm is proposed to solve the optimization problem iteratively till it converges.
- Simulation results show that the proposed algorithm outperforms the greedy algorithm by about 15.7% in terms of the network uplink sum rate. Moreover, the proposed algorithm can improve the system capacity to double the LTE-A scheme.

The remainder of this chapter is organized as follows. The aerial multi-cell network system model is presented in Section 3.2. In section 3.3, we formulate and jointly solve the optimization problem of resource allocation and power control. In Section 3.4, we analyze the computational complexity of the proposed algorithm. Simulation results are presented and analyzed in Section 3.5. Finally, we provide our concluding remarks in Section 3.6.

3.2 System Model

In this section, we present the system model of the considered problem.

3.2.1 Scenario Description

Consider a standalone aerial multi-cell network as shown in Fig.4.1, which is composed of M UAV-BSs, denoted by the set $\mathcal{M}$, N UAV-UEs, and a number of High Altitude Platform (HAP) UAVs which provide the wireless backhaul connectivity for the UAV-BSs. In this system, each UAV-BS $j \in \mathcal{M}$ serves a set of $\mathcal{N}_j$ UAV-UEs in the uplink transmission. Therefore, the set of the total number of UAV-UEs are $\mathcal{N} = \bigcup_{j \in \mathcal{M}} \mathcal{N}_j$. We also consider a single cell cellular network that consists of a BS located at $(0, 0, H_{BS})$ and a number of ground cellular users (CUs). In addition, we assume that there are W non-overlapping WiFi Access Points (WAPs).

We assume that an orthogonal set of finite licensed subchannels C_j^L with uniform bandwidth B_L has been allocated to UAV-BS j. Hence, UAV-BS $j \in \mathcal{M}$ assigns enough resources from the licensed band for each UAV-UE $i \in \mathcal{N}_j$ to retain a predefined uplink data rate of $R_{i,j}^{Licensed}$. For reliable control signal transmission from UAV-UE to UAV-BS, each UAV-UE is only allowed to access one licensed subchannel, and each licensed subchannel is assigned to at most one UAV-UE at each UAV-BS. In addition, the UAV-BSs and UAV-UEs can reinforce the uplink data rate through operating in the unlicensed radio spectrum in order to support a minimum transmission data rate of $QoS_{i,j}, \forall i \in \mathcal{N}, \forall j \in \mathcal{M}$. The bandwidth B_c of the unlicensed channel c is divided by the UAV-cellular system into a set of finite subchannels C^U with uniform bandwidth B_U for efficient resource management. To obtain the highest spectrum efficiency, a frequency reuse factor equal to one in the unlicensed spectrum has been considered. In other words, We assume each UAV-BS $j \in \mathcal{M}$ can use all the unlicensed band to serve its UAV-UEs in the uplink transmission. Thus, each UAV-BS is affected by interference from $M - 1$ UAV-BSs and one WAP, whereas one WAP experiences interference from M UAV-BSs.

As in [72], a 3D space can be filled completely using an arrangement of truncated octahedron structure cells where at the center of each cell, a UAV-BS has been placed. Each structure consists

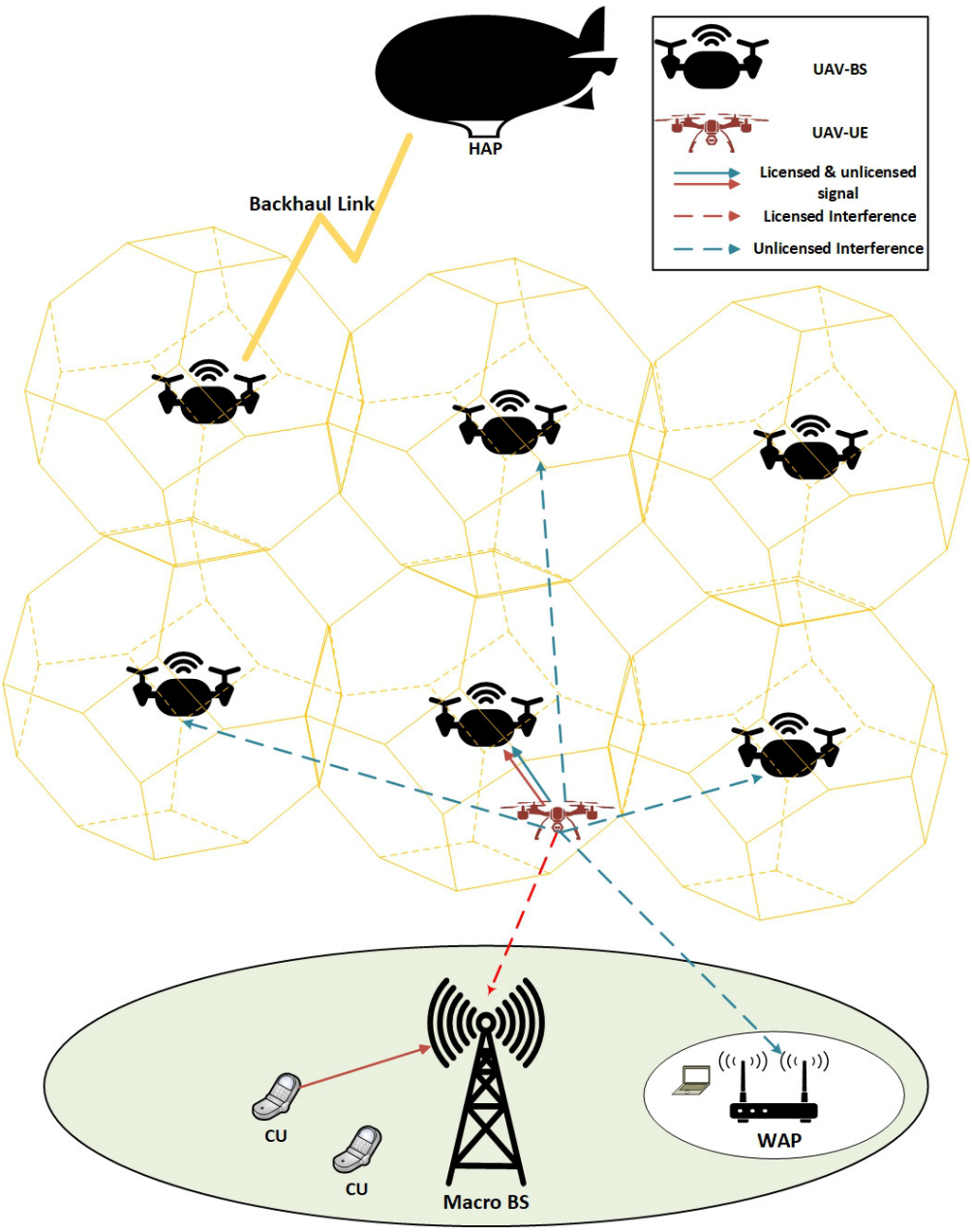

Figure 3.1: A Standalone Aerial Multi-cell Network System Model.

of 14 faces with 6 square and 8 regular hexagonal shapes. The 3D locations of these UAV-BSs can be determined using :

$$L_{a,b,c} = [\, x_0, y_0, z_o] \, + \sqrt{2}R[\, a + b - c, -a + b + c, a - b + c] \,, \tag{3.1}$$

where $[\, x_0, y_0, z_o]$ is the Cartesian coordinates of a given reference location (e.g. the center of the 3D space), a, b, c are integers chosen from set $\{\cdots, -2, -1, 0, 1, 2, \cdots\}$, and R is the edge length of the considered truncated octahedron. After the locations of UAV-BSs have been obtained, these locations will not change within a time slot. In contrast, the UAV-UE can move freely with a speed of $[0, \upsilon_{max}]$ in any time slot [1]. The time slot is chosen to be sufficiently small such that the UAV-UEs' locations can be assumed to be approximately constant within each time slot duration even at maximum UAV-UE's speed as commonly done in the literature [43, 45].

The location of UAV-UE $i \in \mathcal{N}$ in time slot t is denoted as $(\, x_i^t, y_i^t, z_i^t)$, and the UAV-BS $j \in \mathcal{M}$ is located at $(\, x_j, y_j, z_j)$ which have been obtained from equation (3.1). Therefore, in time slot t, the distance between UAV-UE i and UAV-BS j is calculated as

$$d_{i,j}^t = \sqrt{(\, x_i^t - x_j)^{\,2} + (\, y_i^t - y_j)^{\,2} + (\, z_i^t - z_j)^{\,2}}, \tag{3.2}$$

3.2.2 Data Transmission Model

Data Rate in the Licensed Spectrum

When a UAV-BS $j \in \mathcal{M}$ assigns to UAV-UE $i \in \mathcal{N}_j$ a subchannel $k \in C_j^L$, the achieved rate of that user in time slot t is

$$R_{i,j}^{Licensed} = B_L \log_2(\, 1 + \frac{\psi_{i,j}^{k,t} P_{i,j}^{k,t} g_{i,j}^{k,t}}{\sigma^2}) \,. \tag{3.3}$$

where σ^2 is the noise power, $g_{i,j}^{k,t}$ is the free-space channel gain between UAV-UE i and UAV-BS j over subchannel k, and $P_{i,j}^{k,t}$ is the transmit power from UAV-UE i to UAV-BS j over licensed subchannel k. The binary variable $\psi_{i,j}^{k,t} = \{0, 1\}$ represents the subchannel allocation of the

[1] We add the superscript t to some notations to distinguish the fixed parameters from the time-varying parameters.

licensed subchannel k between UAV-UE i and UAV-BS j. We define the licensed subchannels allocation matrix as $\Psi = \left[\psi_{i,j}^{k,t}\right]_{N\times M\times C_j^L}$, where $\psi_{i,j}^{k,t} = 1$ means that subchannel $k \in C_j^L$ is assigned to UAV-UE $i \in \mathcal{N}_j$, and $\psi_{i,j}^{k,t} = 0$ otherwise. The ground CU uplink interference on UAV-BS j is negligible due to the high elevation angle, fading, and shadowing.

Data Rate in the Unlicensed Spectrum

When a UAV-BS $j \in \mathcal{M}$ assigns to UAV-UE $i \in \mathcal{N}_j$ a subchannel $q \in C^U$ from the unlicensed spectrum, the achieved rate of that user in time slot t is

$$R_{i,j}^{Unlicensed,q} = B_U \log_2(1 + \frac{\phi_{i,j}^{q,t} P_{i,j}^{q,t} g_{i,j}^{q,t}}{I_{UAV,j}^{q,t} + \sigma^2}), \tag{3.4}$$

where the binary variable $\phi_{i,j}^{q,t} = \{0, 1\}$ represents the subchannel allocation between UAV-UE i and UAV-BS j over subchannel q, such that $\phi_{i,j}^{q,t} = 1$ means that the subchannel q is assigned to UAV-UE i, and $\psi_{i,j}^{q,t} = 0$ otherwise. $P_{i,j}^{q,t}$ is the transmit power from UAV-UE i to UAV-BS j over unlicensed subchannel q. We define $\Phi = \left[\phi_{i,j}^{q,t}\right]_{N\times M\times C^U}$ and $P_U = \left[P_{i,j}^{q,t}\right]_{N\times M\times C^U}$ as unlicensed subchannels and transmission power allocation matrices, respectively. $I_{UAV,j}^{q,t}$ is the inter-cell interference at UAV-BS j over subchannel q during time slot t, which can be expressed as

$$I_{UAV,j}^{q,t} = \sum_{y\in M\setminus y\neq j} \sum_{x\in\mathcal{N}_y} \phi_{x,y}^{q,t} P_{x,y}^{q,t} g_{x,j}^{q,t}. \tag{3.5}$$

where $\sum_{y\in M\setminus y\neq j} \sum_{x\in\mathcal{N}_y}$ means the sum of the interference from all UAV-UEs that use subchannel q in all the interfering UAV-BSs. The WAP co-channel interference on UAV-BS j is negligible due to the high elevation angle, the wall penetration loss, and the low transmit power of WAP.

If UAV-BS j assigns more than one subchannel to UAV-UE i, then the total achieved rate of that user from the unlicensed band in time slot t is

$$R_{i,j}^{Unlicensed} = \sum_{q\in C^U} \phi_{i,j}^{q,t} R_{i,j}^{Unlicensed,q}. \tag{3.6}$$

UAV-UE QoS

A minimum data rate ($QoS_{i,j}$) is required by each UAV-UE for its applications. When $R_{i,j}^{Licensed} \leq QoS_{i,j}$, each UAV-BS j allows its UAV-UE i to access resources from the unlicensed spectrum to enhance UAV-UE's data rate. Thus, The QoS requirement for UAV-UE i is achieved through the following constraint:

$$R_{i,j} = R_{i,j}^{Licensed} + R_{i,j}^{Unlicensed} \geq QoS_{i,j}. \tag{3.7}$$

3.2.3 Interference Threshold Protection

For Cellular System

We use the Air-to-Ground (A2G) pathloss model between LAP UAV-UE and cellular BS which has been proposed in [84, 85]. In time slot t, the average A2G pathloss from UAV-UE i and BS in dB can be expressed as

$$PL_{i,BS}^{avg,t} = 20\log(\frac{4\pi f_c^L}{c}) + 20\log(d_{i,BS}^t) + P_{LoS,i}^t \eta_{LoS} + (1 - P_{LoS,i}^t)\eta_{NLoS}, \tag{3.8}$$

where f_c^L is the carrier frequency of licensed band, c is the speed of light, $d_{i,BS}^t$ is the distance between UAV-UE i and the cellular BS, η_{LoS} and η_{NLoS} are the average additional losses for LoS and NLoS links, respectively, which depend on environment, and $P_{LoS,i}^t$ is the LoS probability of A2G link which can be denoted as

$$P_{LoS,i}^t = \frac{1}{1 + a\exp(-b(\theta_i^t - a))}, \tag{3.9}$$

where a and b are environmental dependent constants, and $\theta_i^t = sin^{-1}((z_i^t - H_{BS})/d_{i,BS}^t)$ is the elevation angle.

In our system model, reusing the same licensed spectrum leads to mutual interference between the UAV-cellular network and the terrestrial network. Therefore, in order to ensure the coexistence

between the two systems, it is assumed that the total interference introduced from UAV-UEs to the cellular BS on subchannel $k \in C_j^L$ does not exceed a given threshold $I_{Licensed}^{th,k}$, i.e.,

$$\sum_{i \in \mathcal{N}_j} \psi_{i,j}^{k,t} \frac{P_{i,j}^{k,t}}{10^{PL_{i,BS}^{avg,t}/10}} \leq I_{Licensed}^{th,k}, \forall j \in \mathcal{M}, \forall k \in C_j^L. \tag{3.10}$$

For WiFi System

The A2G pathloss model [84] is also considered, where the average pathloss from UAV-UE i to WAP in time slot t can be expressed as

$$PL_{i,WAP}^{avg,t} = 20\log(\frac{4\pi f_c^U}{c}) + 20\log(d_{i,WAP}^t) + P_{LoS,i}^t \eta_{LoS} + (1 - P_{LoS,i}^t)\eta_{NLoS} + \rho, \tag{3.11}$$

where f_c^U is the carrier frequency of unlicensed band, $d_{i,WAP}^t$ is the distance between UAV-UE i and the WAP, ρ is the wall penetration loss, and the other parameters can be derived from equations (3.8)-(3.9).

The non-orthogonality between LTE and WAP respective transmitted signals leads to mutual interference due to the coexistence on the same unlicensed spectrum. Based on [86] and [87], the interference at WAP introduced by the transmission of UAV-UE $i \in \mathcal{N}_j$ on subchannel q can be determined as

$$I_{i,WAP}^q = \int_{d_q - B_c/2}^{d_q + B_c/2} \frac{P_{i,j}^{q,t}}{10^{PL_{i,WAP}^{avg,t}/10}} T_s \left(\frac{sin\ \pi f T_s}{\pi f T_s}\right)^2 df, \tag{3.12}$$

where d_q represents the spectral distance between subchannel q and WAP occupied band B_c, and T_s is the OFDM symbol duration.

We assume that the UAV-cellular network can utilize the unlicensed band c as long as the total interference initiated from all UAV-UEs to the WAP does not exceed $I_{Unlicensed}^{th,B_c}$

$$\sum_{j \in \mathcal{M}} \sum_{i \in \mathcal{N}_j} \sum_{q \in C^U} \phi_{i,j}^{q,t} P_{i,j}^{q,t} O_{i,j}^{q,t} \leq I_{Unlicensed}^{th,B_c}, \tag{3.13}$$

where

$$O_{i,j}^{q,t} = \frac{1}{10^{PL_{i,WAP}^{avg,t}/10}} \int_{d_q - B_c/2}^{d_q + B_c/2} T_s \left(\frac{sin\ \pi f T_s}{\pi f T_s}\right)^2 df. \tag{3.14}$$

3.3 Joint Subchannel Allocation and Power Control

In this section, first, we formulate the joint subchannel allocation and power control optimization problem. Then, we propose an iterative solution for the problem after decomposing it into three sub-problems and solve each of them with the appropriate approach.

3.3.1 Problem Formulation

Since the UAV-cellular network is uplink dominant, the uplink sum-rate of this network is one key metric to evaluate the performance of this network. We aim to maximize the uplink sum-rate of the UAV-UEs for the multi-cell UAV-cellular network by jointly optimizing the subchannel allocation and power control variables for each time slot in both licensed and unlicensed spectrum

$(\Psi, P_L, \Phi, and\ P_U)$. We formulate the optimization problem as follows:

$$\max_{(\Psi, P_L, \Phi, P_U)} \sum_{j \in \mathcal{M}} \sum_{i \in \mathcal{N}_j} R_{i,j},$$

$$\begin{aligned}
&s.t.,\\
&C_1 : R_{i,j} \geq QoS_{i,j}, \forall j \in \mathcal{M}, \forall i \in \mathcal{N}_j\\
&C_2 : \sum_{i \in \mathcal{N}_j} \psi_{i,j}^{k,t} \frac{P_{i,j}^{k,t}}{10^{PL_{i,BS}^{avg,t}/10}} \leq I_{Licensed}^{th,k}, \forall j \in \mathcal{M}, \forall k \in C_j^L\\
&C_3 : \sum_{j \in \mathcal{M}} \sum_{i \in \mathcal{N}_j} \sum_{q \in C^U} \phi_{i,j}^{q,t} P_{i,j}^{q,t} O_{i,j}^{q,t} \leq I_{Unlicensed}^{th,B_c}\\
&C_4 : \sum_{i \in \mathcal{N}_j} \sum_{k \in C_j^L} \psi_{i,j}^{k,t} \leq C_j^L, \forall j \in \mathcal{M}\\
&C_5 : \sum_{i \in \mathcal{N}_j} \psi_{i,j}^{k,t} \leq 1, \forall j \in \mathcal{M}, \forall k \in C_j^L\\
&C_6 : \sum_{k \in C_j^L} \psi_{i,j}^{k,t} \leq 1, \forall j \in \mathcal{M}, \forall i \in \mathcal{N}_j\\
&C_7 : \sum_{i \in \mathcal{N}_j} \sum_{q \in C^U} \phi_{i,j}^{q,t} \leq C^U, \forall j \in \mathcal{M}\\
&C_8 : \sum_{i \in \mathcal{N}_j} \phi_{i,j}^{q,t} \leq 1, \forall j \in \mathcal{M}, \forall q \in C^U\\
&C_9 : \psi_{i,j}^{k,t} = \{0, 1\}, \forall j \in \mathcal{M}, \forall i \in \mathcal{N}_j, \forall k \in C_j^L\\
&C_{10} : \phi_{i,j}^{q,t} = \{0, 1\}, \forall j \in \mathcal{M}, \forall i \in \mathcal{N}_j, \forall q \in C^U\\
&C_{11} : P_{i,j}^{k,t} \leq P_{max}^{k}, \forall j \in \mathcal{M}, \forall i \in \mathcal{N}_j, \forall k \in C_j^L\\
&C_{12} : P_{i,j}^{q,t} \leq P_{max}^{q}, \forall j \in \mathcal{M}, \forall i \in \mathcal{N}_j, \forall q \in C^U
\end{aligned} \tag{3.15}$$

The minimum QoS rate requirement for UAV-UEs is achieved through constraint (C_1). The coexistence with both terrestrial cellular and WiFi systems are secured through constraints (C_2) and (C_3), respectively. Constraints (C_5) and (C_8) guarantee that each licensed and unlicensed subchannel are allocated to at most one UAV-UE per UAV-BS, while constraint (C_6) ensures that each UAV-UE can be assigned to at most one licensed subchannel. The limitation of total

licensed/unlicensed subchannels per UAV-BS is represented by constraints (C_4)/(C_7), respectively. The transmit power of each UAV-UE on both licensed and unlicensed subchannels must be within the permitted range of the total transmitted power on each subchannel as shown in constraints (C_{11}) and (C_{12}), respectively.

The optimization problem in (3.15) is a non-convex Mixed Integer Non-Linear Programming (MINLP) optimization problem which is NP-hard to solve in general. The non-convexity is imputed for two reasons. The first one is the combinatorial nature of licensed and unlicensed subchannel allocation binary variables (Ψ, Φ). The second one is due to the ICI equation in both objective function and constraint (C_1). In the following theorem, we prove that the optimization problem (3.15) is NP-hard.

Theorem 1. Problem (3.15) is NP-hard.

Proof. We prove that optimization problem (3.15) is NP-hard even when we do not consider the licensed band. We construct a simple case of problem (3.15) where there are only two UAV-BSs in which each unlicensed subchannel can serve one UAV-UE from each cell simultaneously. let $\mathcal{N}_1$, $\mathcal{N}_2$, and $\mathcal{C}$ be three disjoint sets of UAV-UEs per cell one, UAV-UEs per cell two, and unlicensed subchannels, respectively, with $|\mathcal{N}_1| = |\mathcal{N}_2| = |\mathcal{C}|$. Set $\mathcal{N}_1$, $\mathcal{N}_2$, and $\mathcal{C}$ satisfy $\mathcal{N}_1 \cap \mathcal{N}_2 = \emptyset$, $\mathcal{N}_1 \cap \mathcal{C} = \emptyset$, and $\mathcal{N}_2 \cap \mathcal{C} = \emptyset$. Let $\mathcal{P}$ be a collection of ordered triples $\mathcal{P} \subseteq \mathcal{N}_1 \times \mathcal{N}_2 \times \mathcal{C}$, where each element in $\mathcal{P}$ consists a UAV-UE from cell 1, a UAV-UE from cell 2, and an unlicensed subchannel. There exists $\overline{P} \subseteq \mathcal{P}$ that for any two distinct triples $(\mathcal{N}_{1,i}, \mathcal{N}_{2,i}, \mathcal{C}_i) \in \overline{P}$ and $(\mathcal{N}_{1,j}, \mathcal{N}_{2,j}, \mathcal{C}_j) \in \overline{P}$, we have $i \neq j$. Therefore, $\overline{P}$ is a three-dimension matching (3-DM) which has been proved to be NP-complete [88]. Moreover, optimization problem (3.15) is $(\mathcal{M}+1)$-dimension matching which is more complicated than the 3-DM problem. Therefore, the problem in (3.15) is NP-hard [43]. ∎

3.3.2 Sub-Optimal Problem Decomposition

Since problem (3.15) is NP-hard, to solve this problem efficiently, we decompose it into three sub-problems, i.e. licensed subchannel allocation and power control, unlicensed subchannel allocation, and power control over unlicensed band sub-problems. First, the licensed resource

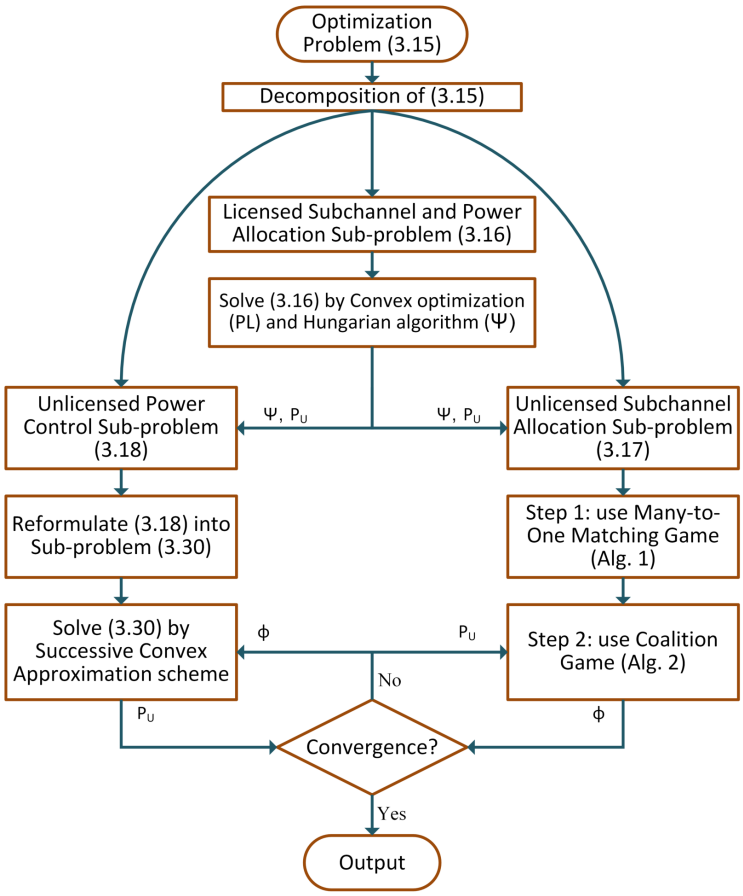

Figure 3.2: Solution process of the problem (3.15)

allocation and power control sub-problem can be expressed as follow:

$$\begin{aligned} &\max_{(\Psi, P_L)} \sum_{j \in \mathcal{M}} \sum_{i \in \mathcal{N}_j} R_{i,j}^{Licensed} \\ &s.t. \quad C_2, C_4, C_5, C_6, C_9, C_{11}. \end{aligned} \tag{3.16}$$

Given the subchannel Ψ and power P_L allocation matrices in the licensed band (achieved data rate from the licensed spectrum) obtained from (3.16), the subchannel allocation sub-problem

and the power control sub-problem in the unlicensed band can be represented as follow:

$$\begin{aligned} &\max_{\Phi} \sum_{j\in\mathcal{M}} \sum_{i\in\mathcal{N}_j} R_{i,j}^{Unlicensed} \\ &s.t. \quad C_1, C_3, C_7, C_8, C_{10}. \end{aligned} \tag{3.17}$$

and

$$\begin{aligned} &\max_{P_U} \sum_{j\in\mathcal{M}} \sum_{i\in\mathcal{N}_j} R_{i,j}^{Unlicensed} \\ &s.t. \quad C_1, C_3, C_{12}. \end{aligned} \tag{3.18}$$

Sub-problems (3.17) and (3.18) have the same objective function with different constraints and variables. The solution of sub-problem (3.17) can be used to solve the sub-problem (3.18), and vice versa repeatedly until converge. We use a matching game with externalities and a coalition formation game to solve sub-problem (3.17) and successive convex approximation (SCA) method for sub-problem (3.18). This solution approach is shown in Fig. 3.2. The details of these approaches are represented in the following subsections.

3.3.3 Subchannel Allocation and Power Control in the Licensed Band Sub-problem

In this subsection, we give a detailed description of the sub-problem (3.16) solution. Since there is no ICI among UAV-BSs in the licensed spectrum, we can decompose sub-problem (3.16) into M distributed sub-problems in which each one is solved based on the solution below at each UAV-BS independently. Each sub-problem is a combinatorial optimization problem concerning Ψ for a fixed P_L. Additionally, it is a concave function with respect to $P_{i,j}^{k,t}$ for a given Ψ. The optimum subchannel allocation and power control in the licensed band can be found by solving two sub-sub-problems iteratively as follows.

1. *power control phase:* For a given Ψ, each sub-problem is concave with respect to P_L. Therefore, the optimal power allocation can be determined based on the KKT conditions [89].

2. *subchannel allocation phase:* For a given P_L, the sub-problem is combinatorial in the variable Ψ, where the Hungarian method [90] is used to obtain the optimal subchannel allocations.

3.3.4 Unlicensed Subchannel Allocation Sub-problem

In this subsection, we propose a solution for sub-problem (3.17) by using a many-to-one matching game with externalities and a coalition formation game.

Matching Game

The unlicensed subchannel allocation sub-problem shown in (3.17) is still NP-hard and cannot be efficiently solved. Therefore, we propose a matching game as introduced in Alg. 1 to solve this sub-problem. The intuition of this matching game is to allocate the unlicensed subchannels in such a way that maximize the uplink sum-rate of the UAV-cellular network while satisfying the QoS requirements of UAV-UE. Thus, lines 3-5 are responsible for calculating the QoS gap for UAV-UEs connected to UAV-BS j between the achieved data rate from the licensed subchannel and the QoS requirement. Line 6 sorts UAV-UEs as the descending order based on their channel gain, and line 7 reorder the elements of the QoS gap vector according to the sorted UAV-UE list. After that, in lines 8-11, ICI is calculated on each unlicensed subchannel and then sort subchannels in ascending order based on the ICI calculated. Finally, lines 12-23 are responsible for allocating the unlicensed subchannels with the least ICI values based on the list obtained from line 11 to the UAV-UE list obtained from line 6 while satisfying the QoS gap of each UAV-UE according to the list given from line 7.

Due to the ICI, a subchannel selection by a UAV-UE is affected by the other UAV-UEs choices for the same subchannel. This is known as the externalities, where traditional preference orders cannot solve it. Therefore, we formulated a coalition matching game as follows to cope with these externalities.

Algorithm 1 Unlicensed Subchannel Allocation for UAV-BS j

Input : QoS, $R^{Licensed}$, P_U, N_j, $\Phi_j^{initial}$
Output : Φ_j
for each $i \in \mathcal{N}_j$ **do**
    Calculate QoS gap by $QG_{i,j} = [QoS_{i,j} - R_{i,j}^{Licensed}]^+$
end for
Sort UAV-UEs from $\mathcal{N}_j$ according to channel gain on descending order
Reorder the elements of QG_j according to $\mathcal{N}_j$
for each subchannel $q \in C^U$ **do**
    Calculate the ICI on each subchannel using eq. (3.5)
end for
Sort subchannels from C^U according to ICI on each subchannel on ascending order
Set $q = 1$
for each $i \in \mathcal{N}_j$ **do**
    Set $RqBW = QG_{i,j}$
    if $RqBW \neq 0$ **then**
        while $RqBW > 0$ **do**
            Set $\phi_{i,j}^q = 1$
            Calculate $R_{i,j}^{Unlicensed,q}$ using eq. (3.6)
            Set $RqBW = RqBW - R_{i,j}^{Unlicensed,q}$
            Set $q = q + 1$
        end while
    end if
end for

Coalition Game

The unlicensed subchannel allocation problem is modeled as a coalitional game to acquire the network utility in terms of the network uplink sum-rate. For each binary parameter $\phi_{i,j}^q = 1$, there is a formed access link between UAV-BS $j \in \mathcal{M}$ and UAV-UE $i \in \mathcal{N}$ on unlicensed subchannel

$q \in C^U$. Therefore, for each unlicensed subchannel $q \in C^U$, there is a maximum M simultaneous access link use this channel through the network since we considered the frequency reuse factor is equal to one.

For the unlicensed subchannel allocation, the game players are the links. We have $\mathcal{L}$ links where each link defined by $j \in \mathcal{M}, i \in \mathcal{N}, q \in C^U$. S_q is the coalition of the links occupying the same subchannel $q \in C^U$. Since there are C^U unlicensed subchannels in the network, the links can be divided into C^U coalitions at most with the following restrictions:

$$\begin{aligned} &\mathcal{L} = S_1 \cup S_2 \cup ... \cup S_{C^U}, \\ &S_q \cap S_k = \emptyset, \forall q, k \in C^U and\ q \neq k. \end{aligned} \tag{3.19}$$

The coalition utility function $U(S_q)$ is defined as the sum rate of all links in coalition S_q, which given by

$$U(S_q) = \sum_{j \in \mathcal{M}} \sum_{i \in \mathcal{N}_j} R_{i,j}^{Unlicensed,q}. \tag{3.20}$$

Since the utility is proportional to the network sum-rate, links tend to form coalitions of different subchannels to maximize the coalitional game utility. Therefore, the game formation definitions are defined based on the content above as follows:

- *Players*: The set of access links is denoted as $\mathcal{L}$.
- *Coalition*: The set of players $\mathcal{L}$ is divided into $|C^U|$ coalitions, according to restrictions given in (4.17).
- *Utility*: $U(S_q)$ is the uplink sum-rate value for each coalition $U(S_q) \subseteq \mathcal{L}$, which is a transferable utility for members in S_q.
- *Strategy*: Players decide to enter or depart a coalition according to the results of the utility comparison between original and new coalition.

Definition 1: (The coalition partition) A coalitional partition is defined as the set $\Theta = \{S_1, ..., S_p\}$ $(1 \leq p \leq |C^U|)$, which partitions the players set $\mathcal{L}$, i.e., $\forall p, S_c \subseteq \mathcal{L}$ are disjoint coalitions such that $\bigcup_{c=1}^{p} S_c = \mathcal{L}$.

In order to maximize the network throughput, preference relation for players to decide whether to join or leave a coalition should be well defined. Instead of initial partition $\Theta = \{S_1, ..., S_p\}$, a group of players prefers to adopt the utilitarian order to organize themselves into a collection of coalitions $\tilde{\Theta} = \{\tilde{S_1}, ..., \tilde{S_p}\}$, which is proposed in [91], [92]. Then the utility relationship between two different partitions can be expressed as

$$\sum_{i=1}^{\tilde{p}} U(\tilde{S}_i) > \sum_{i=1}^{p} U(S_i) \tag{3.21}$$

Definition 2: (Total utility of coalitions) For a partition $\Theta = \{S_1, ..., S_p\}(1 \leq p \leq |C^U|)$, of the set $\mathcal{L}$, the total utility can be calculated as:

$$U(\Theta) = \sum_{i=1}^{p} U(S_i). \tag{3.22}$$

If $U(\tilde{\Theta}) > U(\Theta)$, the partition $\tilde{\Theta}$ has a better performance on total utility. Every coalition in $\tilde{\Theta}$ is the coalition of links which share the same sub-channel. The total utility here is total uplink sum throughput of the network over unlicensed spectrum.

Definition 3: (Preference relation $\succ_l$) For any player l, a preference relation $\succ_l$ is defined as a complete, reflexive, and transitive binary relation over the set of all coalitions that player l may form.

Switch rule 1: for any players $l, l' \in \mathcal{L}, l \in S_p, l' \in S_q, S_p \neq S_q, i' \neq i, j' = j$, players l and l' strictly prefer to switch their coalition with each other ($S_q \succ_l S_p$ and $S_p \succ_{l'} S_q$) when preference relation satisfies

$$U(\{\{S_p \setminus l\} \cup l'\}) + U(\{\{S_q \setminus l'\} \cup l\}) > U(S_p) + U(S_q), S_p, S_q \subseteq \mathcal{L}, S_p \neq S_q, \tag{3.23}$$

then the partition Θ is modified into a new partition as follows

$$\Theta = (\Theta \setminus \{S_p, S_q\}) \cup \{\{S_p \setminus l\} \cup l'\} \cup \{\{S_q \setminus l'\} \cup l\}. \tag{3.24}$$

Switch rule 2: for any players $l \in \mathcal{L}, l \in S_p$, player l strictly prefers to switch its coalition from S_p to coalition S_q ($S_q \succ_l S_p$), $S_q \neq S_p, \forall l' \in S_q, \nexists i' = i, \nexists j' = j$, where preference relation can be defined as follows

$$U(\{S_p \setminus l\}) + U(\{S_q \cup l\}) > U(S_p) + U(S_q), S_p, S_q \subseteq \mathcal{L}, S_p \neq S_q. \tag{3.25}$$

then the partition Θ is modified into a new partition as follows

$$\Theta = (\ \Theta \setminus \{S_p, S_q\})\ \cup \{S_p \setminus l\} \cup \{S_q \cup l\}. \tag{3.26}$$

Based on these definitions and switching rules, the coalition formation game pseudo code is shown in Algorithm 2. As shown in line 3-23, the coalition formation algorithm performs the judgment to determine whether to perform a switch operation based on definition (3). In line 10-17, when there is a link l' inside the selected coalition (S_q) for the same UAV-BS but different UAV-UE, the first coalition switch operation judgment shown in switch rule 1 is examined. If the switch operation satisfies switch rule 1, the switch operation is performed, and the algorithm ends this round of loops and repeats the above operations. If the first switch operation judgment does not meet the switch rule 1, it selects a different coalition S_q and continues examining switch rules. Similarly, in lines 18-22, if there is no any link inside coalition S_q for the same UAV-BS, it examines switch rule 2, and if switch rule 2 is satisfied, it performs the switch operation.

Theorem 2. The final partition Θ_{final} in coalition formation game algorithm is Nash-stable.

Proof. We prove that the final partition Θ_{final} in the coalition game algorithm is Nash-stable. If the final partition Θ_{final} is not Nash-stable. Thus, there must exist:

- Two players $l \in S_p, l' \in S_q, S_p \neq S_q (S_p, S_q \subseteq \Theta_{final})$ such that $S_q \succ_l S_p$ and $S_p \succ_{l'} S_q$. or
- A player $l \in S_p (\ S_p \subseteq \Theta_{final})$ and another coalition $S_q \in \Theta_{final}$ such that $S_q \succ_l S_p$.

Based on our proposed algorithm, for any of the two cases, player l will perform a switch operation with the other player l' or to the available coalition forming a new partition, which conflicts with the fact that Θ_{final} is the final partition. Therefore, the hypothesis that the final partition Θ_{final} is Nash-stable has been proved. ■

Algorithm 2 Coalition Formation Algorithm for Unlicensed Subchannel Allocation

1: Input : The partition Θ from the previous algorithm
2: Output : Final Nash-stable partition Θ_{final}
3: **while** Nash-stable partition is not achieved **do**
4: Randomly choose a link $l \in \mathcal{L}$, and denote its current coalition as $S_p \in \Theta$;
5: Randomly choose another coalition $S_q \in \Theta,\ S_q \neq S_p$;
6: **if** S_q has a link $l' \in \mathcal{L}, i' = i, j' = j$ **then**
7: Set $S_{\overline{q}} = S_q$;
8: Randomly choose another coalition $S_q \in \Theta$, $S_q \neq S_{\overline{q}},\ S_q \neq S_p$;
9: Go back to line 6;
10: **else if** S_q has a link $l' \in \mathcal{L}, i' \neq i, j' = j$ **then**
11: **if** rule satisfies ($S_q \succ_l S_p$ and $S_p \succ_{l'} S_q$) **then**
12: $\Theta = (\ \Theta \setminus \{S_p, S_q\}) \cup \big\{\{S_p \setminus l\} \cup l'\big\} \cup \big\{\{S_q \setminus l'\} \cup l\big\}$;
13: **else**
14: Set $S_{\overline{q}} = S_q$;
15: Randomly choose another coalition $S_q \in \Theta$, $S_q \neq S_{\overline{q}},\ S_q \neq S_p$;
16: Go back to line 6;
17: **end if**
18: **else**
19: **if** rule satisfies ($S_q \succ_l S_p$) **then**
20: $\Theta = (\ \Theta \setminus \{S_p, S_q\}) \cup \{S_p \setminus l\} \cup \{S_q \cup l\}$;
21: **end if**
22: **end if**
23: **end while**

3.3.5 Unlicensed Power Control Sub-problem

The power control sub-problem (3.18) in the unlicensed spectrum is still a non-convex problem owing to the ICI coupling between cells. To solve this sub-problem, we use the successive convex approximation (SCA) approach. SCA method can obtain a solution that satisfies the KKT conditions of the original non-convex problem through approximating it by a series of convex approximations [93]. Thus, we solve the convex approximation problem starting from the initial point and then using the output solution as an initial point for the new convex problem till it converges to a solution that satisfies the KKT conditions of the original non-convex problem. The SCA algorithm is guaranteed to converge after multiple iterations [94].

We first introduce the auxiliary variable $P_{i,j}^{q,t} = e^{\overline{P_{i,j}^{q,t}}}$. Therefore, the sub-problem (3.18) can be reduced to the following:

$$\begin{aligned}
&\max_{\overline{P_U}} \sum_{j\in\mathcal{M}} \sum_{i\in\mathcal{N}_j} \sum_{q\in C^U} \phi_{i,j}^{q,t} \log_2(1+\gamma_{i,j}^{q,t}),\\
&s.t.,\\
&\sum_{q\in C^U} \phi_{i,j}^{q,t} B_U \log_2(1+\gamma_{i,j}^{q,t}) \geq \left[QoS_{i,j} - R_{i,j}^{Licensed}\right]^+, \forall j, \forall i,\\
&\sum_{j\in\mathcal{M}} \sum_{i\in\mathcal{N}_j} \sum_{q\in C^U} \phi_{i,j}^{q,t} e^{\overline{P_{i,j}^{q,t}}} O_{i,j}^{q,t} \leq I_{Unlicensed}^{th,B_c},\\
&\overline{P_{i,j}^{q,t}} \leq \ln(P_{max}^{q}), \forall j \in \mathcal{M}, \forall i \in \mathcal{N}_j, \forall q \in C^U.
\end{aligned} \tag{3.27}$$

where the intermediate variable is given by the following:

$$\gamma_{i,j}^{q,t} = \frac{e^{\overline{P_{i,j}^{q,t}}} g_{i,j}^{q,t}}{\sum_{y\in M\setminus y\neq j} \sum_{x\in\mathcal{N}_y} \phi_{x,y}^{q,t} e^{\overline{P_{x,y}^{q,t}}} g_{x,j}^{q,t} + \sigma^2}. \tag{3.28}$$

The objective function and the first constraint are still non-convex. However, from [95] the lower bound of $f(x) = \log(1+x)$ is given by $\hat{f}(x) = \xi \log x + \upsilon$, where $\xi = \frac{x}{1+x}$ and

$\upsilon = \log(1+x) - \frac{x}{1+x}\log(x)$. This lower bound satisfies the following conditions:

$$\begin{aligned} \hat{f}(x) &< f(x), \\ \hat{f}(x_0) &= f(x_0), \\ \frac{\partial \hat{f}(x)}{x}\,|_{x_0} &= \frac{\partial f(x)}{x}\,|_{x_0}\ . \end{aligned} \tag{3.29}$$

Therefore, the sub-problem (3.27) is reformulated to the following:

$$\begin{aligned} &\max_{\overline{P_U}} \sum_{j\in\mathcal{M}}\sum_{i\in\mathcal{N}_j}\sum_{q\in C^U} \phi_{i,j}^{q,t}\left[\xi_{i,j}^{q,t}\log_2(\gamma_{i,j}^{q,t}) + \upsilon_{i,j}^{q,t}\right], \\ &s.t., \\ &\sum_{q\in C^U} \phi_{i,j}^{q,t}\left[\xi_{i,j}^{q,t}\log_2(\gamma_{i,j}^{q,t}) + \upsilon_{i,j}^{q,t}\right] \geq \left[QoS_{i,j} - R_{i,j}^{Licensed}\right]^+, \\ &\sum_{j\in\mathcal{M}}\sum_{i\in\mathcal{N}_j}\sum_{q\in C^U} \phi_{i,j}^{q,t} e^{\overline{P_{i,j}^{q,t}}} O_{i,j}^{q,t} \leq I_{Unlicensed}^{th,B_c}, \\ &\overline{P_{i,j}^{q,t}} \leq \ln(P_{max}^{q}), \forall j \in \mathcal{M}, \forall i \in \mathcal{N}_j, \forall q \in C^U. \end{aligned} \tag{3.30}$$

Theorem 3. *Problem (3.30) is a convex optimization problem.*

Proof. We examine the convexity of objective function and the first constraint. Since $\log_2(\gamma_{i,j}^{q,t})$ can be rearranged as follow:

$$\log_2(\gamma_{i,j}^{q,t}) = \frac{\ln(\gamma_{i,j}^{q,t})}{\ln(2)} = \frac{1}{\ln(2)}\Big(\ln(g_{i,j}^{q,t}) + \overline{P_{i,j}^{q,t}} - \ln(\sum_{y\in M\setminus y\neq j}\sum_{x\in\mathcal{N}_y} \phi_{x,y}^{q,t} e^{\overline{P_{x,y}^{q,t}}} g_{x,j}^{q,t} + \sigma^2)\Big) \tag{3.31}$$

From above equation, $\log_2(\gamma_{i,j}^{q,t})$ is concave because the log-sum-exponential function is convex [89]. The objective function and the first constraint are combination of concave functions. Therefore, the power control sub-problem in the unlicensed spectrum is a convex optimization problem. ■

3.3.6 Iterative Licensed/Unlicensed Subchannel Allocation and Power Control Algorithm

In this subsection, we introduce an iterative algorithm to solve the optimization problem (3.15), where the three sub-problems are solved iteratively until convergence. The process of the iterative algorithm is summarized in Algorithm 3.

Algorithm 3 Iterative Licensed/Unlicensed Subchannel Allocation and Power Control Algorithm

1: Initialization: $\mathcal{N}$, $\mathcal{M}$, C_j^L, C^U, QoS
2: **Step 1:** solve sub-problem (3.16) in order to get the global optimum of licensed subchannel Ψ and power P_L allocations, and calculate the global optimum $R^{Licensed}$.
3: **Step 2:** use algorithm 1 to allocate unlicensed subchannel to UAV-UEs based on the QoS requirement.
4: **repeat**
5: **Step 3: Coalition Game**: use algorithm 2 to reach Nash-stable unlicensed subchannel allocation.
6: **Step 4: Successive Convex Approximation**: solve sub-problem (3.30) until convergence.
7: **until** Convergence
8: Output: Ψ, P_L, Φ, P_U

Theorem 4. *Algorithm 3 is guaranteed to converge.*

Proof. Algorithm 3 first calculates the optimal global allocations of both subchannels and power in the licensed spectrum. After that, each iteration of Algorithm 3 comprises two sub-problems, the coalition game sub-problem and the SCA sub-problem. In Theorem 2, we argued that the coalition game would reach a Nash-stable partition. In addition, the SCA algorithm guarantees to converge to a local optimum solution that is very close to the global optimum [93]. Since the network uplink sum-rate is improved in each iteration and there is an upper bound for the uplink sum-rate, Algorithm 3 is guaranteed to converge in a limited number of iterations. ■

3.4 Computational Complexity Analysis

In the proposed algorithm, the sub-problem (3.16) is solved first to find the global optimum of power and subchannel in the licensed spectrum. An iterative method has been introduced in which the power assignment sub-problem is solved directly with convex problem solutions, and the subchannel allocation sub-problem is solved efficiently by the Hungarian algorithm. Since the computation of the sub-problem (3.16) is distributed to each UAV-BS, the computational complexity for step 1 of Algorithm 3 is $O(K_1 \times (\mathcal{N}_m C_m^L)^3)$ [90], where K_1 is a constant equivalent to the number of iteration which is very small due to the convexity and the linear programming nature of the power and subchannel allocation sub-problems, respectively.

For the subchannel allocation sub-problem in the unlicensed spectrum, Algorithm 1 (a many-to-one matching game) is used at each UAV-BS to provide UAV-UE with initial subchannel allocations. the complexity of this algorithm is $O(\mathcal{N}_m \cdot C^U)$ [96]. In Algorithm 2, a coalition game is used to solve the matching game's externalities due to the unlicensed spectrum reuse, where the selection of a subchannel in a cell affects the data rate of all the UAV-UEs in the other cells that use the same subchannel. According to the coalition game, the maximum number of links is $|\mathcal{M}| \cdot |C^U|$. By considering the worst-case scenario, each link is examined with $|C^U - 1|$ coalitions. Therefore, the complexity of Algorithm 2 is $O(\mathcal{M}(C^U)^2)$. The exhaustive search algorithm can also be used to obtain the optimal subchannel allocation in the unlicensed band. However, the computation complexity of the optimal algorithm is $O(\mathcal{N}_m^{|\mathcal{M}| \cdot |C^U|})$, which is significantly higher than that of the proposed algorithm.

Finally, the power allocation sub-problem in (3.30) is a convex optimization problem that CVX can efficiently solve. SCA is iteratively solved (3.30) by updating the points of interest up to convergence. The SCA algorithm will be run at most $O(\mathcal{N})$ times [93]. Therefore, the computational complexity for the proposed algorithm is $O(K_1 \times (\mathcal{N}_m C_m^L)^3 + (\mathcal{N}_m C^U) + K_2 \times (\mathcal{M}(C^U)^2 + \mathcal{N}))$, where K_2 is a constant for the number of times the coalition game and the SCA algorithm will run up to convergence which is finite.

Table 3.1: Parameters Values

Parameter	Description	Value
$\mathcal{M}$	Number of LAP UAV-BSs	9
R	Truncated octahedron edge length	400 m
H_{BS}	Height of ground cellular BS	50 m
C_j^L	Number of licensed subchannels	10
C^U	Number of unlicensed subchannels	50
QoS	UAV-UE minimum data rate	4 Mbps
f_c^L	Carrier frequency of licensed band	2 GHz
f_c^U	Carrier frequency of unlicensed band	5 GHz
P_{max}^k	Transmit power on licensed subch.	0.5 Watt
P_{max}^q	Transmit power on unlicensed subch.	0.5 Watt
B_c	Bandwidth of unlicensed channel c	20 MHz
B_L	Licensed subchannel bandwidth	180 KHz
B_U	Unlicensed subchannel bandwidth	180 KHz
σ^2	Noise variance	-114 dBm
η_{LoS}	A2G channel parameter	1 dB
η_{NloS}	A2G channel parameter	20 dB
a	A2G channel parameter	12
b	A2G channel parameter	0.135
ρ	Wall penetration loss	10 dB
$I_{Licensed}^{th,k}$	Interference threshold at cellular BS	-75 dBm
$I_{Unlicensed}^{th,B_c}$	Interference threshold at WAP	-75 dBm

3.5 Simulation Results

In the simulation, we consider a 3D space of size 2.5km $\times$ 2.5km $\times$ 2.5km, in which the locations of the UAV-UEs are uniformly distributed. The centre point of the 3D space is located 1.4km above the surface ground. The simulation parameters are listed in Table I. We compare our proposed algorithm with three other algorithms: greedy, random allocation, and LTE-A. We calculate the global optimum licensed subchannel and power allocation for the first two algorithms by solving sub-problem one. Then, for the greedy algorithm, we utilize Algorithm 1 in which the unlicensed subchannel allocation uses a greedy algorithm, that UAV-UE always selects subchannels in its preference list with the highest utility. For the random allocation algorithm, the unlicensed subchannel allocation is chosen randomly. The last one is the classical LTE-A scheme, where the UAV-BS serves the UAV-UEs in the licensed spectrum only.

Fig. 3.3 shows the total uplink sum-rate of the network achieved by different schemes as a function of the number of UAV-UEs per cell. We can note that the overall sum-rate increases as the number of UAV-UEs increases. Fig. 3.3 shows that when the number of UAV-UEs per cell (n) is between two and three, both the proposed and the greedy algorithms have the same performance, which is slightly better than the LTE-A scheme. The reason for that is, with the low value of n and the availability of the unlicensed spectrum, the two schemes can distribute the unlicensed subchannels among UAV-UEs while maintaining the value of the ICI approximating to zero. However, when the value of n increases from 4 to 10, the ICI turns to be significant; our proposed algorithm achieves nearly 15.7% and 8% improvement in the performance over the other schemes for the low and high level of interference environment, respectively. We also can see that as interference increases, the greedy and random allocation algorithms approximately give the same performance. Moreover, from Fig. 3.3, we can see that the LTE-A can serve only up to five UAV-UEs per cell, while our proposed algorithm can effectively increase the capacity of the network up to ten UAV-UEs per cell.

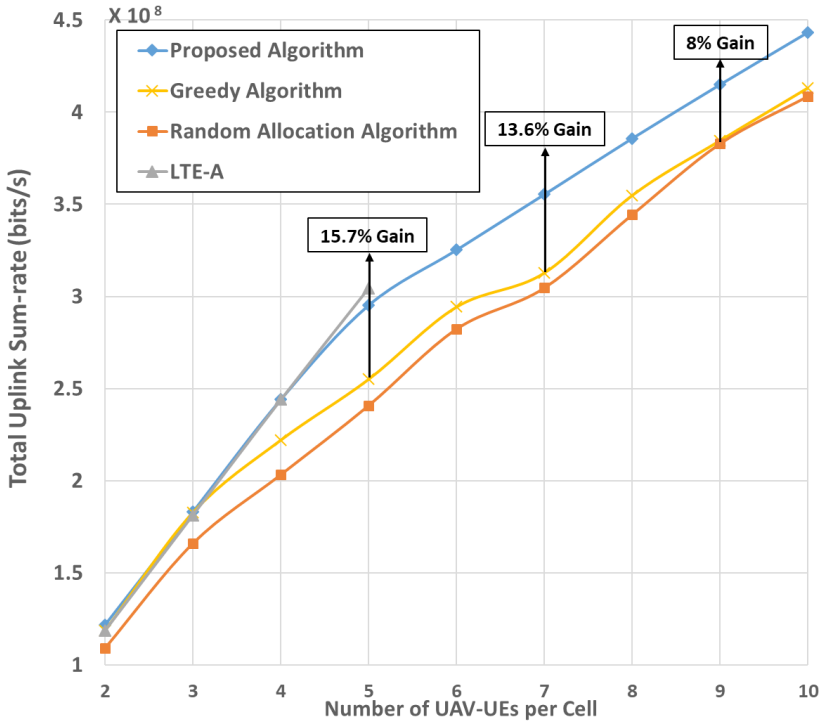

Figure 3.3: Total uplink sum-rate as the number of UAV-UEs per cell varies.

Fig. 3.4 shows the performance of average throughput per UAV-UE for different algorithms. When the value of n is low, the average throughput per UAV-UE for the proposed algorithm is slightly better due to sufficient unlicensed spectrum and ICI absence. Nevertheless, when the value of n equals 5, the LTE-A gives a better performance than the others. In other words, the average throughput achieved using the other schemes decreases as the number of UAV-UEs increases. The reason for that is because as the number of UAV-UEs increases, the ICI value also increases, causing a decrease in the achieved average throughput. However, our proposed algorithm achieves significantly higher performance than the other algorithms. Moreover, the proposed algorithm can double the cell capacity compared to LTE-A while guaranteeing the QoS requirements of the UAV-UEs.

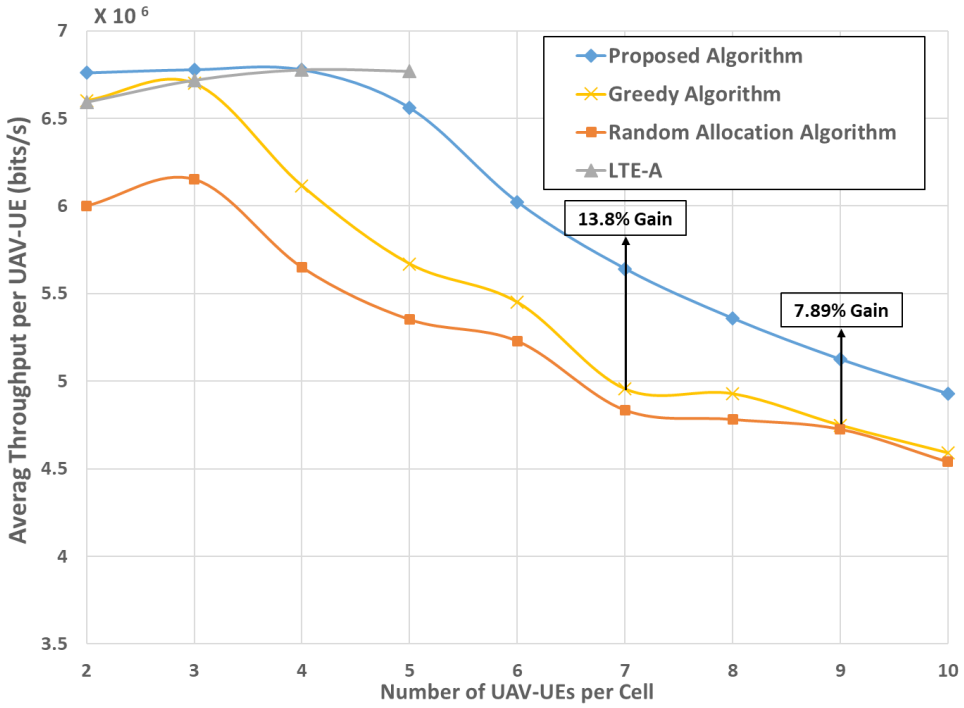

Figure 3.4: Average throughput per UAV-UE for different schemes vs. n (number of UAV-UEs per cell).

Fig. 3.5 shows the UAV-cellular network's interference level on the cellular BS for different numbers of UAV-UEs at two different distances between the cellular BS and the lower level of the 3D UAV-cellular network coverage. Since the greedy and random allocation algorithms use the optimum global allocations in the licensed spectrum, which give the same performance as our proposed algorithm in the licensed spectrum, we compare only the proposed algorithm with the LTE-A. As shown in the figure, the proposed algorithm's interference level on cellular BS for the two different distances is significantly lower than the interference level from LTE-A. Besides, the interference level for the two schemes is much less than the interference threshold level. This is because of the orthogonal distribution of the licensed spectrum among the UAV-BSs, making the UAV-UEs produce low interference per subchannel at the cellular BS.

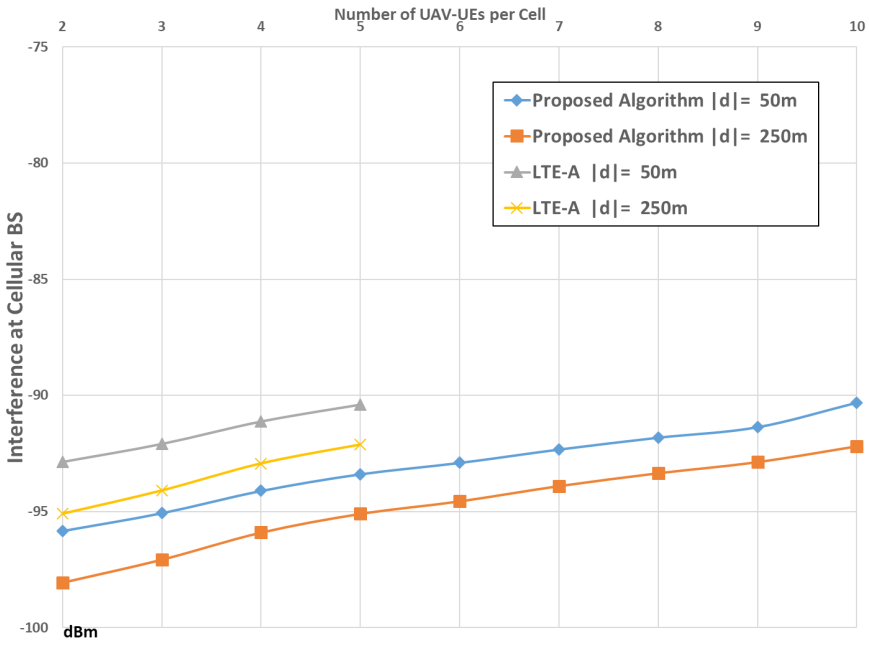

Figure 3.5: Interference value at cellular BS in licensed spectrum vs. n (number of UAV-UEs per cell).

Fig. 3.6 compares the interference level at a WAP for the proposed, greedy, and random allocation algorithms at two different distances between the WAP and the lower level of the 3D UAV-cellular network coverage. The figure shows that the interference level at the WAP increases as the number of UAV-UEs increases since the WAP is affected by all the system's cells, which reuse the entire unlicensed band. The greedy and random allocation schemes produce the same interference levels at the unlicensed band for the different distances since they do not use power control. Again, the proposed algorithm produces significantly lower interference levels over the other schemes for all the different distances. The interference level in the unlicensed spectrum is much less than the threshold level because of the high elevation angle between WAP and UAV-UEs and the wall penetration factor.

Fig. 3.7 shows the convergence of Algorithm 3 that is used to find the local optimal subchannel and power allocation in both licensed and unlicensed spectrum by iteratively solving (3.15). As seen in the figure, Algorithm 3 converges after a finite number of iterations.

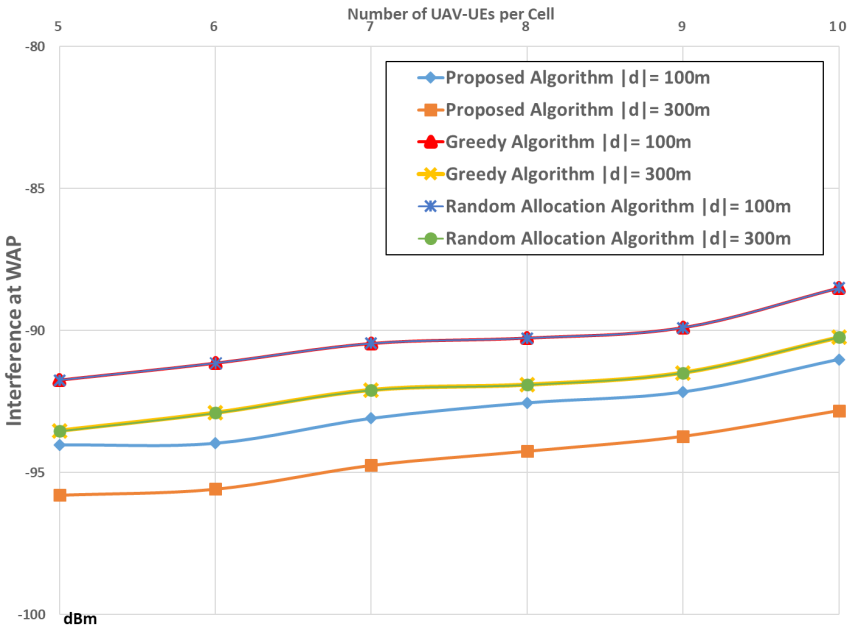

Figure 3.6: Interference value at WAP in unlicensed spectrum vs. number of UAV-UEs per cell.

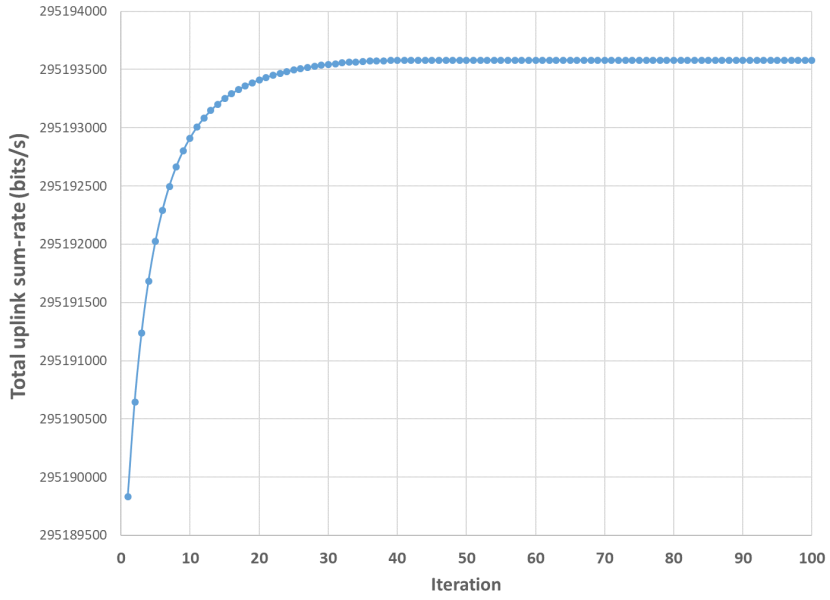

Figure 3.7: Convergence of Algorithm 3.

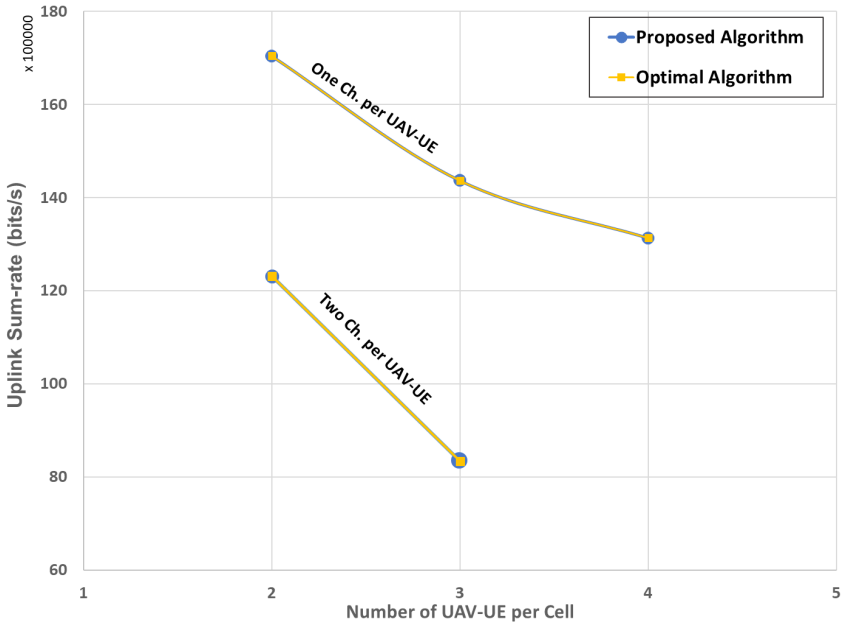

Figure 3.8: Comparison with the Optimal Algorithm

In Fig. 3.8, we show that the matching game with externalities and coalition game proposed in Algorithms 1 and 2 reach a Nash-stable solution. Therefore, we use the brute force algorithm to find the optimal subchannel allocation for given power allocation and compare it with the result of the proposed algorithm. Due to the large searching space, we test it for a small network ($\mathcal{M} = 3$, $C^U = 6$ $R_{licensed} = 0$). Fig. 3.8 shows that Algorithms 1 and 2 give the same optimal uplink sum-rate value as the optimal algorithm.

3.6 Summary

In this chapter, we have proposed channel resource allocation and interference management strategies to enhance resource utilization and improve system capacity for a novel aerial multi-cell network. Considering the co-channel interference with terrestrial cellular and WiFi systems, we have jointly optimized channel resource allocation and transmit power of UAV-UEs in the licensed and unlicensed spectrum to maximize the uplink sum rate while considering the QoS

of UAV-UE and the inter-cell interference. In order to solve this NP-hard problem, we first decompose it into three subproblems and then propose an iterative algorithm consisting of convex optimization, the Hungarian algorithm, a matching game with externalities and a coalition game, and SCA techniques to jointly solve them. Based on the simulation results, the proposed network and algorithm significantly improve the system performance in terms of the network capacity and the overall uplink sum rate compared to other schemes. In the next chapter, we will integrate the terrestrial cellular network with the aerial network and investigate the association, interference, and dynamic spectrum management strategies considering multi-cell and multi-operator scenarios.

Chapter 4

Joint User Association, Power Control, and Dynamic Spectrum Sharing for Integrated Aerial-Terrestrial Multi-Operator Network

In this chapter, we propose a novel integrated aerial-terrestrial multi-operator network. In the proposed network, each operator deploys a number of Unmanned Aerial Vehicle-Base Stations (UAV-BSs) besides the terrestrial Macro Base Station (MBS), where each BS reuses the operator's licensed band to provide downlink connectivity for UAV-Users (UAV-UEs). In addition, the operators allow the UAV-UE, whose demand cannot be satisfied by the licensed band, to compete with others to obtain bandwidth resources from the unlicensed spectrum. Considering inter-cell and inter-operator interference in the licensed and unlicensed spectrum, the user association, power allocation, and dynamic spectrum sharing are jointly optimized to maximize the network throughput while ensuring the UAV-UEs' data rate requirements. The formulated optimization problem is divided into two sequential subproblems: user association and power control in the licensed spectrum; and dynamic spectrum allocation and user association in the unlicensed spectrum. We propose a distributed iterative algorithm consisting of a matching game, coalition game, and successive convex approximation to solve the former subproblem efficiently. Afterwards, in the latter subproblem, we use a matching game to associate UAV-UEs with the UAV-BSs for

each operator in the unlicensed spectrum. Then, we propose a three-layer auction algorithm to allocate the unlicensed spectrum dynamically between operators. Simulation results show that, in the licensed spectrum, the proposed network and algorithm significantly improve network throughput per operator than using the conventional terrestrial network alone. Moreover, the achieved system throughput of the proposed algorithms with the additional use of the unlicensed spectrum is 86.8% higher than using the licensed spectrum only.

4.1 Background and Motivation

The next-generation cellular network needs to satisfy the high expected demand from cellular-connected UAVs as new users to the cellular network [97]. The applications of UAVs are expected to overgrow during the next decade [98,99]. However, this exponential growth in the UAV network comes with another pressure on the already congested terrestrial cellular network [100]. More specifically, the high uplink/downlink interference and base station antennas down-tilt produce a challenge for the terrestrial network to provide seamless connectivity to UAV-UE [3, 101]. In addition, sharing the limited spectrum of the terrestrial network with ground cellular users (CUs) could impact the network performance due to interference and decrease the operators' profit [102].

To overcome these challenges, the aerial network, which considers an essential part of the next-generation cellular network, can be leveraged to provide cellular connectivity to UAV-UEs. However, integrating the aerial network with the terrestrial network needs to overcome several challenges the new network faces, such as user association, interference and resource management, and spectrum management [103]. In addition, when multi-operators extend their cellular service to the unlicensed spectrum, the issue of how to share the band with multiple operators to overcome the inter-operator interference arises.

This chapter's main contribution is a novel integrated aerial-terrestrial multi-cell multi-operator network. We formulate a joint user association, power control, and dynamic spectrum allocation optimization problem to maximize the system sum rate, considering the UAV-UE data rate requirements and the inter-cell and inter-operator interference in the licensed and unli-

censed spectrums. To the best of our knowledge, this is the first work to consider an integrated aerial-terrestrial network that considers multi-cell and multi-operator scenarios in licensed and unlicensed spectrums, respectively. The main contributions of this paper are as follows:

- We propose a novel integrated aerial-terrestrial multi-operator network in which each BS provides cellular connectivity to UAV-UEs by reusing the complete licensed spectrum (multi-cell scenario). In addition, network operators allow UAV-UE, whose achieved data rate from the licensed spectrum has not fulfilled its demand, to compete with others to obtain bandwidth from the unlicensed spectrum.
- Considering multi-cell and multi-operator scenarios in licensed and unlicensed spectrum, an optimization problem is formulated to maximize the network throughput by jointly optimizing the user association, power control, and dynamic spectrum management while ensuring the UAV-UE data rate requirement.
- To solve the coupling issue that arises due to considering the multi-cell scenario, we propose a distributed iterative algorithm based on a matching game, coalition game and successive convex approximation to solve the joint user association and power control subproblem in the licensed spectrum.
- To design dynamic spectrum management that solves the inter-operator interference issue in the unlicensed spectrum and overcomes the aerial network high dynamics, we propose a three-layer auction algorithm to allocate the unlicensed spectrum band dynamically among operators.
- Simulation results show that the proposed network and algorithms can significantly improve the operator's network throughput in the licensed band by 22% compared with the terrestrial network. In addition, the total network sum rate from licensed and unlicensed bands is 86.8% higher than using cellular service in licensed spectrum only.

The rest of this chapter is organized as follows. Section 4.2 introduces the system model of the integrated aerial-terrestrial network. We provide the optimization problem formulation

and decomposition in Section 4.3. Section 4.4 describes the solution algorithm of the joint user association and power control subproblem in the licensed spectrum. Section 4.5 illustrates the solution algorithm of the user association and dynamic spectrum allocation subproblem in the unlicensed spectrum. Simulation results are presented in Section 4.6. Section 4.7 states the conclusion.

4.2 System Model

In this section, we first describe the network model of the integrated aerial-terrestrial network architecture and then present the channel pathloss models and data rate calculations in the licensed and unlicensed spectrum.

4.2.1 Network Model

In the system model shown in Fig. 4.1, we consider an integrated ariel-terrestrial multi-operator network in the downlink transmission. Each operator deploys multiple UAV-BSs, besides the terrestrial Macro BS (MBS), to provide efficient cellular services for UAV-UEs. Consider a set $\mathcal{S}$ of S operators, in which the operator $s \in \mathcal{S}$ serves a set $\mathcal{N}^s = \{1, 2, \cdots, N^s\}$ of N^s UAV-UEs and a set $\mathcal{M}^s = \{0, 1, 2, \cdots, M^s\}$ of M^s BSs, where the MBS is indexed by 0 and the UAV-BSs are indexed by $(1, 2, \cdots, M^s)$. We assume that for operator s, the location of MBS is $\{0, 0, z_{BS}\}$ and location of UAV-BS $m \in \mathcal{M}^s/\{0\}$ is $\{x_m, y_m, z_m\}$.

We assume each operator has its licensed spectrum, which is reused by all the BSs of the operator to fulfill the spectrum efficiency of next-generation networks. As a result, for operator s, the UAV-UE $n \in \mathcal{N}^s$ associate with the BS $m \in \mathcal{M}^s$ is suffered from inter-cell interference (ICI) from all the other M^s cells. Due to the high demand data rate required by some applications (e.g. virtual reality, augmented reality, etc.) [104], the data rate over the licensed spectrum ($R_n^{l,s}$) could not attain the requested data rate ($R_n^{l,s} < R_n^{Req.}$). Therefore, we assume that operators can compete to extend the service by reusing a total of B_{total}^U bandwidth from the unlicensed spectrum. In order to ensure the proposed architecture has a low impact on the existing WiFi system in the

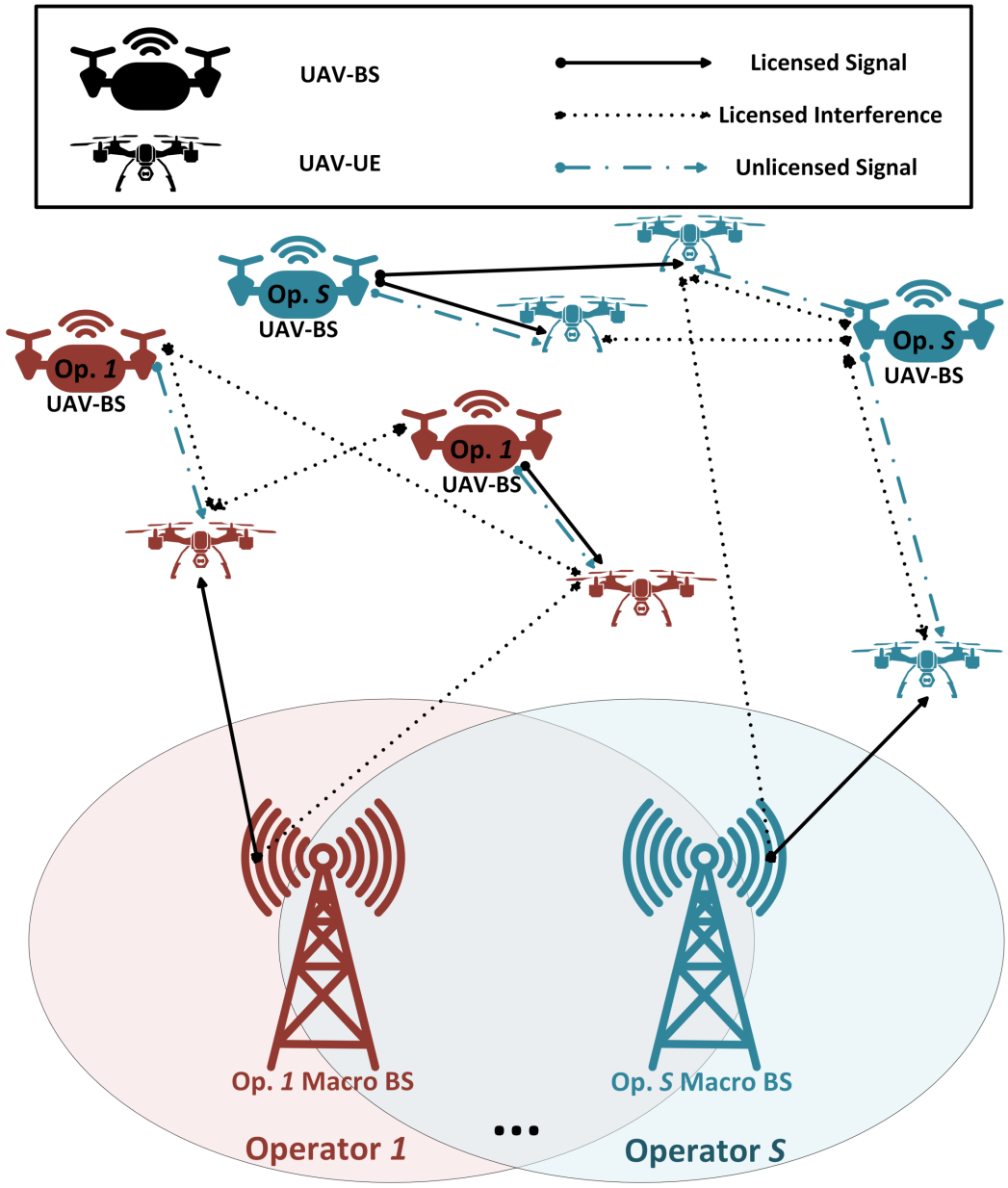

Figure 4.1: Integrated aerial-terrestrial multi-operator network model.

unlicensed spectrum, we assume that only the UAV-BSs can serve the UAV-UEs in the unlicensed spectrum [105]. In other words, the MBS can not operate in the unlicensed band due to its high

transmit power and its antenna's down-tilt. Nevertheless, allowing multiple operators to access the unlicensed spectrum without management could severely degrade the performance due to the severe inter-operator interference among the operators. Since the operators need to compete to obtain the limited unlicensed spectrum for their potential UAV-UEs, a controller is needed to control the dynamic auction operation (DAO) to achieve efficient on-demand spectrum allocation. This controller could be a ground or an air unit based on the operators' methodology to provide backhaul connectivity to the aerial network. Since The aerial network could obtain the backhaul connectivity from either MBS or HAP, we set a HAP to provide the backhaul connectivity for the aerial network, where an auction controller (HAP-AC).

4.2.2 Channel Model

In our proposed network, we consider two different types of channel models as follows: (1) Air-to-Air (A2A) channel model (between UAV-BS and either HAP or UAV-UEs); and (2) Ground-to-Air (G2A) channel model (between MBS and UAV-UEs).

A2A Channel Model

The channels among UAV-BSs, HAP, and UAV-UEs are typically dominated by LoS links. Based on 3GPP TR 36.777, the path loss from UAV-BS $m \in \mathcal{M}^s \setminus \{0\}$ to UAV-UE $n \in \mathcal{N}^s$ during time slot t is given by:

$$PL_{mn}^{v,s}(t) = 30.9 + (22.25 - 0.5\log_{10}|z_n(t) - z_m|) \cdot \log_{10} d_{mn}^{s}(t) + 20\log_{10} f_c^v, \tag{4.1}$$

where $v \in \{l, u\}$ refers to licensed or unlicensed spectrum; $d_{mn}^{s}(t)$ is the 3D distance between UAV-BS m and UAV-UE n located at $\{x_n(t), y_n(t), z_n(t)\}$ within the operator s during time slot t, which calculated as $d_{mn}^{s}(t) = \sqrt{(x_m - x_n(t))^2 + (y_m - y_n(t))^2 + (z_m - z_n(t))^2}$; z_m is the UAV-BS m height; and f_c^v is the carrier frequency of licensed or unlicensed spectrum.

G2A Channel Model

According to [106], the downlink path loss between the MBS $m = \{0\} \subset \mathcal{M}^s$ and UAV-UE $n \in \mathcal{N}^s$ during time slot t can be calculated as:

$$PL_{mn}^{v,s}(t) = P_{LoS} PL_{mn}^{LoS}(t) + \left(1 - P_{LoS}\right) PL_{mn}^{NLoS}(t), \tag{4.2}$$

where the path loss in line-of-sight (LoS) and non-LoS (NLoS) case can be calculated by:

$$PL_{mn}^{LoS}(t) = 28.0 + 22 \log_{10}\left(d_{mn}^{s}(t)\right) + 20 \log_{10}\left(f_c^v\right), \tag{4.3}$$

$$PL_{mn}^{NLoS}(t) = -17.5 + \left(46 - 7 \log_{10}(z_n(t))\right) \cdot \log_{10}(d_{mn}^{s}(t)) + 20 \log_{10}(40\pi f_c^v/3), \tag{4.4}$$

and the LoS probability is given by:

$$P_{LoS} = \frac{d_1}{d_{mn}^{2d}} + \exp\left(-\frac{d_{mn}^{2d}}{p_1}\right)\left(1 - \frac{d_1}{d_{mn}^{2d}}\right), \tag{4.5}$$

where d_1 and p_1 are altitude-dependent parameters with $d_1 = \max(460 \log_{10}(z_n(t)), 18)$ and $p_1 = 4300 \log_{10}(z_n(t)) - 3800$; and d_{mn}^{2d} is the 2D distance between MBS and UAV-UE n.

4.2.3 Data Rate

For Licensed Spectrum

We assume that the spectrum efficiency per UAV-UE $n \in \mathcal{N}^s$ associated with BS $m \in \mathcal{M}^s$ of operator s in time slot t is as follows:

$$r_{mn}^{l,s}(t) = \log_2\left(1 + \frac{P_m^{l,s}(t) g_{mn}^{l,s}(t)}{\sum_{m' \in \mathcal{M}^s \setminus \{m\}} P_{m'}^{l,s}(t) g_{m'n}^{l,s}(t) + N_0}\right), \tag{4.6}$$

where $P_m^{l,s}(t)$ is the transmit power spectral density (PSD) at the BS m in the licensed band. Define the channel gain between UAV-UE n and BS m as $g_{mn}^{l,s}(t) = 10^{-PL_{mn}^{l,s}(t)/10}$, which can be derived from equation (2)-(5) for $m = \{0\}$ and from equation (1) for $m \in \mathcal{M}^s \setminus \{0\}$. N_0 is the PSD of the noise, and $\sum_{m' \in \mathcal{M}^s \setminus \{m\}} P_{m'}^{l,s}(t) g_{m'n}^{l,s}(t)$ is the amount of inter-cell interference at UAV-UE n.

Let $B^{l,s}$ be the amount of licensed spectrum allocated for operator $s \in \mathcal{S}$. Then, the achievable transmission rate of UAV-UE n associated with BS m from the licensed spectrum during time slot t can be expressed as:

$$R_{mn}^{l,s}(t) = \lambda_{mn}^{l,s} \cdot \frac{B^{l,s}}{\sum_{n \in \mathcal{N}^s} \lambda_{mn}^{l,s}} \cdot r_{mn}^{l,s}(t), \tag{4.7}$$

where $\lambda^{l,s}$ is the user association index of operator s in the licensed spectrum, in which $\lambda_{mn}^{l,s} = 1$ when UAV-UE n is associated with BS m of operator s, and $\lambda_{mn}^{l,s} = 0$ otherwise; and $\sum_{n \in \mathcal{N}^s} \lambda_{mn}^{l,s}$ is the number of UAV-UEs associated with BS m.

For Unlicensed Spectrum

we assume that the spectrum efficiency per UAV-UE $n \in \mathcal{N}^s$ under UAV-BS $m \in \mathcal{M}^s \setminus \{0\}$ of operator $s \in \mathcal{S}$ during time slot t is as following:

$$r_{mn}^{u,s}(t) = \log_2\left(1 + \frac{P_m^{u,s} g_{mn}^{u,s}(t)}{N_0}\right), \tag{4.8}$$

where $P_m^{u,s}$ is the transmit PSD at the UAV-BS m of operator s in the unlicensed band, which is fixed. Define the channel gain between UAV-UE n and UAV-BS m in the unlicensed spectrum during time slot t as $g_{mn}^{u,s}(t) = 10^{-PL_{mn}^{u,s}(t)/10}$, which can be derived from equation (1).

Thus, the UAV-UE n associated with UAV-BS m could achieve a data rate in the unlicensed spectrum during time slot t as expressed below:

$$R_{mn}^{u,s}(t) = \lambda_{mn}^{u,s} \cdot B_n^{u,s}(t) \cdot r_{mn}^{u,s}(t), \tag{4.9}$$

where $\lambda_{mn}^{u,s}$ is the association index between UAV-UE $n \in \mathcal{N}^s$ and UAV-BS $m \in \mathcal{M}^s \setminus \{0\}$ in the unlicensed spectrum; and $B_n^{u,s}(t)$ is the assigned unlicensed bandwidth for UAV-UE n during time slot t.

Finally, the achievable sum data rate of UAV-UE n over the licensed and unlicensed spectrum bands during time slot t is:

$$\mathcal{R}_n^s(t) = \sum_{m \in \mathcal{M}^s} R_{mn}^{l,s}(t) + \sum_{m \in \mathcal{M}^s \setminus \{0\}} R_{mn}^{u,s}(t). \tag{4.10}$$

4.3 Problem formulation and decomposition

Given the system model in the previous section, our goal is to maximize the total downlink sum rate of the network by jointly optimizing power allocation and user association in the licensed spectrum and dynamic spectrum allocation and user association in the unlicensed spectrum. In addition, two types of interference are considered in the formulated problem: inter-cell interference in the licensed band and inter-operator interference in the unlicensed spectrum. Thus, the optimization problem is formulated as follows:

$$
\begin{aligned}
&\max_{(\lambda^L, P^L, \lambda^U, B^U)} \sum_{s\in\mathcal{S}} \sum_{n\in\mathcal{N}^s} \mathcal{R}_n^s(t), \\
&s.t., \\
&C_1 : \mathcal{R}_n^s(t) \geq R_n^{Req.}, \forall s \in \mathcal{S}, \forall n \in \mathcal{N}^s, \\
&C_2 : \sum_{m\in\mathcal{M}^s} \lambda_{mn}^{l,s} = 1, \forall s \in \mathcal{S}, \forall n \in \mathcal{N}^s, \\
&C_3 : 0 \leq \sum_{s\in\mathcal{S}} \sum_{n\in\mathcal{N}^s} B_n^{u,s}(t) \leq B_{total}^U, \\
&C_4 : \sum_{m\in\mathcal{M}^s\setminus\{0\}} \lambda_{mn}^{u,s} \leq 1, \forall s \in \mathcal{S}, \forall n \in \mathcal{N}^s, \\
&C_5 : \lambda_{mn}^{l,s} \in \{0,1\}, \forall s \in \mathcal{S}, \forall n \in \mathcal{N}^s, \forall m \in \mathcal{M}^s, \\
&C_6 : \lambda_{mn}^{u,s} \in \{0,1\}, \forall s \in \mathcal{S}, \forall n \in \mathcal{N}^s, \forall m \in \mathcal{M}^s \setminus \{0\}, \\
&C_7 : 0 \leq P_m^{l,s}(t) \leq P_m^{l,max}, \forall s \in \mathcal{S}, \forall m \in \mathcal{M}^s,
\end{aligned}
\tag{4.11}
$$

where constraint C_1 denotes that the achieved data rate through the licensed and unlicensed spectrum of each UAV-UE should meet the requested data rate; constraint C_2 ensures that each UAV-UE is associated with exactly one BS in the licensed spectrum; constraint C_3 guarantees that the total assigned unlicensed bandwidth resources must be less than or equal to the total available spectrum in the unlicensed band; constraint C_4 ensures that each UAV-UE is associated at most with one UAV-BS in the unlicensed spectrum; constraints C_5 and C_6 show that the user association coefficients in the licensed and unlicensed spectrum are binary; and $P_m^{l,max}$ is the maximum transmit PSD of BS m in the licensed spectrum.

The formulated problem is a non-convex mixed-integer non-linear programming (MINLP) optimization problem [107], which is generally NP-hard. Therefore, to solve this problem efficiently, we decouple the optimization problem into two sequence subproblems: the user association and power control in the licensed spectrum; and the user association and dynamic spectrum allocation in the unlicensed spectrum.

4.3.1 Stage One: Joint User Association and Power Control Subproblem Formulation in the Licensed Spectrum

The joint user association and power control subproblem in the licensed spectrum is written as:

$$\begin{aligned} &\max_{(\lambda^L, P^L)} \sum_{s\in\mathcal{S}} \sum_{n\in\mathcal{N}^s} \sum_{m\in\mathcal{M}^s} R_{mn}^{l,s}(t), \\ &s.t., \\ &C_2, C_5, and\ C_7. \end{aligned} \tag{4.12}$$

Since each operator has a licensed spectrum band, we decompose subproblem (4.12) into S subproblems to decrease the computational complexity of the system. Each subproblem aims to independently maximize the operator's sum rate in the licensed spectrum. The optimization subproblem of operator $s \in \mathcal{S}$ is expressed as follows:

$$\begin{aligned} &\max_{(\lambda^L, P^L)} \sum_{n\in\mathcal{N}^s} \sum_{m\in\mathcal{M}^s} \lambda_{mn}^{l,s} \cdot \frac{B^{l,s}}{\sum_{n\in\mathcal{N}^s} \lambda_{mn}^{l,s}} \cdot r_{mn}^{l,s}(t), \\ &s.t., \\ &C_2^{'}: \sum_{m\in\mathcal{M}^s} \lambda_{mn}^{l,s} = 1, \forall n \in \mathcal{N}^s, \\ &C_5^{'}: \lambda_{mn}^{l,s} \in \{0,1\}, \forall n \in \mathcal{N}^s, \forall m \in \mathcal{M}^s, \\ &C_7^{'}: 0 \le P_m^{l,s}(t) \le P_m^{l,max}, \forall m \in \mathcal{M}^s, \end{aligned} \tag{4.13}$$

where constraint ($C_2^{'}$) emphasizes that each UAV-UE $n \in \mathcal{N}^s$ is associated with exactly one BS. Constraint ($C_5^{'}$) indicates that the user association coefficient in the licensed spectrum $\lambda_{mn}^{l,s}$ can be only 0 or 1. Constraint ($C_7^{'}$) ensures that the BS transmit PSD in the licensed spectrum remains in the required range.

4.3.2 Stage Two: Joint User Association and Dynamic Spectrum Allocation Subproblem Formulation in the Unlicensed Band

In this phase, we aim to maximize the network sum rate achieved from the unlicensed spectrum. After solving the previous subproblem, operators allow the UAV-UEs, which achieved data rate from the licensed band less than the requested data rate $\left(R_n^{l,s} < R_n^{Req}\right)$, to extend their cellular service to the unlicensed spectrum. As mentioned before, the MBS is not within the set of BSs that extend service to the unlicensed band to prevent the impact of coexistence interference on the WiFi system. However, the inter-operator interference issue in the unlicensed spectrum due to the multi-operator case will severely degrade the network performance if not managed. Due to the aerial network's high dynamics, a dynamic spectrum sharing mechanism is essential to ensure satisfactory system performance. Therefore, this subproblem aims to maximize the total sum rate in the unlicensed spectrum by optimizing the user association and dynamically allocating the unlicensed band between the operators, which is written as:

$$
\begin{aligned}
&\max_{(\lambda^U, B^U)} \sum_{s\in\mathcal{S}} \sum_{n\in\mathcal{N}^s} \sum_{m\in\mathcal{M}^s\setminus\{0\}} \lambda_{mn}^{u,s} \cdot B_n^{u,s}(t) \cdot r_{mn}^{u,s}(t), \\
&s.t., \\
&C_1: \sum_{m\in\mathcal{M}^s\setminus\{0\}} \lambda_{mn}^{u,s} \cdot B_n^{u,s}(t) \cdot r_{mn}^{u,s}(t) \geq \left[R_n^{Req.} - R_n^{l,s}\right]^+, \forall s \in \mathcal{S}, \forall n \in \mathcal{N}^s, \\
&C_3: 0 \leq \sum_{s\in\mathcal{S}} \sum_{n\in\mathcal{N}^s} B_n^{u,s}(t) \leq B_{total}^U, \\
&C_4: \sum_{m\in\mathcal{M}^s\setminus\{0\}} \lambda_{mn}^{u,s} = 1, \forall s \in \mathcal{S}, \forall n \in \mathcal{N}^s \\
&C_6: \lambda_{mn}^{u,s} \in \{0,1\}, \forall s \in \mathcal{S}, \forall n \in \mathcal{N}^s, \forall m \in \mathcal{M}^s \setminus \{0\}.
\end{aligned}
\tag{4.14}
$$

4.4 User Association and Power Control in the Licensed Band

For operator $s \in \mathcal{S}$, the optimization subproblem (4.13) is still a non-convex MINLP optimization problem. Therefore, we decouple it into two sub-subproblems: user association sub-subproblem

and power control sub-subproblem, which are respectively written below as:

$$\begin{aligned} &\max_{\lambda^L} \sum_{n\in\mathcal{N}^s}\sum_{m\in\mathcal{M}^s} \lambda_{mn}^{l,s}\cdot\frac{B^{l,s}}{\sum_{n\in\mathcal{N}^s}\lambda_{mn}^{l,s}}\cdot r_{mn}^{l,s}(t), \\ &s.t., \quad C_2^{'} \text{ and } C_5^{'}, \end{aligned} \tag{4.15}$$

and

$$\begin{aligned} &\max_{P^L} \sum_{n\in\mathcal{N}^s}\sum_{m\in\mathcal{M}^s} \lambda_{mn}^{l,s}\cdot\frac{B^{l,s}}{\sum_{n\in\mathcal{N}^s}\lambda_{mn}^{l,s}}\cdot r_{mn}^{l,s}(t), \\ &s.t., \quad C_7^{'}. \end{aligned} \tag{4.16}$$

In this section, we propose an efficient algorithm to obtain a sub-optimal solution to subproblem (4.13) by solving its two sub-subproblems (4.15) and (4.16) iteratively. A traditional matching game cannot solve the user association sub-subproblem (4.15) due to externalities, in which the choice of a UAV-UE by a BS is affected by the selection of the other UAV-UEs for that specific BS. Therefore, a matching and coalition game are proposed to cope with these externalities and solve this sub-subproblem efficiently. Then, a successive convex approximation method is utilized to solve the non-convex power control sub-subproblem (4.16). In the following, the two sub-subproblems solution methods are discussed first, then we provide the iterative algorithm and discuss its convergence and complexity.

4.4.1 User Association

Matching Game

For operators $s \in \mathcal{S}$, we consider two disjoint finite sets of players, $\mathcal{M}^s$ and $\mathcal{N}^s$. A matching game is defined as a function of $\Omega : \mathcal{M}^s \rightarrow \mathcal{N}^s$, such that:

- $\Omega(n) = m \Longleftrightarrow \Omega(m) = n, \forall n \in \mathcal{N}^s, \forall m \in \mathcal{M}^s$.
- $|\Omega(n)| = 1, \forall n \in \mathcal{N}^s$.

The first item shows that if UAV-UE n is matched to BS m, then BS m is also matched to UAV-UE n. The second item implies that each UAV-UE is matched to one BS only.

Each UAV-UE of the set $\mathcal{N}^s$ ranks the BSs of the set $\mathcal{M}^s$ by preference relation $\succ$. The notation $\psi^n_{m_1} \succ_n \psi^n_{m_2}$ means that UAV-UE n prefers the BS m_1 over m_2 if $\psi^n_{m_1} > \psi^n_{m_2}$, where the utility ($\psi^n_m$) of UAV-UE n for BS m is calculated using equation (4.6).

Next, we propose a coalition game, along with UAV-UE transfer, to overcome the externalities of the matching game.

Coalition Game

For each operator $s \in \mathcal{S}$, we denote π_i as the coalition of the BS $i \in \mathcal{M}^s$ which is a set of UAV-UEs associated with this BS. The utility of UAV-UE n in the coalition π_i is calculated using equation (4.7). Since there are $M^s + 1$ BSs in the operator s network, the set of UAV-UEs $\mathcal{N}^s$, who are the players, is divided among the $|M^s + 1|$ coalitions. The formation of coalitions should satisfy the following constraints:

$$\begin{aligned} &\mathcal{N}^s = \pi_0 \cup \pi_1 \cup ... \cup \pi_{M^s}, \\ &\pi_m \cap \pi_j = \emptyset, \forall m, j \in \mathcal{M}^s and\ m \neq j, \end{aligned} \tag{4.17}$$

where $U(\pi_m)$ is the utility of coalition m that is written as:

$$U(\pi_m) = \sum_{n \in \pi_m} R^{l,s}_{mn}, \tag{4.18}$$

which represents the sum data rate in the licensed bands of all the UAV-UEs associated with the BS m.

Definition 1: (A coalition set total utility) The total utility of a coalitional set Θ, where $\Theta = \{\pi_0, ..., \pi_{M^s}\}$, is calculated as:

$$U(\Theta) = \sum_{m=0}^{M^s} U(\pi_m), \tag{4.19}$$

which represents the sum data rate in the licensed spectrum band of all the UAV-UEs by the association defined by Θ.

The preference relation for UAV-UEs to choose whether to leave or join a coalition must be determined to maximize the operator's sum rate in the licensed spectrum. Instead of initial coalition set $\Theta = \{\pi_0, ..., \pi_{M^s}\}$, a group of UAV-UEs choose to depart or enter a coalition, which forms a new coalition set $\tilde{\Theta} = \{\tilde{\pi}_0, ..., \tilde{\pi}_{M^s}\}$, based on the utility comparison results between the initial and current coalition set [91], [92]. The utility relationship between the new and current coalition sets is defined as:

$$\sum_{m=0}^{M^s} U(\tilde{\pi}_m) > \sum_{m=0}^{M^s} U(\pi_m), \tag{4.20}$$

Thus, $U(\tilde{\Theta}) > U(\Theta)$ means that the coalition set $\tilde{\Theta}$ achieves a superior total utility than Θ.

Switching rule: for any UAV-UE $n \in \mathcal{N}^s$ and $n \in \pi_m$, UAV-UE n strictly prefers to switch its coalition from π_m to coalition π_j ($\pi_j \succ_n \pi_m$), if and only if:

$$U(\{\pi_m \setminus n\}) + U(\{\pi_j \cup n\}) > U(\pi_m) + U(\pi_j), \pi_m, \pi_j \subseteq \mathcal{N}^s, \pi_m \neq \pi_j, \tag{4.21}$$

Therefore, the coalition set Θ is adjusted into a new coalition set as follows

$$\Theta = (\Theta \setminus \{\pi_m, \pi_j\}) \cup \{\pi_m \setminus n\} \cup \{\pi_j \cup n\}. \tag{4.22}$$

Theorem 5. The coalition game's final coalition set Θ_{final} is stable.

Proof. If the final coalition set Θ_{final} is not stable, then there must exist a UAV-UE $n \in \pi_p (\pi_p \subseteq \Theta_{final})$ and another coalition $\pi_q \subseteq \Theta_{final}$ such that $\pi_q \succ_l \pi_p$. However, in this case, UAV-UE n will perform a switch operation to the available coalition forming a new coalition set based on the coalition game formulation [108]. Therefore, the final coalition set Θ_{final} is stable. ■

4.4.2 Power Control

The power control sub-subproblem (4.16) is still a non-convex optimization problem due to the ICI coupling between BSs. Therefore, we use the successive convex approximation (SCA) method to solve this sub-subproblem efficiently [93]. Based on [94], the SCA approach is guaranteed to converge in a finite number of iterations.

Algorithm 4 Iterative User Association and Power control Algorithm in the Licensed Spectrum for Operator s

Initialization: $\mathcal{N}^s$, $\mathcal{M}^s$, $P_m^{L,max}$
Step 1: Matching Game
Input: $\mathcal{N}^s$, $\mathcal{M}^s$.
Output: Initial user association λ_{ini}^L.
for each UAV-UE $n \in \mathcal{N}^s$ **do**
    Calculate $r_{mn}^{l,s}$ with the help of (4.6);
    Sort BSs according to $r_{mn}^{l,s}$ in descending order;
    Match UAV-UE with the most preferred BS in its list.
end for
repeat
    Step 2: Coalition Game
    Input: Initial coalition set Θ_{ini} from previous step
    Output: Coalition set Θ_{final} (user association λ^L)
    while stable coalition set is not achieved **do**
        Choose a UAV-UE $n \in \mathcal{N}^s$ randomly and refer to its current coalition as $\pi_m \in \Theta$;
        Choose randomly another coalition $\pi_j \in \Theta$, $\pi_j \neq \pi_m$;
        if Switch rule $(\pi_j \succ_n \pi_m)$ is fulfilled **then**
            $\Theta = (\Theta \setminus \{\pi_m, \pi_j\}) \cup \{\pi_m \setminus n\} \cup \{\pi_j \cup n\}$
        end if
    end while
    Step 3: Successive Convex Approximation
    Solve sub-subproblem (4.23) until convergence.
until Convergence
Output: λ^L, P^L

We first use the auxiliary variable $P_m^{l,s}(t) = e^{q_m^{l,s}(t)}$. Then, according to [95], $\hat{f}(x) = \xi \log x + \upsilon$ is the lower bound of $f(x) = \log(1+x)$, where $\xi = \frac{x}{1+x}$ and $\upsilon = \log(1+x) - \frac{x}{1+x}\log(x)$.

Therefore, we can reformulate the sub-subproblem (4.16) as:

$$\begin{aligned} &\max_{q^L} \sum_{n\in\mathcal{N}^s}\sum_{m\in\mathcal{M}^s} \lambda_{mn}^{l,s}\frac{B^{l,s}}{\sum_{n\in\mathcal{N}^s}\lambda_{mn}^{l,s}}[\,\xi_{mn}^{l,s}\log_2(\,\gamma_{mn}^{l,s})\,+\upsilon_{mn}^{l,s}] \\ &s.t., \\ &\quad q_m^{l,s}(t)\le \ln(\,P_m^{L,max})\,,\forall m\in\mathcal{M}^s, \end{aligned} \tag{4.23}$$

where γ_{mn}^{L} is the signal-to-interference-plus-noise ratio (SINR) in the licensed spectrum, which is given by the following:

$$\gamma_{mn}^{l,s}=\frac{e^{q_m^{l,s}(t)}g_{mn}^{l,s}(t)}{\sum_{m'\in\mathcal{M}^s\setminus\{m\}}e^{q_{m'}^{l,s}(t)}g_{m'n}^{l,s}(t)+N_0}. \tag{4.24}$$

Theorem 6. *Problem (4.23) is a convex optimization problem.*

Proof. In order to check the convexity of the optimization sub-subproblem (4.23), we rearrange $\log_2(\,\gamma_{i,j}^{q,t})$ to be as follow:

$$\log_2(\gamma_{mn}^{l,s})=\frac{\ln(\gamma_{mn}^{l,s})}{\ln(2)}=\frac{1}{\ln(2)}\Big(\,\ln(g_{mn}^{l,s}(t))\;+\;q_m^{l,s}(t)-\ln(\sum_{m'\in\mathcal{M}^s\setminus\{m\}}e^{q_{m'}^{l,s}(t)}g_{m'n}^{l,s}(t)+\sigma^2)\Big). \tag{4.25}$$

Based on [89], the above function is concave since the log-sum-exponential function is convex. Therefore, since the objective function of (4.23) is a combination of concave functions, the optimization sub-subproblem is convex. ■

4.4.3 Iterative User Association and Power Control Algorithm

Theorem 7. *The convergence of Algorithm 4 is guaranteed.*

Proof. Algorithm 4 determines near-optimal user association and power allocation in the licensed band, where each iteration includes a coalition game and SCA approach. Based on [93], the SCA approach guarantees the convergence to local optimum close to the global optimum.

Besides, as proofed in Theorem 5, the coalition game would reach a stable coalition set. Therefore, the convergence of Algorithm 4 is guaranteed in a finite number of iterations since the operator's sum rate in the licensed spectrum has an upper bound and is improved in each iteration. ■

4.4.4 Computational Complexity Analysis

In this subsection, we analyze the computational complexity of the proposed Algorithm 4. For the user association sub-subproblem of operator s, we first use a matching game to initially associate UAV-UEs with BSs, with a complexity of $(\mathcal{M}^s \cdot \mathcal{N}^s)$ [96]. Afterwards, we introduce a coalition game to solve the externalities of the previous matching game. Based on the coalition game formulation, in the worst case, each UAV-UE needs to examine $|\mathcal{M}^s|$ of coalitions. Thus, the complexity of the coalition game is $\mathcal{O}(\mathcal{M}^s \cdot \mathcal{N}^s)$. The optimal user association sub-subproblem could also be solved using the exhaustive search algorithm. However, the optimal algorithm has a computational complexity equal to $\mathcal{O}((\mathcal{N}^s)^{|\mathcal{M}^s|})$, which is exceptionally high. The power control sub-subproblem is solved efficiently using the CVX package since the problem is convex. Based on [93], the SCA method solves the optimization problem iteratively by updating the points of interest till convergence, which iterate for at most $\mathcal{O}(\mathcal{M}^s)$ times. Therefore, the computational complexity for the proposed algorithm 4 is $\mathcal{O}((\mathcal{M}^s \cdot \mathcal{N}^s) + K \times (\mathcal{M}^s \cdot \mathcal{N}^s + \mathcal{M}^s))$, where K denotes the number of iterations that the SCA method and coalition game would iterate before convergence, which is a finite constant.

4.5 Dynamic Unlicensed Spectrum Allocation and User Association

To solve the subproblem (4.14) of user association and dynamic spectrum allocation in the unlicensed band, we decouple it into two sub-subproblems: user association sub-subproblem and dynamic spectrum allocation sub-subproblem; which are respectively written below as:

$$\max_{\lambda^U} \sum_{s\in\mathcal{S}} \sum_{n\in\mathcal{N}^s} \sum_{m\in\mathcal{M}^s\setminus\{0\}} \lambda_{mn}^{u,s} \cdot B_n^{u,s}(t) \cdot r_{mn}^{u,s}(t), \quad s.t., \;\; C_4 \text{ and } C_6, \tag{4.26}$$

and

$$\max_{B^U} \sum_{s\in\mathcal{S}} \sum_{n\in\mathcal{N}^s} \sum_{m\in\mathcal{M}^s\setminus\{0\}} \lambda_{mn}^{u,s} \cdot B_n^{u,s}(t) \cdot r_{mn}^{u,s}(t), \quad s.t., \;\; C_1 \text{ and } C_3. \tag{4.27}$$

In order to decrease the computational complexity of the system, the user association sub-subproblem is divided into $|\mathcal{S}|$ sub-subproblems; thus, each operator independently uses a matching game to associate the UAV-UEs with UAV-BS. For the dynamic spectrum allocation sub-subproblem, UAV-UEs need to compete with each other to strive for the limited unlicensed spectrum, which is hard to fulfill all the bandwidth requirements of UAV-UEs. Thus, we propose a three-layers auction framework to dynamically allocate the unlicensed spectrum among operators to prevent inter-operator interference.

4.5.1 Matching Game

Similar to the matching game used in the licensed spectrum, two disjoint finite sets of players, $\mathcal{M}^s \setminus \{0\}$ and $\mathcal{N}^s$, are considered. We define the matching game as a function of $\Omega : \mathcal{M}^s \setminus \{0\} \rightarrow \mathcal{N}^s$, such that:

- $\Omega(n) = m \Longleftrightarrow \Omega(m) = n, \forall n \in \mathcal{N}^s, \forall m \in \mathcal{M}^s \setminus \{0\}$.
- $|\Omega(n)| = 1, \forall n \in \mathcal{N}^s$.

Each UAV-UE of the set $\mathcal{N}^s$ ranks the UAV-BSs of the set $\mathcal{M}^s \setminus \{0\}$ by preference relation $\succ$, in which the utility ψ_m^n of UAV-UE n for UAV-BS m is calculated using equation (4.8).

4.5.2 Dynamic Auction Operation

This subsection proposes a three-layers dynamic auction operation (DAO) to solve the dynamic spectrum allocation sub-subproblem in the unlicensed spectrum (4.27). The three layers are the UAV-UEs layer, Operators layer, and HAP-AC layer. The dynamic auction operation coordinates competition relations between operators for the supply-demand of unlicensed bandwidth.

In the auction process, each UAV-UE $n \in \mathcal{N}^s$ associated with UAV-BS $m \in \mathcal{M}^s \setminus \{0\}, \forall s \in \mathcal{S}$, calculates $d_n^s(t)$, which denotes the bandwidth demand from the unlicensed spectrum based on

$$d_n^s(t) = \frac{\left[R_n^{Req} - R_n^l\right]^+}{r_{mn}^{u,s}(t)} \tag{4.28}$$

Afterwards, the UAV-UE submits its demand priority pair (a_n^s, d_n^s), where a_n^s is a predetermined value that indicates the maximum acceptable price of UAV-UE n under operator s and is related to (4.8). We use a_n^s to determine the demand priority degree, in which as the a_n^s increase, the bandwidth demand priority degree is higher.

We define the dynamic bidding matrix as $B(t) = \{b_s(t), s = 1, 2, ..., S\}$, where $b_s(t) \in [0, B_{total}^U]$. $b_s(t) > 0$ means operator $s \in \mathcal{S}$ can help UAV-UEs bid for the unlicensed bandwidth of HAP-AC, otherwise $b_s(t) = 0$. The dynamic bidding matrix values are expressed as

$$b_s(t) \in [0, B_{total}^U], \forall s \in \mathcal{S}, \tag{4.29}$$

$$\sum_{s=1}^{S} b_s(t) \leq B_{total}^U. \tag{4.30}$$

Define q_n^s as the UAV-UE layer's received unlicensed bandwidth resources, where $q_n^s \in [0, B_{total}^U]$. $q_n^s > 0$ means UAV-UE $n \in \mathcal{N}^s$ actually obtained unlicensed bandwidth, while $q_n^s = 0$ means the bid is failed. We define the operators layer's unlicensed spectrum allocation matrix as $Q(t) = \{q_s^{op}, s = 1, 2, ..., S\}$, where $q_s^{op} = \sum_{n \in \mathcal{N}^s} q_n^s$. The unlicensed spectrum allocation matrix is defined as:

$$q_s^{op} \in [0, B_{total}^U], \forall s \in \mathcal{S}, \tag{4.31}$$

$$\sum_{s=1}^{S} q_s^{op} \leq B_{total}^U. \tag{4.32}$$

We design the operator $\mathcal{U}_s^{\mathcal{S}}(t)$ and HAP-AC $\mathcal{U}^C(t)$ layers' utility functions to ensure competition in the DAO. When operator s assists UAV-UE n to bid, the operator-UAV link utility function is expressed as $U_n^s = a_n^s - P_A$, where P_A implies the current price of the DAO. We consider that only $\mathcal{N}_{new}^s$ UAV-UEs with $R_n^{l,s} < R_n^{Req}$ and $a_n^s > P_A$ are qualified to engage in this auction. Thus, we can update the current bandwidth demand of operator s to be

$$b_s(t) = \sum_{n \in \mathcal{N}_{new}^s} d_n^s(t). \tag{4.33}$$

Therefore, the operator layer utility function is defined as

$$\mathcal{U}_s^{\mathcal{S}}(t) = \sum_{n \in \mathcal{N}_{new}^s} U_n^s \cdot d_n^s(t) = \sum_{n \in \mathcal{N}_{new}^s} (\, a_n^s - P_A) \cdot d_n^s(t), \tag{4.34}$$

and the HAP-AC side utility function can be expressed as

$$\mathcal{U}^C(t) = \sum_{s=1}^{S} (\, P_A - P_{base,s}) \cdot b_s(t), \tag{4.35}$$

where $P_{base,s}$ represents the cost of the operator s to provide the unlicensed bandwidth resource unit for UAV-UE. Thus, we consider $P_{base,s}$ as the minimum price of the operator s bidding. We can observe that $a_n^s > P_{base,s}$ is guaranteed for each UAV-UE $n \in \mathcal{N}_{new}^s$ in the bidding procedures.

Therefore, the dynamic spectrum allocation sub-subproblem optimal solution refers to the solution of spectrum band allocation that maximizes the social welfare, which is formulated as a linear programming optimization problem as:

$$\begin{aligned} &\max_{q_n^s} \sum_{s \in \mathcal{S}} \sum_{n \in \mathcal{N}^s} (\, a_n^s - P_{base,s}) \cdot q_n^s, \\ &s.t., \\ &C_1 : q_n^s \geq d_n^s(t), \forall s \in \mathcal{S}, \forall n \in \mathcal{N}^s, \\ &C_2 : \sum_{s \in \mathcal{S}} \sum_{n \in \mathcal{N}^s} q_n^s \leq B_{total}^U, \end{aligned} \tag{4.36}$$

Algorithm 5 Dynamic Spectrum Allocation and User Association in the Unlicensed Spectrum

Initialization: $\mathcal{S}$, $\mathcal{N}^s$, $\mathcal{M}^s \setminus \{0\}$, $R_n^{l,s}$, $R_n^{Req.}$.

Stage I: Matching Game

for each operator $s \in \mathcal{S}$ **do**

  for each UAV-UE $n \in \mathcal{N}^s$ **do**

    Calculate $r_{mn}^{u,s}$ with the help of (4.8);

    Sort UAV-BSs according to $r_{mn}^{u,s}$ in descending order;

    Match UAV-UE with the most preferred UAV-BS in the preference list.

  end for

end for

Stage II: Dynamic Auction Operation (DAO)

for each operator $s \in \mathcal{S}$ **do**

  for each UAV-UE $n \in \mathcal{N}^s$ **do**

    Calculate $d_n^s(t)$ by using (4.28),

    Submit the demand priority pair (a_n^s, d_n^s) to the operator s.

  end for

  Operator s computes the initial bidding value based on (4.33), and sent it to HAP-AC.

end for

Set iteration counter (i) equals 1;

while $[\sum_{s=1}^{S} b_s(t) - B_{total}^U]_i \geq \Delta$ **do**

  if $[\sum_{s=1}^{S} b_s(t) - B_{total}^U]_i \cdot [\sum_{s=1}^{S} b_s(t) - B_{total}^U]_{i-1} > 0$ **then**

    Set $P_A = P_A + \varepsilon$;

    Update $B(t)$ and $\mathcal{U}_s^{\mathcal{S}}(t)$ based on (4.34).

  else

    Set $\varepsilon = -0.5\varepsilon$;

    Set $P_A = P_A + \varepsilon$;

    Update $B(t)$ and $\mathcal{U}_s^{\mathcal{S}}(t)$ based on (4.34).

  end if

  i = i + 1;

end while

$Q(t) = B(t)$, and the HAP-AC allocates the unlicensed spectrum among the operators.

Output: λ^U, B^U

Instead of submitting the complete bidding information of all UAV-UEs to HAP-AC, which has high complexity, we propose a DAO with low complexity, where the HAP-AC only receives the bidding requests from the operators. The main idea is that the operators assist their UAV-UEs in getting the unlicensed spectrum resources from the HAP-AC. First, UAV-UEs submit the demand priority pairs (a_n^s, d_n^s) to their operators. Afterwards, each operator updates its current bandwidth demand $b_s(t)$ and utility function $\mathcal{U}_s^{\mathcal{S}}(t)$ according to the current auction price using (4.33) and (4.34), respectively.

The deal price P_A^* is determined until $[\sum_{s=1}^{S} b_s(t) - B_{total}^U] < \Delta$, where $\Delta = \max\{d_n^s(t)\}$. The residue of the unlicensed band is distributed uniformly among operators. Lastly, the bandwidth allocation matrix indicates the final bidding matrix. A fast-slow combination technique is proposed to modify the step size value dynamically in order to find the auction deal price efficiently. Stage II in Algorithm 5 shows the mathematical description of the DAO. If the complete unlicensed spectrum has not been demanded in full at the DAO beginning, we set $P_A = P_{base,s}$ for each operator.

4.6 Performance Evaluation

In this section, we evaluate and compare the performances of our proposed approaches in both licensed and unlicensed spectrum under different system conditions and with other approaches.

4.6.1 Simulation Setup

In the simulations, we consider three different operators where each operator has 6 BSs (one MBS and 5 UAV-BSs), and each operator has 20 MHz licensed bandwidth. In addition, a total of 20 MHz unlicensed spectrum are shared between the operators. We consider a cube of 2 Km $\times$ 2 Km $\times$ 1 Km, in which both UAV-BSs and UAV-UEs are uniformly distributed within this area. Unless stated otherwise, parameter settings are presented in Table 4.1.

Table 4.1: Value of the Simulation Parameters

Parameter	Description	Value
$\mathcal{S}$	Number of operators	3
$\mathcal{M}^s$	Number of BSs per operator s	6
P^L_{MBS}	Macro BS PSD in licensed band	-24 dBm/Hz
P^L_m	UAV-BS PSD in licensed band	-22 dBm/Hz
P^U_m	UAV-BS PSD in unlicensed band	-22 dBm/Hz
N_0	Noise PSD	-170 dBm/Hz
f^l_c	Carrier frequency of licensed band	2 GHz
f^u_c	Carrier frequency of unlicensed band	5 GHz
R^{Req}_n	UAV-UE average requested data rate	1 Mbps
B^L_s	Per operator s licensed bandwidth	20 MHz
B^U	Total unlicensed bandwidth	20 MHz

First, we evaluate our proposed algorithm 4, which maximizes the per operator sum rate in the licensed spectrum, with two well-known user association algorithms (MAX-SINR algorithm and Random algorithm). In addition, the performance of using a terrestrial network of two MBS, without using UAV-BSs, has been examined in this comparison.

4.6.2 Algorithm 4 Results for Joint User Association and Power Control in the Licensed Band

Figure 4.2 represents the average achievable data rate per UAV-UE for different numbers of UAV-UEs per operator in the licensed spectrum. The figure shows that the proposed algorithm

4 achieves a higher average data rate than other schemes, even when the number of UAV-UEs is high and the inter-cell interference is severe. It also shows that the average data rate per UAV-UE decreases as the number of UAV-UEs increases because the total achieved sum rate per operator has a maximum limit.

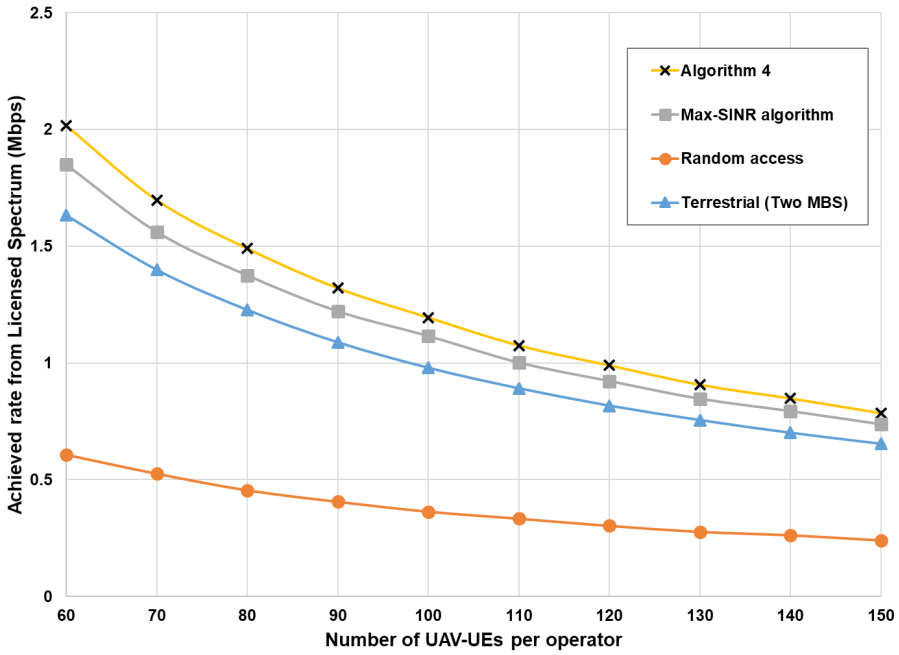

Figure 4.2: The comparison of average achieved rate per user among UAV-UEs per operator.

In Figure 4.3, we represent the total achieved per-operator sum rate in the licensed spectrum for all the comparing algorithms. It shows that our proposed algorithm has better results than all the other algorithms. Specifically, our proposed algorithm can achieve around 9 percent and 22 percent higher total sum rate per operator than the Max-SINR algorithm and the terrestrial network, respectively. The reason is that interference management through power control decreases inter-cell interference's impact significantly when the number of BSs increases. In addition, considering the coupling issue when associating UAV-UEs with BSs prevents a BS from being more congested than other BSs.

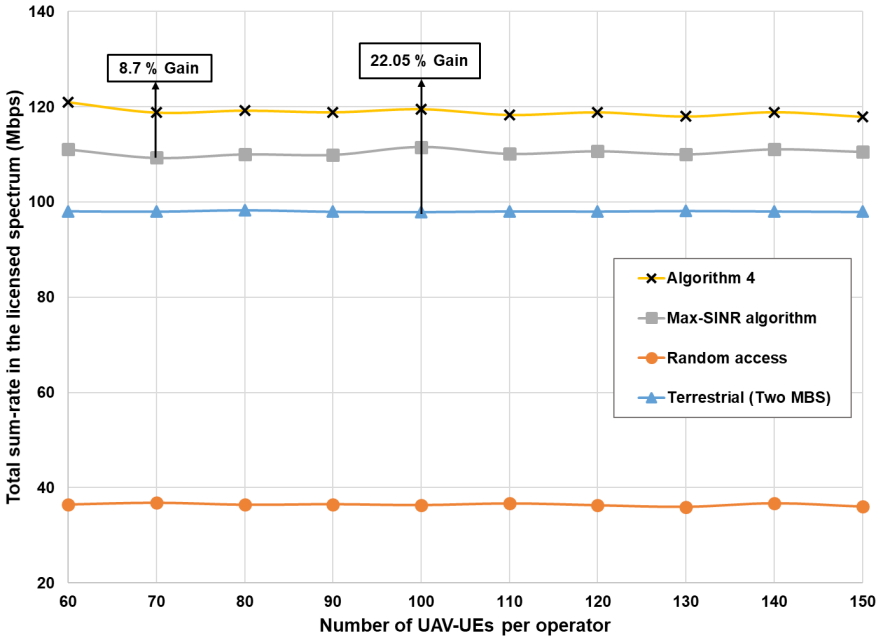

Figure 4.3: The comparison of total sum rate among UAV-UEs per operator.

Figure 4.4 shows the impact of the number of BSs on the total achieved sum rate per operator in the licensed spectrum. As can be seen, when the number of BSs increases, the total achieved sum rate also increases. Furthermore, again, our algorithm achieves higher performance than the Max-SINR algorithm. In contrast, for the Random association algorithm, as the number of BSs increases, the sum rate decreases due to the high impact of the inter-cell interference.

Figure 4.5 shows that the convergence of the proposed Algorithm 4 is guaranteed in a limited number of iterations.

Next, we compare the performance of the Algorithm 5 in the unlicensed spectrum with the existing spectrum management algorithms.

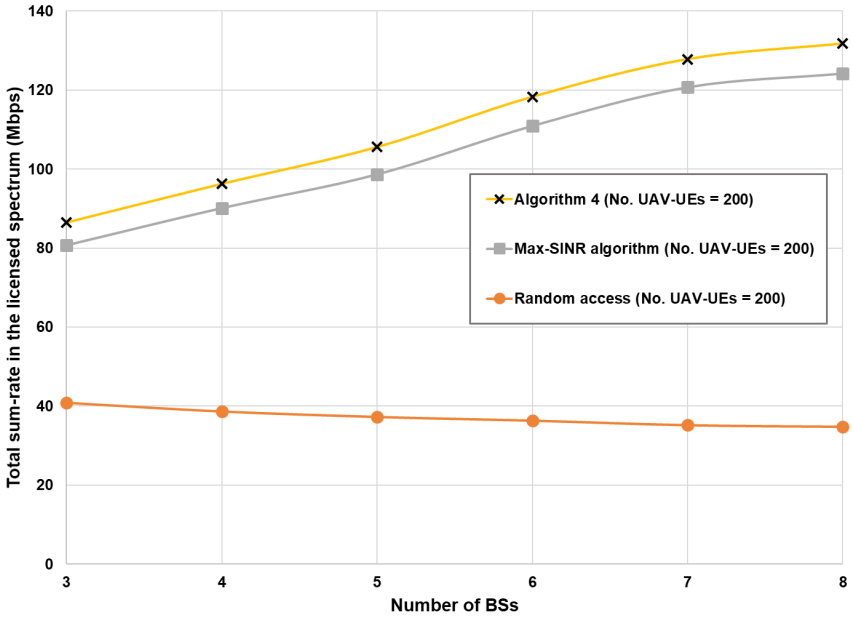

Figure 4.4: The comparison of total sum rate among BSs per operator.

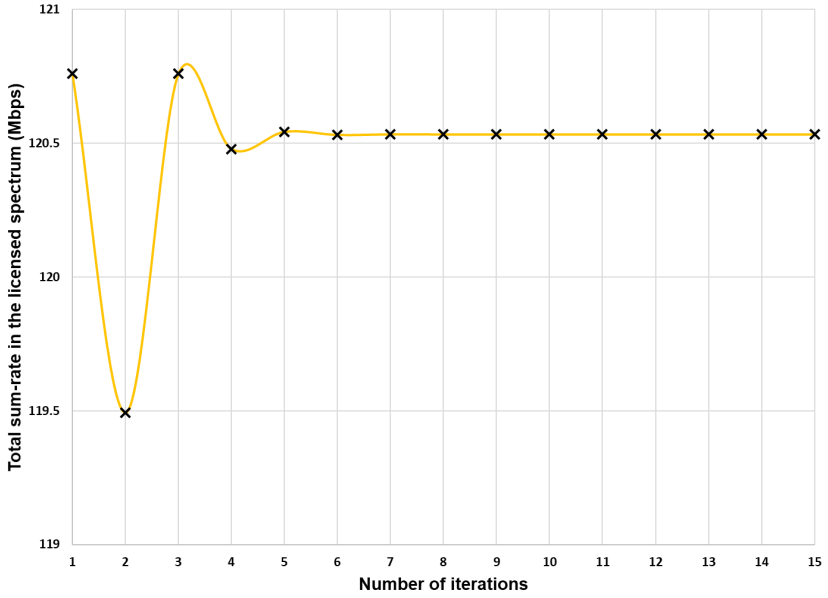

Figure 4.5: Convergence of Algorithm 4.

4.6.3 Algorithm 5 Results of User Association and Dynamic Spectrum Management in the Unlicensed Band

The output of Algorithm 4 is used as a baseline for the achieved data rate from the licensed spectrum before extending the service to the unlicensed band of all compared algorithms. We compare the proposed Algorithm 5 with two different spectrum management algorithms. The first algorithm is fixed assignment or uniform spectrum distribution, where all operators will be assigned with the same amount of unlicensed spectrum without considering their load demand. The second algorithm is the game-theoretic approach developed in [60], where each operator sends a bandwidth request to a coordinator, who then distributes the unlicensed spectrum among the operators as a ratio based on their load demand. Afterwards, each operator distributes the assigned bandwidth over the users using the game theory.

We consider that each of the three operators owns 5 UAV-BSs that can extend the cellular service to the unlicensed band. We consider three scenarios while simulating the above algorithms in the unlicensed spectrum. The considered scenarios are as follows:

- In **Scenario 1**, the number of UAV-UEs subscribing with operator one is 100, operator two is 200 and operator three is 300.
- In **Scenario 2**, we consider a uniform distribution where each operator serves 250 UAV-UEs through their network.
- In **Scenario 3**, the number of UAV-UEs served by operator one is 400, by operator two is 550, and by operator three is 700.

To measure the satisfaction level of UAV-UEs about their achieved data rate, we use the average proportion of satisfied UAV-UEs ($|\tilde{\mathcal{N}}^{s}_{Sat.}|$) per operator over all the operators [60], which is represented as follows:

$$Rate\ Satisfaction = \frac{\sum_{s\in\mathcal{S}} \frac{|\tilde{\mathcal{N}}^{s}_{Sat.}|}{|\tilde{\mathcal{N}}^{s}|}}{|\mathcal{S}|}. \tag{4.37}$$

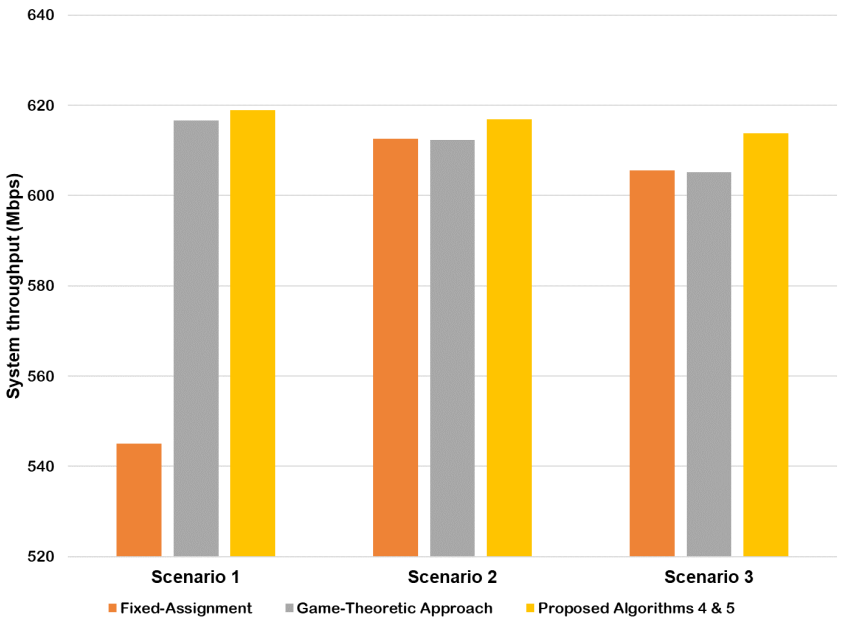

Figure 4.6: Total system throughput vs. different scenarios.

Figure 4.6 shows the total system throughput achieved for each algorithm under different scenarios. Our proposed system model can achieve about 87% gain in system throughput by extending the service to the unlicensed spectrum compared to using the licensed band only. Moreover, the proposed algorithm 5 achieves higher performance than the other two spectrum management schemes, especially in scenario 1, where it can be observed that the fixed assignment algorithm performs poorly when there is a load difference among operators. In addition, although the game-theoretic approach performs similarly to the proposed algorithm 5 in scenario 1, the actual performance could be much less. The reason is the lack of incentive for operators to honestly inform about their actual load demand. Therefore, in this case, if all the operators falsely demand the complete unlicensed spectrum, the game-theoretic approach will achieve a performance close to the fixed-assignment algorithm. In contrast, in proposed algorithm 5, if the operator requests higher unlicensed bandwidth than his actual demand, this would lead to a higher current auction price.

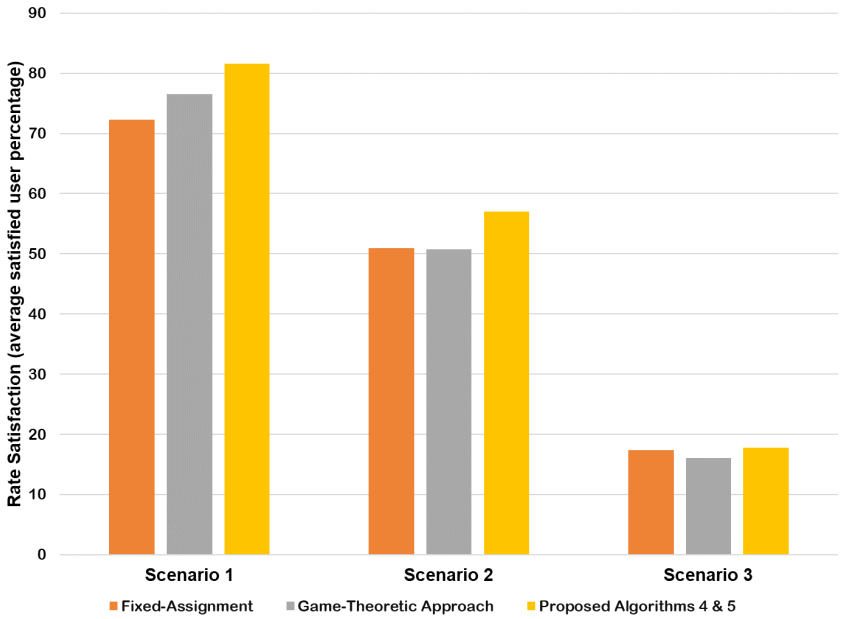

Figure 4.7: Rate satisfaction vs. different scenarios.

Figure 4.7 shows the average percentage of satisfied users who successfully achieved at least their minimum request data rate under different scenarios. As can be seen, the proposed algorithms 4 & 5 achieve an average percentage of rate satisfaction around four and six folds the proposed algorithm 4 alone in scenarios 1 and 2, respectively. Moreover, the proposed algorithm 5 achieves a higher data rate satisfaction percentage among UAV-UEs compared to the other two spectrum management schemes under all scenarios.

In Figures 4.8, 4.9, and 4.10, we show the total achieved system throughput against different unlicensed spectrum bandwidths. Figure 4.8 shows that our proposed algorithm achieves a significantly higher total system throughput than Fixed-assignment algorithms when there is a load difference between operators. Again, even though the game-theoretic approach has comparable performance to the proposed algorithm 5, the lack of incentive for operators to honestly demand unlicensed bandwidth would end up in a performance similar to the fixed-assignment algorithm.

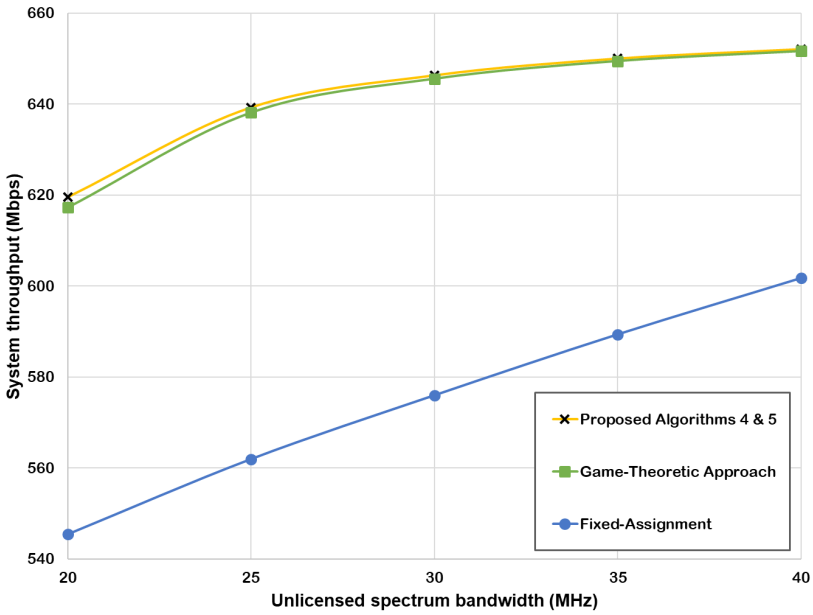

Figure 4.8: System throughput against different unlicensed spectrum bandwidth for **Scenario 1**.

Figure 4.9 shows that the fixed-assignment and game-theoretic approaches have the same performance under equal load distribution among operators. However, the proposed algorithm still performs better than the other two schemes. Figure 4.10 also shows that our proposed algorithm works much better than the other schemes in cases where there is a severely crowded network scenario with different load distributions among operators.

Figure 4.11 shows the rate satisfaction percentage against different unlicensed spectrum bandwidths for all three scenarios. As can be seen, the proposed algorithm achieves a significantly higher satisfaction rate from the user's point of view over the other algorithms in all scenarios. In scenario 2, the average percentage of the rate satisfied UAV-UEs is around 8% higher in the proposed algorithm compared to the other two schemes, which perform similarly.

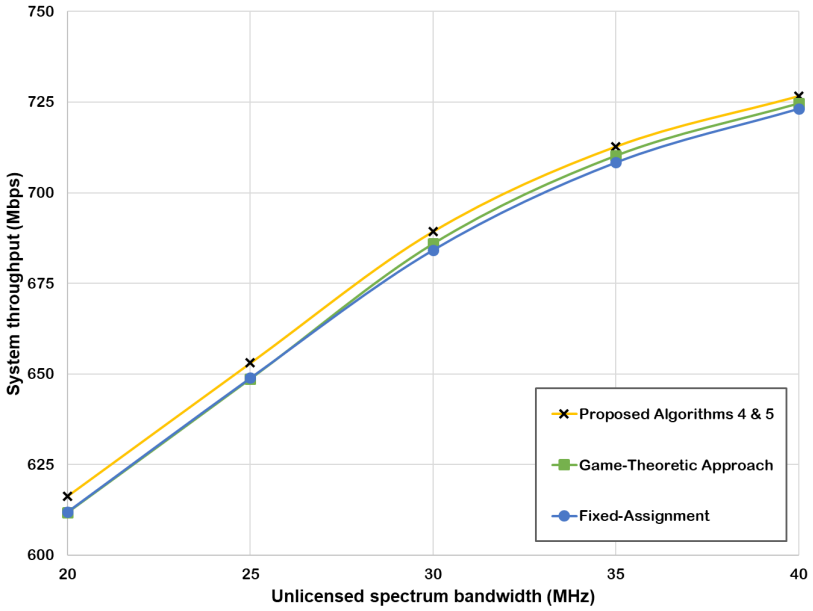

Figure 4.9: System throughput against different unlicensed spectrum bandwidth for **Scenario 2**.

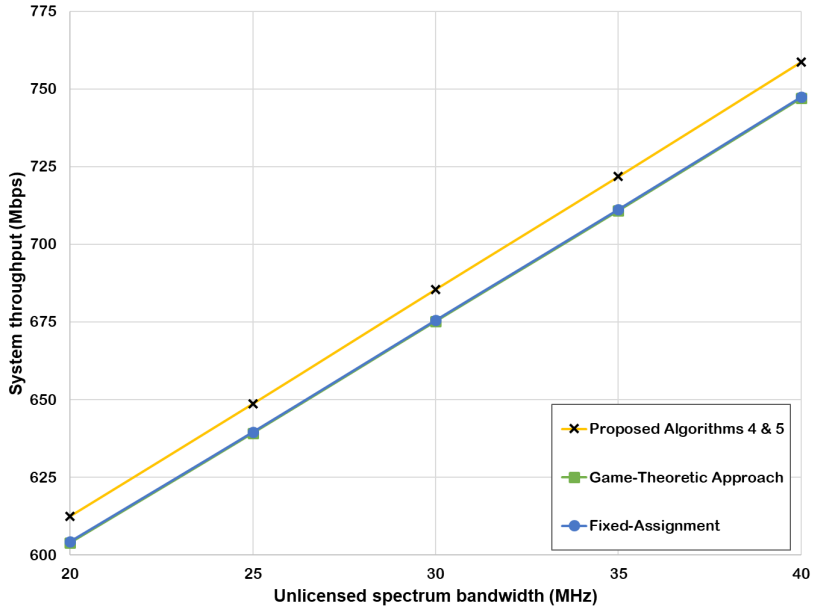

Figure 4.10: System throughput against different unlicensed spectrum bandwidth for **Scenario 3**.

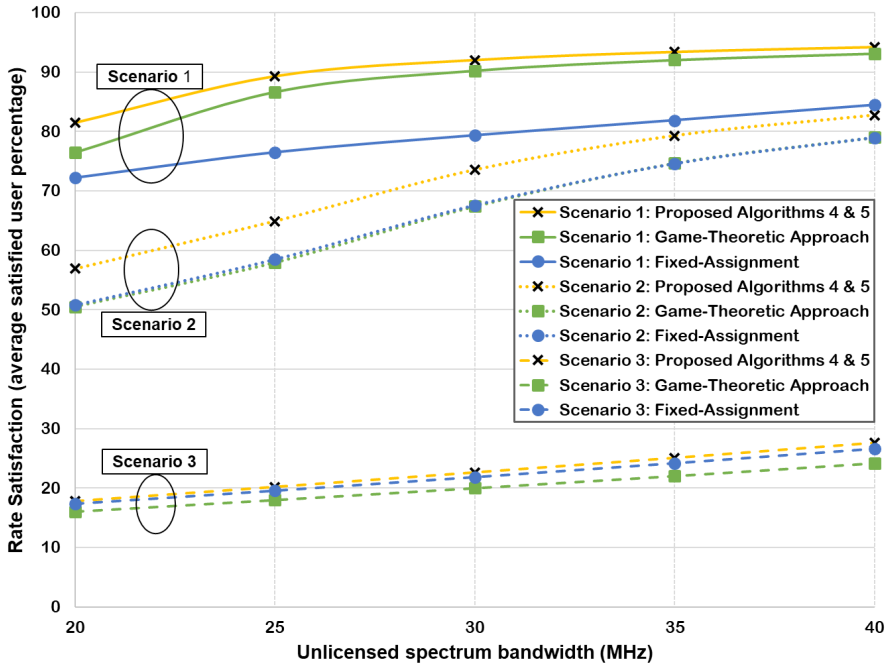

Figure 4.11: Rate satisfaction vs. different unlicensed spectrum bandwidth.

Figures 4.12 and 4.13 show the convergence speed performance for different initial auction prices. As shown in Figure 4.12, current auction price stabilizes and converges to the final theoretical analysis price. Figure 4.13 shows the changes in the total unlicensed bandwidth demand of the operators under the current auction price. Regardless of the initial auction price, the dynamic auction operation converges speedily to the theoretical analysis optimal value, which is represented in a black dashed line.

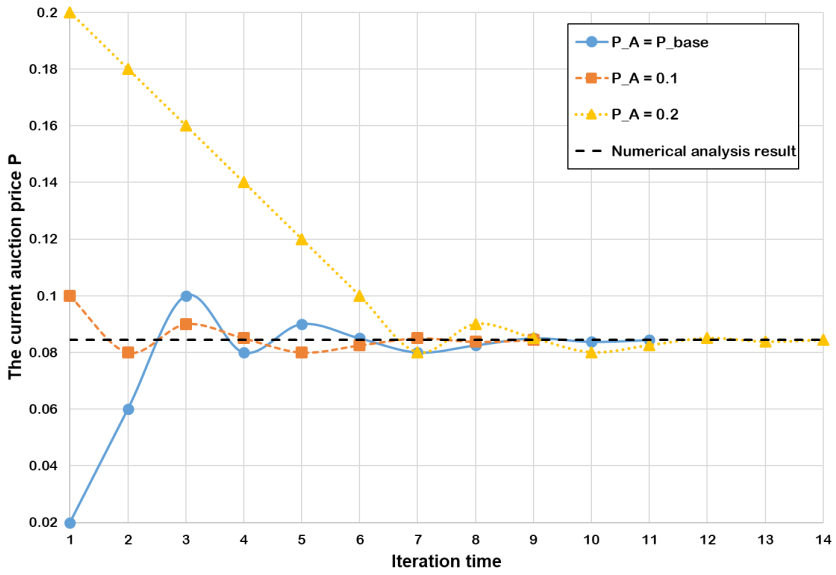

Figure 4.12: Variation of auction price.

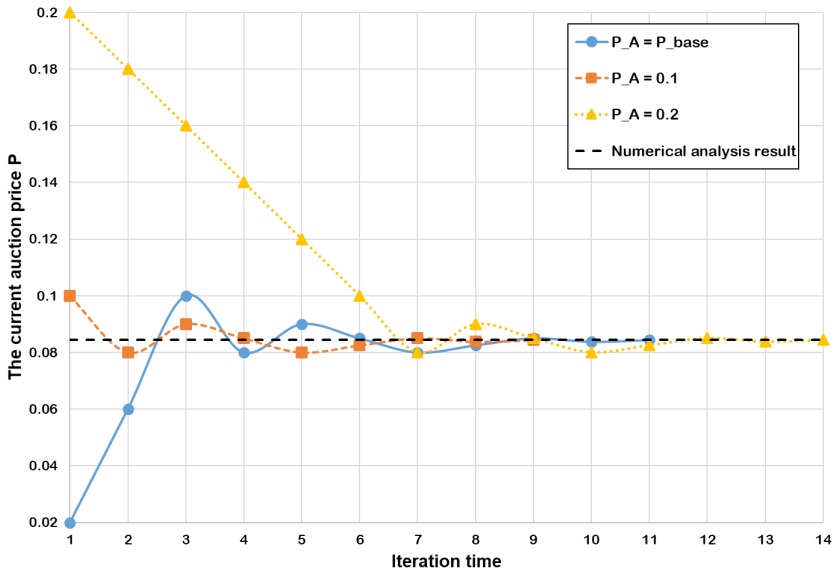

Figure 4.13: Variation of total unlicensed bandwidth bidding.

4.7 Summary

We have proposed a novel integrated aerial-terrestrial multi-operator network, considering inter-cell and inter-operator interference in licensed and unlicensed spectrum. Two algorithms have been presented to solve the joint user association and power control subproblem in licensed spectrum and the dynamic spectrum allocation and user association subproblem in unlicensed spectrum, respectively. Simulation results have demonstrated that with the proposed algorithms and integrating the aerial network with the terrestrial network, each operator can achieve a significantly higher network sum rate from the licensed spectrum than the terrestrial network alone. Moreover, the overall network throughput from licensed and unlicensed spectrum are nearly doubled than that from the licensed spectrum alone.

Chapter 5

Conclusion and Future Work

In this chapter, we summarize the main results and contributions of this thesis and present our future research directions.

5.1 Main Research Contributions

In this thesis, we have investigated channel resource allocation, user association, power control, and dynamic spectrum management for cellular-connected UAVs in 6G. Specifically, three resource and interference management strategies have been proposed for two new aerial networks. First, we have proposed a novel standalone aerial multi-cell network enabling the UAV-BSs to provide cellular service to the UAV-UEs by reusing the licensed and unlicensed spectrum. Under the proposed network, a joint subchannel allocation and power control framework to maximize the uplink network throughput has developed, considering a realistic multi-cell case scenario, the QoS of UAV-UE, and the coexistence with terrestrial cellular and WiFi systems. Second, we have proposed a novel integrated aerial-terrestrial network in which a joint user association and power control algorithm has developed. Third, a dynamic spectrum management strategy has been designed to overcome the inter-operator interference in the unlicensed spectrum for an aerial multi-operator network. The main contributions of this thesis are summarized as follows.

1. A joint subchannel allocation and power control strategy have been proposed over licensed and unlicensed spectrum in a novel aerial multi-cell network. The proposed approach considers the QoS of UAV-UE, the coexistence with terrestrial cellular and WiFi systems, and the inter-cell interference to improve the overall uplink network throughput. We have proposed an iterative algorithm consisting of convex optimization, a Hungarian algorithm, a matching game with externalities and a coalition game, and an SCA technique to efficiently solve the NP-hard optimization problem. The proposed algorithm provides an optimal resource allocation and interference management framework with low computational complexity for complex interference environments. The work allows the cellular network operators to duplicate the network throughput and capacity and enhance the spectrum efficiency.

2. A novel integrated aerial-terrestrial multi-operator network has been proposed, in which each BS (UAV-BSs and MBS) reuses the operator's licensed spectrum to provide downlink connectivity for UAV-UEs. Moreover, the operators allow the UAV-UEs to compete with others to obtain unlicensed bandwidth from the unlicensed spectrum to fulfill the QoS of UAV-UEs. Under the proposed network, a joint user association and power control scheme in the licensed spectrum and a dynamic spectrum management strategy in the unlicensed spectrum have been proposed to maximize the total network throughput, considering the inter-cell and inter-operator interference in the licensed and unlicensed spectrum, respectively. The main contributions of the proposed strategies are as follows.

    (a) A distributed iterative algorithm that jointly optimizes the user association and the BS transmit power has been developed to maximize the operator network throughput in the licensed spectrum. The proposed scheme significantly improves the operator sum rate and enhances spectrum utilization efficiency in the complex interference multi-cell environment.

    (b) A three-layers auction framework has been proposed to dynamically allocate the unlicensed spectrum bandwidth between the competitive UAV-UEs from different operators while ensuring the prevention of inter-operator interference. The proposed architecture and framework allow cellular operators to overcome the rigorous chal-

lenge of increasing network capacity with the spectrum resources shortage by reusing the unlicensed spectrum.

In summary, this thesis has investigated resource and interference management in the licensed and unlicensed spectrum for a novel integrated aerial-terrestrial multi-operator network in three aspects: optimizing UAV-UEs subchannels and power allocations, optimizing the user association and BSs transmit power, and dynamically allocating unlicensed spectrum bandwidth. Moreover, different types of interference have been considered, including inter-cell interference, co-channel interference with existing terrestrial cellular and WiFi systems, and inter-operator interference. The proposed architecture and approaches should provide valuable guidelines for future research in designing resource and interference management schemes and spectrum utilization enhancement for the complex interference environments of aerial networks in 6G.

5.2 Future Research Directions

For future research, I plan to investigate two novel aerial network architectures that support the exponential growth of cellular-connected UAV applications.

1. **Wireless Virtualization Architecture for Aerial Networks:** Wireless virtualization includes the abstraction and sharing of physical resources of Infrastructure Providers (InPs) with different parties such as Virtual Aerial Network Operators (VANOs). Specifically, physical resources such as radio frequency and UAV-BSs are owned and managed by InPs, while VANOs rent those physical resources from InPs and provide wireless services to their subscribed UAV. This architecture aims to build network operators without owning any physical telecommunication infrastructure to achieve optimal wireless infrastructure use and revenue maximization for InPs. However, the resource allocation approach plays a central role in enhancing spectrum efficiency, energy efficiency, data rate, and quality of service (QoS) in aerial networks. We plan to propose a novel wireless virtualization architecture for aerial networks and a dynamic pricing framework to ensure revenue maximization for InP and VANOs while ensuring the UAV-UE minimum data rate requirements.

2. **Blockchain-enable Spectrum Trading for Aerial Network** Spectrum trading is envisioned as a new paradigm for improving spectrum utilization efficiency. Operators desire to share their licensed resources for effective resource management and increased profit. Nonetheless, security and privacy challenges in the aerial network deter operators from collaborating with one another for spectrum trading, such as the double spending attack problem. Lately, blockchain technology has received overwhelming attention for secure spectrum trading thanks to its security features. However, the following research gaps remain to be addressed: (1) How fair, trusted, and secure is the centralized network broker between buyers and sellers? (2) Beyond the economic aspect of resource trading, what technical dynamic resource sharing procedures can be applied for efficient resource management of the limited network resource? (3) What network performance gains will enable the joint integration of blockchain and aerial network to offer 6G? We plan to propose a novel hierarchical framework for blockchain-based resource trading among aerial network operators (ANOs) in aerial multi-operator networks.

References

[1] G. T. R. 36.777, "Technical specification group radio access network; study on enhanced LTE support for aerial vehicles (release 15)," 3GPP, Tech. Rep., Dec. 2017.

[2] F. A. Administration, "FAA aerospace forecast fiscal years 2022–2042," [online]. Available: https://www.faa.gov/sites/faa.gov/files/2022-06/Unmanned_Aircraft_Systems.pdf, 2022, [accessed 11-September-2022].

[3] A. Baltaci, E. Dinc, M. Ozger, A. Alabbasi, C. Cavdar, and D. Schupke, "A survey of wireless networks for future aerial communications (FACOM)," *IEEE Communications Surveys & Tutorials*, vol. 23, no. 4, pp. 2833–2884, 2021.

[4] H. Peng, H. Wu, and X. S. Shen, "Edge intelligence for multi-dimensional resource management in aerial-assisted vehicular networks," *IEEE Wireless Communications*, vol. 28, no. 5, pp. 59–65, Oct. 2021.

[5] G. Geraci, A. Garcia-Rodriguez, M. M. Azari, A. Lozano, M. Mezzavilla, S. Chatzinotas, Y. Chen, S. Rangan, and M. Di Renzo, "What will the future of UAV cellular communications be? a flight from 5G to 6G," *IEEE Communications Surveys & Tutorials*, vol. 24, no. 3, pp. 1304–1335, 2022.

[6] M. Mozaffari, W. Saad, M. Bennis, Y.-H. Nam, and M. Debbah, "A tutorial on UAVs for wireless networks: Applications, challenges, and open problems," *IEEE Communications Surveys & Tutorials*, 2019.

[7] R. Shahzadi, M. Ali, H. Z. Khan, and M. Naeem, "UAV assisted 5G and beyond wireless networks: A survey," *Journal of Network and Computer Applications*, vol. 189, p. 103114, Sep. 2021.

[8] A. Fotouhi, H. Qiang, M. Ding, M. Hassan, L. G. Giordano, A. Garcia-Rodriguez, and J. Yuan, "Survey on UAV cellular communications: Practical aspects, standardization advancements, regulation, and security challenges," *IEEE Communications Surveys & Tutorials*, 2019.

[9] X. Jiang, M. Sheng, Z. Nan, X. Chengwen, L. Weidang, and W. Xianbin, "Green UAV communications for 6G: A survey," *Chinese Journal of Aeronautics*, vol. 35, no. 9, pp. 19–34, Sep. 2022.

[10] A. Masaracchia, Y. Li, K. K. Nguyen, C. Yin, S. R. Khosravirad, D. B. Da Costa, and T. Q. Duong, "UAV-enabled ultra-reliable low-latency communications for 6G: A comprehensive survey," *IEEE Access*, Oct. 2021.

[11] L. Gupta, R. Jain, and G. Vaszkun, "Survey of important issues in UAV communication networks," *IEEE Communications Surveys & Tutorials*, vol. 18, no. 2, pp. 1123–1152, 2016.

[12] Y. Zeng, R. Zhang, and T. J. Lim, "Wireless communications with unmanned aerial vehicles: Opportunities and challenges," *IEEE Communications Magazine*, vol. 54, no. 5, pp. 36–42, 2016.

[13] NOKIA, "F-cell technology from nokia bell labs revolutionizes small cell deployment by cutting wires, costs and time," [online]. Available: https://www.nokia.com/about-us/news/releases/2016/10/03/, Oct. 2016.

[14] Huawei, "Connected aerial vehicle live," [online]. Available: https://www.huawei.com/en/industry-insights/outlook/mobile-broadband/xlabs/use-cases/mbbf2017-connected-aerial-vehicle-live.

[15] H. Nawaz, H. M. Ali, and A. A. Laghari, "UAV communication networks issues: a review," *Archives of Computational Methods in Engineering*, vol. 28, no. 3, pp. 1349–1369, 2021.

[16] Z. Ullah, F. Al-Turjman, and L. Mostarda, "Cognition in UAV-aided 5G and beyond communications: A survey," *IEEE Transactions on Cognitive Communications and Networking*, vol. 6, no. 3, pp. 872–891, Sep. 2020.

[17] H. Yang, B. Hu, and L. Wang, "A deep learning based handover mechanism for UAV networks," in *2017 20th International Symposium on Wireless Personal Multimedia Communications (WPMC)*. IEEE, 2017, pp. 380–384.

[18] C. Zhang, W. Zhang, W. Wang, L. Yang, and W. Zhang, "Research challenges and opportunities of UAV millimeter-wave communications," *IEEE Wireless Communications*, vol. 26, no. 1, pp. 58–62, Feb. 2019.

[19] A. A. Khuwaja, Y. Chen, N. Zhao, M.-S. Alouini, and P. Dobbins, "A survey of channel modeling for UAV communications," *IEEE Communications Surveys & Tutorials*, vol. 20, no. 4, pp. 2804–2821, 2018.

[20] C. H. Liu, Z. Chen, J. Tang, J. Xu, and C. Piao, "Energy-efficient UAV control for effective and fair communication coverage: A deep reinforcement learning approach," *IEEE Journal on Selected Areas in Communications*, vol. 36, no. 9, pp. 2059–2070, Sep. 2018.

[21] R. Amorim, H. Nguyen, P. Mogensen, I. Z. Kovács, J. Wigard, and T. B. Sørensen, "Radio channel modeling for UAV communication over cellular networks," *IEEE Wireless Communications Letters*, vol. 6, no. 4, pp. 514–517, 2017.

[22] B. Hu, H. Yang, L. Wang, and S. Chen, "A trajectory prediction based intelligent handover control method in UAV cellular networks," *China Communications*, vol. 16, no. 1, pp. 1–14, 2019.

[23] P. K. Chittoor, B. Chokkalingam, and L. Mihet-Popa, "A review on UAV wireless charging: Fundamentals, applications, charging techniques and standards," *IEEE access*, vol. 9, pp. 69 235–69 266, May 2021.

[24] Z. Feng, L. Ji, Q. Zhang, and W. Li, "Spectrum management for mmWave enabled UAV swarm networks: Challenges and opportunities," *IEEE Communications Magazine*, vol. 57, no. 1, pp. 146–153, Jan. 2019.

[25] M. M. Azari, F. Rosas, and S. Pollin, "Cellular connectivity for UAVs: Network modeling, performance analysis and design guidelines," *IEEE Transactions on Wireless Communications*, vol. 18, no. 7, pp. 3366–3381, July 2019.

[26] B. Shang, V. Marojevic, Y. Yi, A. S. Abdalla, and L. Liu, "Spectrum sharing for UAV communications: Spatial spectrum sensing and open issues," *IEEE Vehicular Technology Magazine*, vol. 15, no. 2, pp. 104–112, Jun. 2020.

[27] M. Campion, P. Ranganathan, and S. Faruque, "A review and future directions of UAV swarm communication architectures," in *2018 IEEE international conference on electro/information technology (EIT)*. IEEE, 2018, pp. 0903–0908.

[28] R. Amer, W. Saad, and N. Marchetti, "Mobility in the sky: Performance and mobility analysis for cellular-connected UAVs," *IEEE Transactions on Communications*, vol. 68, no. 5, pp. 3229–3246, May 2020.

[29] M. M. Azari, G. Geraci, A. Garcia-Rodriguez, and S. Pollin, "UAV-to-UAV communications in cellular networks," *IEEE Transactions on Wireless Communications*, vol. 19, no. 9, pp. 6130–6144, Sep. 2020.

[30] Y. Gao, L. Xiao, F. Wu, D. Yang, and Z. Sun, "Cellular-connected UAV trajectory design with connectivity constraint: A deep reinforcement learning approach," *IEEE Transactions on Green Communications and Networking*, vol. 5, no. 3, pp. 1369–1380, Sep. 2021.

[31] W. Shi, J. Li, W. Xu, H. Zhou, N. Zhang, S. Zhang, and X. Shen, "Multiple drone-cell deployment analyses and optimization in drone assisted radio access networks," *IEEE Access*, vol. 6, pp. 12 518–12 529, 2018.

[32] Z. Mao, F. Hu, W. Wu, H. Wu, and X. Shen, "Joint distributed beamforming and backscattering for UAV-assisted WPSNs," *IEEE Transactions on Wireless Communications*, early access articles.

[33] A. Dhekne, M. Gowda, and R. R. Choudhury, "Cell tower extension through drones: Poster," in *Proceedings of the 22nd Annual International Conference on Mobile Computing and Networking*, 2016, pp. 456–457.

[34] C. Zhang and W. Zhang, "Spectrum sharing for drone networks," *IEEE Journal on Selected Areas in Communications*, vol. 35, no. 1, pp. 136–144, 2016.

[35] Q. Wu, Y. Zeng, and R. Zhang, "Joint trajectory and communication design for multi-UAV enabled wireless networks," *IEEE Transactions on Wireless Communications*, vol. 17, no. 3, pp. 2109–2121, 2018.

[36] M. Mozaffari, W. Saad, M. Bennis, and M. Debbah, "Mobile internet of things: Can UAVs provide an energy-efficient mobile architecture?" in *2016 IEEE global communications conference (GLOBECOM)*. IEEE, 2016, pp. 1–6.

[37] Y. Zeng, J. Lyu, and R. Zhang, "Cellular-connected UAV: Potential, challenges, and promising technologies," *IEEE Wireless Communications*, vol. 26, no. 1, pp. 120–127, Feb. 2019.

[38] Y. Zeng, X. Xu, S. Jin, and R. Zhang, "Simultaneous navigation and radio mapping for cellular-connected UAV with deep reinforcement learning," *IEEE Transactions on Wireless Communications*, vol. 20, no. 7, pp. 4205–4220, Jul. 2021.

[39] Y.-J. Chen and D.-Y. Huang, "Joint trajectory design and BS association for cellular-connected UAV: An imitation-augmented deep reinforcement learning approach," *IEEE Internet of Things Journal*, vol. 9, no. 4, pp. 2843–2858, Feb. 2022.

[40] R. Zhang, M. Wang, L. X. Cai, Z. Zheng, X. Shen, and L.-L. Xie, "LTE-unlicensed: The future of spectrum aggregation for cellular networks," *IEEE Wireless Communications*, vol. 22, no. 3, pp. 150–159, 2015.

[41] G. R1-155275, "Discussion on starting and ending of LAA transmission," 3GPP TSG RAN WG1 Meeting 82, Tech. Rep., Oct. 2015.

[42] R. Liu, Q. Chen, G. Yu, G. Y. Li, and Z. Ding, "Resource management in LTE-U systems: Past, present, and future," *IEEE Open Journal of Vehicular Technology*, vol. 1, pp. 1–17, 2019.

[43] S. Zhang, H. Zhang, B. Di, and L. Song, "Cellular UAV-to-X communications: design and optimization for multi-UAV networks," *IEEE Transactions on Wireless Communications*, vol. 18, no. 2, pp. 1346–1359, Feb. 2019.

[44] J. Lyu and R. Zhang, "Network-connected UAV: 3D system modeling and coverage performance analysis," *IEEE Internet of Things Journal*, vol. 6, no. 4, pp. 7048–7060, Aug. 2019.

[45] U. Challita, W. Saad, and C. Bettstetter, "Interference management for cellular-connected UAVs: A deep reinforcement learning approach," *IEEE Transactions on Wireless Communications*, vol. 18, no. 4, pp. 2125–2140, Apr. 2019.

[46] S. Zhang, Y. Zeng, and R. Zhang, "Cellular-enabled UAV communication: A connectivity-constrained trajectory optimization perspective," *IEEE Transactions on Communications*, vol. 67, no. 3, pp. 2580–2604, Mar. 2019.

[47] C. Zhan and Y. Zeng, "Energy-efficient data uploading for cellular-connected UAV systems," *IEEE Transactions on Wireless Communications*, vol. 19, no. 11, pp. 7279–7292, Nov. 2020.

[48] B. Khamidehi and E. S. Sousa, "Federated learning for cellular-connected UAVs: Radio mapping and path planning," in *GLOBECOM 2020-2020 IEEE Global Communications Conference*. IEEE, 2020, pp. 1–6.

[49] N. Senadhira, S. Durrani, X. Zhou, N. Yang, and M. Ding, "Uplink NOMA for cellular-connected UAV: Impact of UAV trajectories and altitude," *IEEE Transactions on Communications*, vol. 68, no. 8, pp. 5242–5258, Aug. 2020.

[50] L. Liu, S. Zhang, and R. Zhang, "Multi-beam UAV communication in cellular uplink: Cooperative interference cancellation and sum-rate maximization," *IEEE Transactions on Wireless Communications*, vol. 18, no. 10, pp. 4679–4691, Oct. 2019.

[51] M. M. U. Chowdhury, W. Saad, and I. Güvenç, "Mobility management for cellular-connected UAVs: A learning-based approach," in *2020 IEEE International Conference on Communications Workshops (ICC Workshops)*. IEEE, 2020, pp. 1–6.

[52] J. Cui, Y. Liu, and A. Nallanathan, "Multi-agent reinforcement learning-based resource allocation for UAV networks," *IEEE Transactions on Wireless Communications*, vol. 19, no. 2, pp. 729–743, Feb. 2020.

[53] W. Shi, J. Li, H. Wu, C. Zhou, N. Cheng, and X. Shen, "Drone-cell trajectory planning and resource allocation for highly mobile networks: A hierarchical DRL approach," *IEEE Internet of Things Journal*, vol. 8, no. 12, pp. 9800–9813, Jun. 2021.

[54] R. Ding, F. Gao, and X. S. Shen, "3D UAV trajectory design and frequency band allocation for energy-efficient and fair communication: A deep reinforcement learning approach," *IEEE Transactions on Wireless Communications*, vol. 19, no. 12, pp. 7796–7809, Dec. 2020.

[55] C. Qiu, Z. Wei, X. Yuan, Z. Feng, and P. Zhang, "Multiple UAV-mounted base station placement and user association with joint fronthaul and backhaul optimization," *IEEE Transactions on Communications*, vol. 68, no. 9, pp. 5864–5877, Sep. 2020.

[56] W. Feng, N. Zhao, S. Ao, J. Tang, X. Zhang, Y. Fu, D. K. C. So, and K.-K. Wong, "Joint 3D trajectory and power optimization for uav-aided mmWave MIMO-NOMA networks," *IEEE Transactions on Communications*, vol. 69, no. 4, pp. 2346–2358, Apr. 2021.

[57] N. Cherif, W. Jaafar, H. Yanikomeroglu, and A. Yongacoglu, "On the optimal 3D placement of a UAV base station for maximal coverage of UAV users," in *GLOBECOM 2020-2020 IEEE Global Communications Conference*. IEEE, 2020, pp. 1–6.

[58] M. Chen, W. Saad, and C. Yin, "Liquid state machine learning for resource and cache management in LTE-U unmanned aerial vehicle (UAV) networks," *IEEE Transactions on Wireless Communications*, vol. 18, no. 3, pp. 1504–1517, Mar. 2019.

[59] D. Athukoralage, I. Guvenc, W. Saad, and M. Bennis, "Regret based learning for UAV assisted LTE-U/WiFi public safety networks," in *2016 IEEE Global Communications Conference (GLOBECOM)*. IEEE, 2016, pp. 1–7.

[60] A. K. Bairagi, N. H. Tran, W. Saad, Z. Han, and C. S. Hong, "A game-theoretic approach for fair coexistence between LET-U and Wi-Fi systems," *IEEE Transactions on Vehicular Technology*, vol. 68, no. 1, pp. 442–455, Jan. 2019.

[61] H. Zhang, Y. Xiao, L. X. Cai, D. Niyato, L. Song, and Z. Han, "A multi-leader multi-follower Stackelberg game for resource management in LTE unlicensed," *IEEE Transactions on Wireless Communications*, vol. 16, no. 1, pp. 348–361, Jan. 2017.

[62] A. K. Bairagi, N. H. Tran, W. Saad, and C. S. Hong, "Bargaining game for effective coexistence between LET-U and Wi-Fi systems," in *NOMS 2018-2018 IEEE/IFIP Network Operations and Management Symposium*. IEEE, 2018, pp. 1–8.

[63] A. K. Bairagi, N. H. Tran, and C. S. Hong, "A multi-game approach for effective co-existence in unlicensed spectrum between LTE-U system and Wi-Fi access point," in *2018 International Conference on Information Networking (ICOIN)*. IEEE, 2018, pp. 380–385.

[64] U. Challita, L. Dong, and W. Saad, "Proactive resource management for LTE in unlicensed spectrum: A deep learning perspective," *IEEE transactions on wireless communications*, vol. 17, no. 7, pp. 4674–4689, Jul. 2018.

[65] B. Qian, H. Zhou, T. Ma, K. Yu, Q. Yu, and X. Shen, "Multi-operator spectrum sharing for massive IoT coexisting in 5G/B5G wireless networks," *IEEE Journal on Selected Areas in Communications*, vol. 39, no. 3, pp. 881–895, Mar. 2021.

[66] T. Wang and R. Adve, "Fair licensed spectrum sharing between two MNOs using resource optimization in multi-cell multi-user MIMO networks," *IEEE Transactions on Wireless Communications*, vol. 21, no. 8, pp. 6714–6730, Aug. 2022.

[67] S. Zheng, T. Han, Y. Jiang, and X. Ge, "Smart contract-based spectrum sharing transactions for multi-operators wireless communication networks," *IEEE Access*, vol. 8, pp. 88 547–88 557, May 2020.

[68] S. Zhang, W. Quan, J. Li, W. Shi, P. Yang, and X. Shen, "Air-ground integrated vehicular network slicing with content pushing and caching," *IEEE Journal on Selected Areas in Communications*, vol. 36, no. 9, pp. 2114–2127, Sep. 2018.

[69] J. Zhou, D. Tian, Z. Sheng, X. Duan, and X. Shen, "Joint mobility, communication and computation optimization for UAVs in air-ground cooperative networks," *IEEE Transactions on Vehicular Technology*, vol. 70, no. 3, pp. 2493–2507, Mar. 2021.

[70] Y. Li, S. Xu, Y. Wu, and D. Li, "Network energy efficiency maximization in UAV-enabled air-ground integrated deployment," *IEEE Internet of Things Journal*, early access articles.

[71] W. Mei, Q. Wu, and R. Zhang, "Cellular-connected UAV: Uplink association, power control and interference coordination," *IEEE Transactions on Wireless Communications*, vol. 18, no. 11, pp. 5380–5393, Nov. 2019.

[72] M. Mozaffari, A. T. Z. Kasgari, W. Saad, M. Bennis, and M. Debbah, "Beyond 5G with UAVs: Foundations of a 3D wireless cellular network," *IEEE Transactions on Wireless Communications*, vol. 18, no. 1, pp. 357–372, Jan. 2019.

[73] F. Pervez, L. Zhao, and C. Yang, "Joint user association, power optimization and trajectory control in an integrated satellite-aerial-terrestrial network," *IEEE Transactions on Wireless Communications*, vol. 21, no. 5, pp. 3279–3290, May 2022.

[74] D. Saluja, R. Singh, K. Choi, and S. Kumar, "Design and analysis of aerial-terrestrial network: A joint solution for coverage and rate," *IEEE Access*, vol. 9, pp. 81 855–81 870, Jun. 2021.

[75] M. M. Azari, S. Solanki, S. Chatzinotas, O. Kodheli, H. Sallouha, A. Colpaert, J. F. M. Montoya, S. Pollin, A. Haqiqatnejad, A. Mostaani *et al.*, "Evolution of non-terrestrial networks from 5G to 6G: A survey," *IEEE Communications Surveys & Tutorials*, early access articles.

[76] B. Li, Z. Fei, and Y. Zhang, "UAV communications for 5G and beyond: Recent advances and future trends," *IEEE Internet of Things Journal*, vol. 6, no. 2, pp. 2241–2263, Apr. 2019.

[77] D. Mishra and E. Natalizio, "A survey on cellular-connected UAVs: Design challenges, enabling 5G/B5G innovations, and experimental advancements," *Computer Networks*, vol. 182, p. 107451, 2020.

[78] N. Cheng, W. Xu, W. Shi, Y. Zhou, N. Lu, H. Zhou, and X. Shen, "Air-ground integrated mobile edge networks: Architecture, challenges, and opportunities," *IEEE Communications Magazine*, vol. 56, no. 8, pp. 26–32, Aug. 2018.

[79] W. Mei, Q. Wu, and R. Zhang, "Cellular-connected UAV: Uplink association, power control and interference coordination," *IEEE Transactions on wireless communications*, vol. 18, no. 11, pp. 5380–5393, Nov. 2019.

[80] Y. Huang, Q. Wu, T. Wang, G. Zhou, and R. Zhang, "3D beam tracking for cellular-connected UAV," *IEEE Wireless Communications Letters*, vol. 9, no. 5, pp. 736–740, May 2020.

[81] M. M. U. Chowdhury, P. Sinha, and I. Güvenç, "Handover-count based velocity estimation of cellular-connected UAVs," in *2020 IEEE 21st International Workshop on Signal Processing Advances in Wireless Communications (SPAWC)*. IEEE, 2020, pp. 1–5.

[82] W. Shi, J. Li, N. Cheng, F. Lyu, S. Zhang, H. Zhou, and X. Shen, "Multi-drone 3-D trajectory planning and scheduling in drone-assisted radio access networks," *IEEE Transactions on Vehicular Technology*, vol. 68, no. 8, pp. 8145–8158, Aug. 2019.

[83] N. Cheng, W. Quan, W. Shi, H. Wu, Q. Ye, H. Zhou, W. Zhuang, X. S. Shen, and B. Bai, "A comprehensive simulation platform for space-air-ground integrated network," *IEEE Wireless Communications*, vol. 27, no. 1, pp. 178–185, Feb. 2020.

[84] A. Al-Hourani, S. Kandeepan, and A. Jamalipour, "Modeling air-to-ground path loss for low altitude platforms in urban environments," in *2014 IEEE global communications conference*. IEEE, 2014, pp. 2898–2904.

[85] A. Al-Hourani, S. Kandeepan, and S. Lardner, "Optimal LAP altitude for maximum coverage," *IEEE Wireless Communications Letters*, vol. 3, no. 6, pp. 569–572, 2014.

[86] W. Xu, B. Li, Y. Xu, and J. Lin, "Lower-complexity power allocation for LTE-U systems: A successive cap-limited waterfilling method," in *2015 IEEE 81st Vehicular Technology Conference (VTC Spring)*. IEEE, 2015, pp. 1–6.

[87] T. LeAnh, N. H. Tran, D. T. Ngo, Z. Han, and C. S. Hong, "Orchestrating resource management in LTE-unlicensed systems with backhaul link constraints," *IEEE Transactions on Wireless Communications*, vol. 18, no. 2, pp. 1360–1375, Feb. 2019.

[88] D. S. Johnson and M. R. Garey, *Computers and intractability: A guide to the theory of NP-completeness*. W.H. Freeman, 1979.

[89] S. Boyd, S. P. Boyd, and L. Vandenberghe, *Convex optimization*. Cambridge university press, 2004.

[90] H. W. Kuhn, "The Hungarian method for the assignment problem," *Naval research logistics quarterly*, vol. 2, no. 1-2, pp. 83–97, 1955.

[91] M. A. Alim, T. Pan, M. T. Thai, and W. Saad, "Leveraging social communities for optimizing cellular device-to-device communications," *IEEE Transactions on Wireless Communications*, vol. 16, no. 1, pp. 551–564, Jan. 2017.

[92] W. Saad, Z. Han, M. Debbah, A. Hjorungnes, and T. Basar, "Coalitional game theory for communication networks," *IEEE Signal Processing Magazine*, vol. 26, no. 5, pp. 77–97, Sep. 2009.

[93] A. Abdelnasser and E. Hossain, "Resource allocation for an OFDMA cloud-RAN of small cells underlaying a macrocell," *IEEE Transactions on Mobile Computing*, vol. 15, no. 11, pp. 2837–2850, Nov. 2016.

[94] B. R. Marks and G. P. Wright, "A general inner approximation algorithm for nonconvex mathematical programs," *Operations research*, vol. 26, no. 4, pp. 681–683, 1978.

[95] M. Sami and J. N. Daigle, "User association and power control for UAV-enabled cellular networks," *IEEE Wireless Communications Letters*, vol. 9, no. 3, pp. 267–270, Mar. 2020.

[96] M. W. Baidas, M. S. Bahbahani, E. Alsusa, K. A. Hamdi, and Z. Ding, "Joint D2D group association and channel assignment in uplink multi-cell NOMA networks: A matching-theoretic approach," *IEEE Transactions on Communications*, vol. 67, no. 12, pp. 8771–8785, Sep. 2019.

[97] W. Mei and R. Zhang, "Aerial-ground interference mitigation for cellular-connected UAV," *IEEE Wireless Communications*, vol. 28, no. 1, pp. 167–173, Feb. 2021.

[98] T. Zeng, M. Mozaffari, O. Semiari, W. Saad, M. Bennis, and M. Debbah, "Wireless communications and control for swarms of cellular-connected UAVs," in *2018 52nd Asilomar Conference on Signals, Systems, and Computers*. IEEE, 2018, pp. 719–723.

[99] Y. Zeng, Q. Wu, and R. Zhang, "Accessing from the sky: A tutorial on UAV communications for 5G and beyond," *Proceedings of the IEEE*, vol. 107, no. 12, pp. 2327–2375, Dec. 2019.

[100] W. Zhang, L. Li, N. Zhang, T. Han, and S. Wang, "Air-ground integrated mobile edge networks: A survey," *IEEE Access*, vol. 8, pp. 125 998–126 018, 2020.

[101] J. Angjo, I. Shayea, M. Ergen, H. Mohamad, A. Alhammadi, and Y. I. Daradkeh, "Handover management of drones in future mobile networks: 6G technologies," *IEEE access*, vol. 9, pp. 12 803–12 823, 2021.

[102] M. A. Jasim, H. Shakhatreh, N. Siasi, A. H. Sawalmeh, A. Aldalbahi, and A. Al-Fuqaha, "A survey on spectrum management for unmanned aerial vehicles (UAVs)," *IEEE Access*, vol. 10, pp. 11 443–11 499, 2022.

[103] M. Mozaffari, X. Lin, and S. Hayes, "Toward 6G with connected sky: UAVs and beyond," *IEEE Communications Magazine*, vol. 59, no. 12, pp. 74–80, 2021.

[104] L. Zhang and J. Chakareski, "UAV-assisted edge computing and streaming for wireless virtual reality: Analysis, algorithm design, and performance guarantees," *IEEE Trans. Veh. Technol.*, vol. 71, no. 3, pp. 3267–3275, Mar. 2022.

[105] A. S. Matar and X. Shen, "Joint subchannel allocation and power control in licensed and unlicensed spectrum for multi-cell UAV-cellular network," *IEEE Journal on Selected Areas in Communications*, vol. 39, no. 11, pp. 3542–3554, Nov. 2021.

[106] A. Al-Hourani and K. Gomez, "Modeling cellular-to-UAV path-loss for suburban environments," *IEEE Wireless Communications Letters*, vol. 7, no. 1, pp. 82–85, Feb. 2018.

[107] D. Bertsimas and J. N. Tsitsiklis, *Introduction to linear optimization*. Athena Scientific Belmont, MA, 1997, vol. 6.

[108] Y. Wang, Y. Niu, H. Wu, Z. Han, B. Ai, and Q. Wang, "Sub-channel allocation for device-to-device underlaying full-duplex mmWave small cells using coalition formation games," *IEEE Trans. Veh. Technol.*, vol. 68, no. 12, pp. 11 915–11 927, Dec. 2019.